8-2016

The impacts of biopolymer-ionic liquid interactions on the utilization of lignocellulosic biomass

Jing Wang
University of Tennessee, Knoxville, jwang76@vols.utk.edu

To the Graduate Council:

I am submitting herewith a dissertation written by Jing Wang entitled "The impacts of biopolymer-ionic liquid interactions on the utilization of lignocellulosic biomass." I have examined the final electronic copy of this dissertation for form and content and recommend that it be accepted in partial fulfillment of the requirements for the degree of Doctor of Philosophy, with a major in Biosystems Engineering.

Nicole Labbe, Major Professor

We have read this dissertation and recommend its acceptance:

Douglas G. Hayes, Thomas G. Rials, Thomas Zawodzinski, David P. Harper

Accepted for the Council:
Dixie L. Thompson

Vice Provost and Dean of the Graduate School

(Original signatures are on file with official student records.)

The impacts of biopolymer-ionic liquid interactions on the utilization of lignocellulosic biomass

A Dissertation Presented for the
Doctor of Philosophy
Degree
The University of Tennessee, Knoxville

Jing Wang
August 2016

DEDICATION

This dissertation is dedicated to my parents, Baolin Wang and Yanmei Li and my husband Bo Zhang.

ACKNOWLEDGEMENTS

I sincerely thank my major advisor, Dr. Nicole Labbé, for her tremendous guidance and support of my doctorate program. I thank Drs. Douglas G. Hayes, Thomas Zawodzinski, Timothy G. Rials and David P. Harper for serving on my committee and their valuable questions and comments during preparation of this dissertation. I also appreciate the help and support from Drs. Amit Naskar and Stephen Chmely.

I am very grateful for the kindness, help and encouragement from my groupmates, Ms. Choo Hamilton, Dr. Pyoung Chung Kim, Ms. Anna Kim, Ms. Lindsey Kline and Dr. Jingming Tao, and all staff of the Department of Biosystems Engineering and Soil Science and the Center for Renewable Carbon.

I express my special thanks to my family and my friends for their love, prayers, encouragement and continuous support. I would like to thank God for many blessings during my Ph. D. study. I can complete my study because he always gives me strength.

ABSTRACT

In the bioenergy field, the recalcitrance of lignocellulosic biomass has been mainly attributed to lignin. Many ionic liquid (IL) pretreatments were performed to maximize the removal of lignin. However, those methods seriously degraded lignin and hemicellulose, and could generate lignin or hemicellulose for developing an integrated biorefinery that utilizes efficiently the whole biomass. To fulfill the requirements of the integrated biorefineries, this dissertation explored the interactions between biopolymers and IL for a better utilization of lignocellulosic biomass as feedstock. By removing a large portion of hemicellulose, through an autohydrolysis, this physical and chemical barrier for IL diffusion was dismantled and the interactions of the remaining biopolymers with 1-ethyl-3-methylimidazolium acetate were distinctly improved, which significantly enhanced the dissolution ability of biomass in this IL. The percentage of dissolution of biomass increased by a factor of 8 with the highest severity autohydrolysis (160 °C for 60 min) at 100 °C. Furthermore, rheological data showed that autohydrolyzed biomass-IL solution had adequate viscosity for film casting. Therefore, biomass films were directly cast from the solution, coagulated with a solvent and generated materials free of any cracks or wrinkles. The properties of the films highly depended on the coagulant. The film coagulated in methanol showed the most homogeneous texture, and the best thermal and mechanical properties. These characteristics could mainly be explained by the impacts of low polarity of methanol on the morphology and chemical composition of biomass films. Finally, an efficient fractionation process was investigated. Autohydrolyzed biomass was activated under mild IL conditions (60 °C for 3 h) and was then subjected to an enzymatic saccharification. The superior carbohydrates conversion kinetics resulted from a

combination of both treatments. The process isolated 87 wt% of cellulose and 81 wt% of hemicellulose in the carbohydrates fractions, and 70 wt% of the lignin with a purity of 90.1%. The main linkages present in the biomass were preserved during the fractionation process. Overall, the successful production of biomass films and the complete fractionation of lignocellulosic biomass demonstrated that the improved interactions of biopolymers with IL by hemicellulose extraction paved the way for a better utilization of lignocellulosic biomass.

TABLE OF CONTENTS

LIST OF TABLES

LIST OF FIGURES

CHAPTER ONE

INTRODUCTION AND BACKGROUND

1.1 Motivation

Lignocellulosic biomass has been investigated as a resource to generate biofuels, biochemical, and other bioproducts. A variety of pretreatment methods has been designed to decrease the recalcitrance of lignocellulosic biomass and produce ethanol and other bioproducts from cellulose. A majority of these methods treated lignin as structural barrier preventing the interaction between cellulose and IL, therefore they were designed to remove lignin from the biomass by pretreatment under high severity (mostly temperature). During these pretreatments, lignin and hemicellulose were always highly degraded and often ended in the waste streams. To improve the profitability and sustainability of biorefineries, an advanced process that can either use the whole biomass as feedstock or isolate each biopolymer with high purity and yield for downstream processing is required.

1.2 Main goal and objectives

The overall goal of this dissertation is to understand the interactions between biopolymers and IL for a better utilization of lignocellulosic biomass. Accordingly, achieving this overall goal requires fulfilment of three sub-objectives:

1. To improve the interactions of lignocellulosic biopolymers with IL through an autohydrolysis step.
2. To completely dissolve these biopolymers in IL and directly produce high-value films from biomass-IL solution.
3. To fractionate IL-activated lignocellulosic biomass and generate high purity and yield of biopolymer fractions.

1.3 Lignocellulosic biomass and bioenergy

Concerns to reduce crude oil imports, diminish CO_2 emission, and promote long term economy of the United States have motivated research over the last 35 years in renewable domestic sources to substitute petroleum.[1] Lignocellulosic biomass has been considered as a potential valuable feedstock to produce renewable fuels and other bioproducts because it is the most abundant renewable resource and has been largely underutilized.[2] The US environment protection agency established the Renewable Fuel Standards in 2005 mandating a minimum volume of renewable fuel for transportation. The actual volume of domestic biofuel in the calendar years of 2014, 2015 and 2016 showed that the final requirement for cellulosic biofuel has grown steadily (Table 1.1). Lignocellulosic biomass is the major resource for the production of cellulosic biofuel.

Table 1.1 Final Renewable Fuel Volumes (reproduced from ref.[3])

	2014	2015	2016
Cellulosic biofuel (million gallons)	33	123	230
Biomass-based diesel (billion gallons)	1.63	1.73	1.90
Advanced biofuel (billion gallons)	2.67	2.88	3.61
Renewable fuel (billion gallons)	16.28	16.93	18.11

1.4 Lignocellulosic biomass composition and its recalcitrance

Lignocellulose is a composite material that makes up plant cell walls. Its primary composition of polymeric carbohydrates (cellulose and hemicellulose) and aromatic polymer lignin, make up at least 90 % of dry matter of lignocellulose. Plant cell wall structure and microfibril cross-section are shown in Figure 1.1.

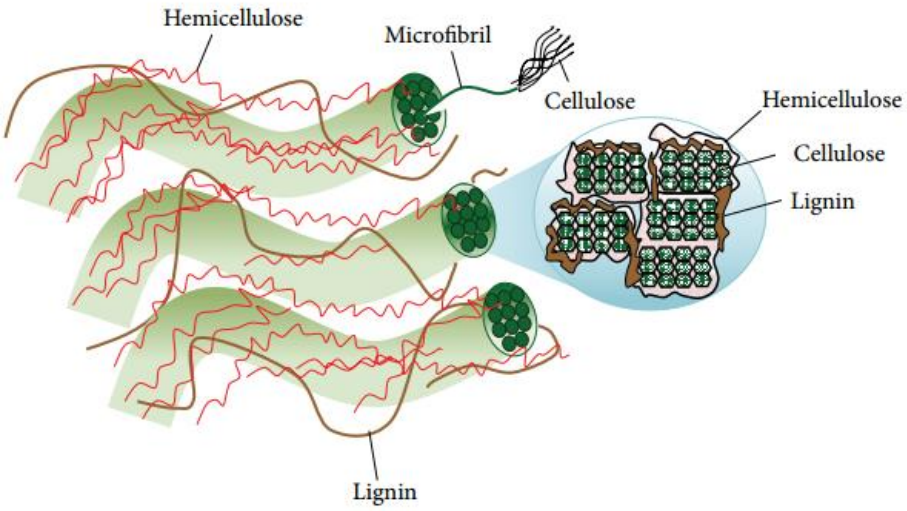

Figure 1.1 Plant cell wall structure and microfibril cross-section adapted from ref.[4]

1.4.1 Cellulose

The main polysaccharide in woody plant is cellulose. The units of *D*-glucopyranose monomer are linked to each other by 1-4-β glycosidic bonds (Figure 1.2) and generate the homopolysaccharide with approximately 10-15,000 degree of polymerization.[5] The β conformation of pyranose rings and the three hydroxyl groups in an equatorial position enable the packing of numerous cellulose strands into cellulose sheet by hydrogen-bonding interaction (Figure 1.3). The sheets are believed to interact mostly through van der Waals interactions.[5] The intermolecular hydrogen-bonding and van der Waals interactions between sheets allow intimate and ordered packing of cellulose strands. The structural characteristics of cellulose microfibrils contribute to the polymer's insolubility in water and most organic solvents.[6] Moreover, cellulose strands are embedded in the matrix of the other two biopolymers, hemicellulose and lignin, which strengthen the insolubility and

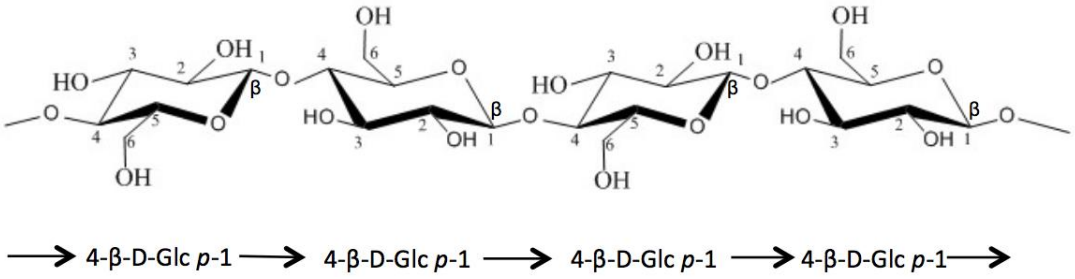

Figure 1.2 Cellulose structure.

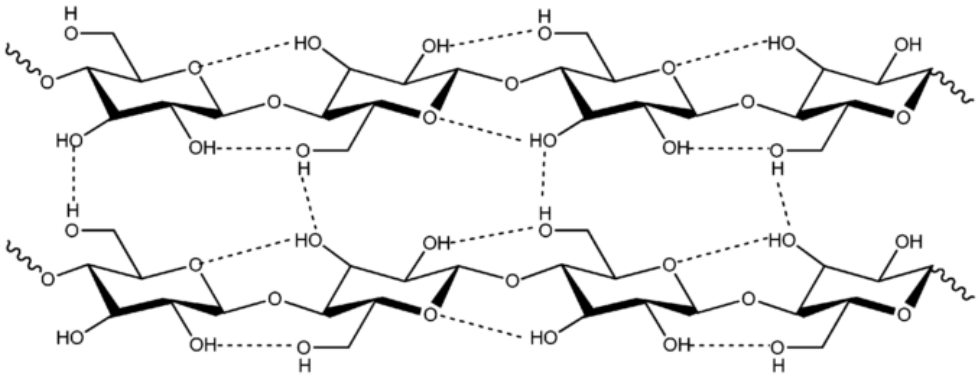

Figure 1.3 Intermolecular and intramolecular hydrogen bonding interactions in cellulose adapted from ref.[11]

complexity of lignocellulosic biomass (Figure 1.1). The native state of cellulose in biomass (cellulose I) can be transformed to less crystallized structure and thermodynamically more favorable structure, i.e. cellulose II, via some processes, regeneration (solubilization and recrystallization)[7], mercerization (alkali treatment)[7], ball-milling[8] and subcritical water[9]. Cellulose II has antiparallel strands and some hydrogen bonds between sheets.[7, 10]

1.4.2 Hemicellulose

Hemicellulose is a branched polymer with lower degree of polymerization around 100–200[12] and described as an amorphous matrix material covering the cellulose fibrils by forming hydrogen bonds with cellulose fibrils. Hemicellulose is also thought to entangle with lignin and form covalent bonds with lignin (mainly α-benzyl ether linkages).[13, 14]

Hemicellulose is a hetero-polysaccharide comprising of both hexose (glucose, mannose and galactose) and pentose (xylose and arabinose) (Figure 1.4). The structure of hemicellulose is more complex than cellulose. A few of subclasses of hemicellulose have been found from various plant species, including glucuronoxylans, arabinoxylans, linear mannans, glucomannans, galactomannans, galactoglucomannans, β-glucans, and xyloglucans.[15] In general, xylans and mannans are the most prevalent polysaccharides of hemicellulose. The predominant hemicellulose in hardwood is xylan, more specifically an O-acetyl-4-O-methylglucurono-β-D-xylan. On the contrary, galactoglucomannan (15–20% dry weight) is the dominant hemicellulose in softwood; xylan is approximately 7–10% of the softwood dry weight.[15] Xylan in the cell wall of many species plant are in the acetated form. Biely et al. first demonstrated the negative effect of acetyl side groups on the enzymatic saccharification of hemicellulose.[16] Deacetylation of biomass can

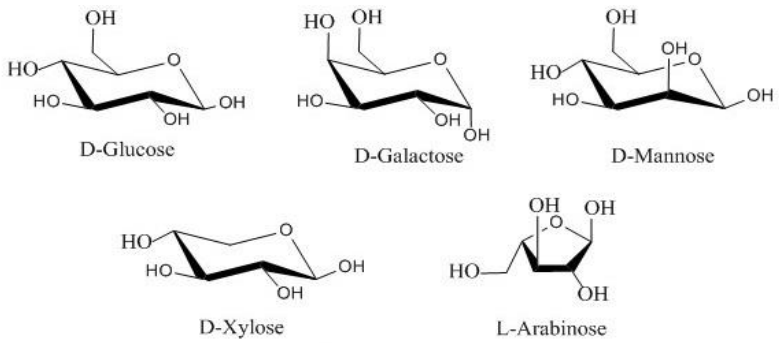

Figure 1.4 Hexoses and pentoses in hemicellulose.

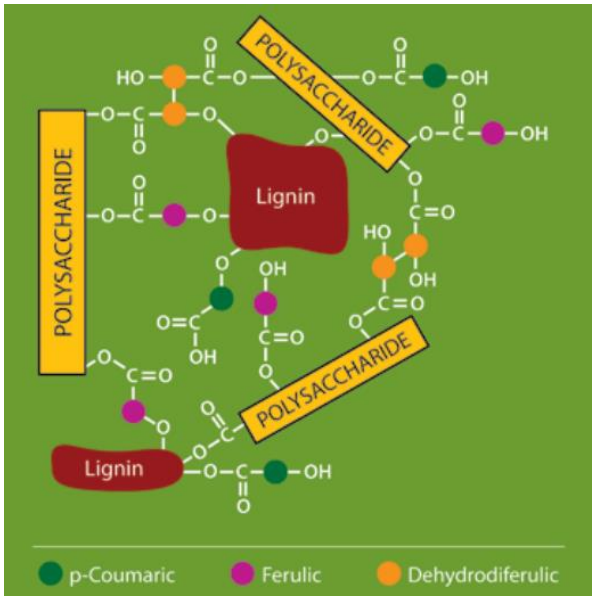

Figure 1.5 Cross-links between polysaccharides and lignin adapted from ref.[14]

much improve the enzymatic accessibility and increase the carbohydrates conversion.[17, 18]

1.4.3 Lignin

Lignin is the second most abundant biopolymer on the planet, surpassed only by cellulose. It accounts for approximately 30 % of the organic carbon in the biosphere and 15-30 % of the dry weight of woody plants.[19] Lignin is bonded to the cellulose and hemicellulose polysaccharides and acts as a structural and protective element in the cell wall around the carbohydrate constituents, preventing biomass breakdown (Figure 1.1 and Figure 1.5).[14]

Lignin carries the highest specific energy content and possesses the most abundant functional groups of lignocellulosic biomass. A number of studies have explored the structure of lignin. Although the exact structure of native lignin remains unclear, the dominant constituents of lignin have been elucidated. Lignin is described as a phenyl-propanoid (C9) polyphenol mainly linked by arylglycerol ether bonds between the monomeric phenolic p-coumaryl alcohol (H), coniferyl alcohol (G) and syringyl alcohol (S) units (Figure 1.6 and Figure 1.7).[20] The primary inter-unit linkages in native lignin are shown in Figure 1.7. The amount of lignin differs from plant to plant, with lignin content generally decreasing in the order of softwood, hardwood, and grasses, respectively. Softwood lignin is mainly composed of G units with low level of H units, hardwood lignin consists principally of G and S units with trace amount of H units, and grass lignin is composed of S, G, and H units.[19]

Milled wood lignin (MWL) first isolated by Björkman in 1956, has been considered as the representative of native lignin in lignocellulosic biomass.[21] The name MWL was first

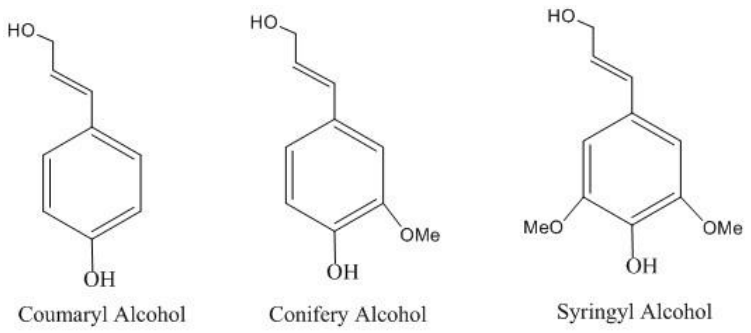

Figure 1.6 Structures of three lignin precursors**.**

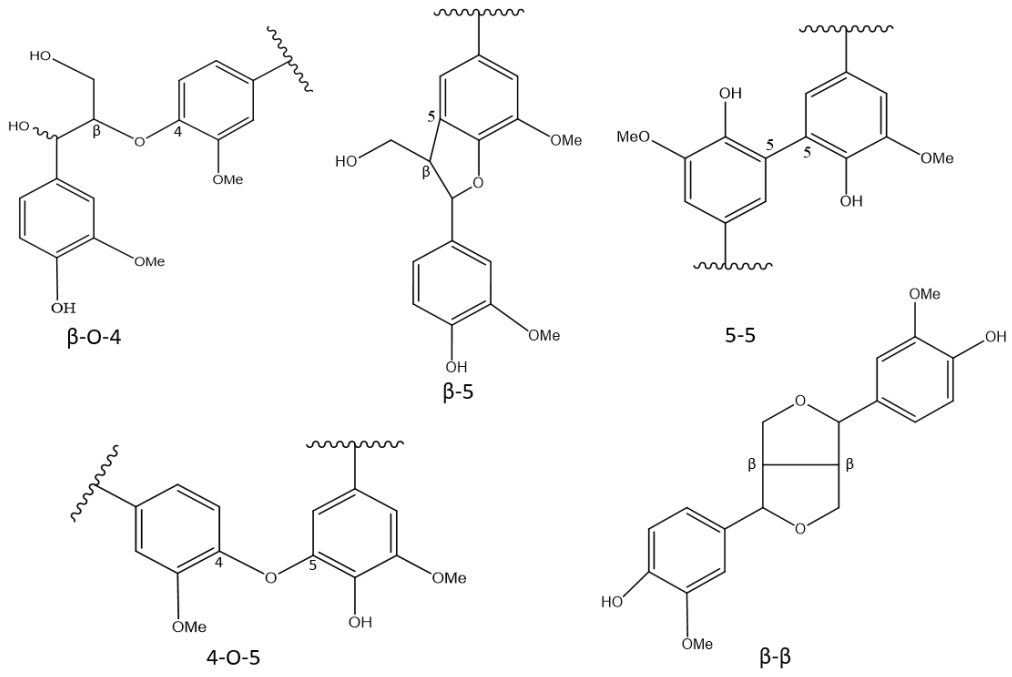

Figure 1.7 Primary inter-unit linkages in native lignin reproduced from ref.[19]

presented in the “Studies on finely divided wood Part 1. Extraction of lignin with neutral solvents”.[21] In this paper, the 'standard method-MWL' is provided. Briefly, wood is reduced to pass a 20 mesh screen, pre-extracted to remove resins etc., ground for 48 hrs. in a Lampén mill (12 g. charge) and 48 hrs. in a vibrational ball mill (6 g. charge), using toluene for dispersion, and extracted with aqueous dioxane. After evaporation of the solvent, lignin is dissolved in an aqueous acetic acid solution, precipitated by addition of water, dried, dissolved in 1,2-dichloroethane/ethanol (2/1, v/v), precipitated with ethyl ether, washed, and dried. A faintly cream-colored, ash-free powder, i.e. MWL, is obtained. The molecular weight of MWL from spruce has been reported to be about 11,000 (weight average) or about 60 phenyl-propane units.[21]

Most structural characterizations of native lignin have been achieved by solution-state nuclear magnetic resonance spectroscopy of MWL.[22-28] Although MWL is very useful for lignin studies, it cannot provide the comprehensive information of native lignin, because structural changes take place during the lignin isolation process. The evidences below are supporting this statement:

1. The process does not allow the entire lignin fraction to be isolated. Normally, only 15-20% of the entire lignin is extracted as a dioxane-soluble. For example, 18.1% of total lignin from pine[29] and 11.6% of total lignin from spruce have been reported. Low molecular weight lignin was easier to extract than high molecular weight lignin by the process.[30]
2. The severe ball milling process results in lignin structure alterations. The degree of polymerization is reduced with new free-phenolic end groups and new side-chain groups, side-chain oxidation and side-chain degradation.[20] For instance, the

vibratory-milling processes have been demonstrated to induce condensation[29] and side-chain oxidation[31] as well as increase amounts of condensed phenolic hydroxyl and carboxylic acid groups[32]. Therefore, while MWL is considered as today as the most native lignin, it is clear that lignin undergoes several modifications during its isolation. A new lignin isolation method is still needed to extract lignin with minimum degradation and modification.

1.5 Pretreatment of lignocellulosic biomass

Lignocellulosic biomass has complex structural and chemical properties that make it highly resistant to pretreatment to release sugars from chemicals and enzymes.[33] The insolubility of lignocellulosic biomass in water and conventional organic solvents has prevented its efficient utilization as a feedstock to produce biofuels and biomaterials. To overcome this recalcitrance, a wide variety of pretreatment processes has been developed to deconstruct plant cell walls. The goals of pretreatment technologies are to alter or remove structural and compositional impediments in order to improve enzyme accessibility and increase yields of fermentable sugars from cellulose (Figure 1.8).[1, 34, 35] Pretreatment technologies are classified into four categories: physical and mechanical (milling and grinding), physicochemical (autohydrolysis, steam explosion), chemical (acidic, alkaline and oxidative), and biological (using white rot fungi).[36]

1.5.1 Kraft pulping process

The Kraft process is a major chemical pulping technique, accounting for 98 percent of chemical pulp production in the United States and 92 percent of chemical pulp production in the world.[37] During this treatment, wood chips are pretreated with a mixture of at

Figure 1.8 Schematic of the goal of pretreatment on lignocellulosic biomass adapted from ref.[35]

temperature between 150-180 °C for about 2 h.[38] The pretreatment causes hydroxide and hydrosulfide anions to depolymerize lignin into smaller water/alkali soluble fragments.[39] The removal of lignin and hemicellulose liberates cellulose from the wood matrix.

The major chemical reactions of the pulping process include lignin fragmentation (alpha- and beta-aryl ether cleavage in free phenolic units, enol ether formation, alpha- and beta-aryl ether cleavage in etherified units and C-C bond cleavage), lignin condensation, and the cleavage of lignin bonding to carbohydrates.[39] The residual liquor from the pulping process, “black liquor”, is a highly complex solution including lignin, hemicellulose, organic components, sodium salts, and sulfur compounds. It contains more than half of the energy content of the wood fed into the digester of a Kraft pulp mill. The recycling of black-liquor and the pretreatments for black liquor to produce high-value products have been studied worldwide. Although lignin can be recovered through several separating methods, the primary use of Kraft lignin is as a low-grade energy source in combustion.[40] The other disadvantages of this pulping process include high capital cost, high energy consumption, and low pulp yields.[41]

1.5.2 Other pretreatment processes

Other pretreatment technologies have been developed and reviewed.[1] These pretreatment technologies focus on disrupting the lignin-carbohydrate complex, breaking down lignin and hemicellulose, and decreasing the crystallinity of cellulose. For example, dilute acid pretreatment has been developed to process a wide range of lignocellulosic biomass.[42, 43] The pretreatment is always conducted with low concentration of acid (less than 4%) in the range of 120 to 210 °C. Various acids have been applied, but sulfuric acid is the most widely used one due to its inexpensiveness.[42] The major effect of dilute acid pretreatment is to hydrolyze a high percentage of hemicellulose and lignin, disrupt lignin structure, and further enhance the accessibility of cellulose for enzymes. However, the complete conversion of cellulose in the acid-pretreated biomass by enzyme saccharification can be hardly achieved since the cellulose crystallinity is not adequately modified by this method.[44, 45] In addition, acid-based approaches can lead to the formation of by-products of aliphatic carboxylic acid and phenolic compounds by the hydrolysis of hemicellulose and lignin.[46]

Similar to dilute acid pretreatment, some other pretreatment technologies are able to increase the accessible area of cellulose as well (Table 1.2). Most of the methods can distinctly increase the accessibility of cellulose in order to provide fermentable sugars for biofuel purposes. However, these pretreatment processes could not really take advantage of the other two major components, lignin and hemicellulose, of the biomass. In addition, these severe pretreatments with high temperature and long reaction time also result in the delignification and the production of by-products, which inhibit downstream processes.[46] For instance, the alkaline methods have been reported to produce by-products including

Table 1.2 Effect of various pretreatment methods on the chemical composition and chemical/physical structure of lignocellulosic biomass (reproduced from ref.[1])

	Increase accessible area	Decrystallize cellulose	Remove hemicellulose	Remove lignin	Alter lignin structure
Uncatalyzed steam explosion	■		■		■
Liquid hot water	■	ND	■		■
pH controlled hot water	■	ND	■		ND
Flow-through liquid hot water	■	ND	■	■	■
Dilute acid	■		■	■	■
Flow-through acid	■		■	■	■
AFEX	■	■	■	■	■
ARP	■	■	■	■	■
Lime	■	ND	■	■	■

■ : Major effect AFEX: Ammonia fiber/freeze explosion

■ : Minor effect ARP: Ammonia recycled percolation

ND: Not determine

acetic acid, hydroxyl acids, dicarboxylic acids and phenolic compounds.[46]

1.6 Biomass fractionation

Pretreatment methods designed to produce biofuels from carbohydrates have limited profitability of biorefineries.[47] Lignin with highly reactive functional groups represents a significant possibility to produce high value-added chemicals or materials.[48] Therefore, pretreatment technologies need to be improved to fractionate lignocellulosic biomass and utilize each major component (Figure 1.9).

Biorefineries should follow the model of the petrochemical industry by integrating low value fuel with the production of high value chemicals derived from each primary component of lignocellulose (Figure 1.9 and Table 1.3).[47] Even if the new generation biorefineries are challenged by high cost, the ability to incorporate high value chemical

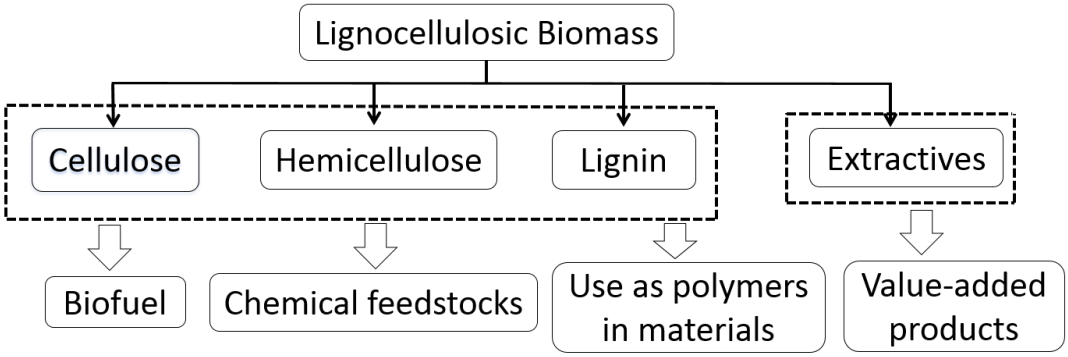

Figure 1.9 Possible applications of the major components from lignocellulosic biomass modified and reproduced from ref.[49]

Table 1.3 The top 10 chemicals from carbohydrates and lignin. Reprinted from ref.[51]

Products from carbohydrates	Products form lignin
Succinic, fumaric and malic acids	Thermochemical products (gasification, pyrolysis, combustion)
2, 5-Furandicarboxylic acid	Macromolecules (carbon fibers, polymer modifiers, resins adhesives)
3-Hydroxypropionic acid	BTX
Aspartic acid	Phenol
Glucaric acid	Substituted coniferols (propylphenol, eugenol, aryl ethers, etc.)
Glutamic acid	Oxidized lignin monomers (vanillin, syringaldehyde)
Itaconic acid	Diacids from chemical transformations
Levulinic acid	Diacids from biochemical transformations
3-Hydroxybutyrolactone	Aromatic polyols (cresols, catechols)
Glycerol	Cyclohexane and substituted cyclohexanes
Sorbitol Xylitol/arabinitol	Quinones

products in an integrated operation will provide a revenue stream.[50, 51] Therefore, advanced processes that satisfy the requirements of integrated biorefineries must exhibit the ability to isolate each primary component of lignocellulosic biomass.[47] Organosolv and ionic liquid processes have been proposed and designed to meet these requirements.[52]

1.6.1 Organosolv process

Organosolv process exposes lignocellulosic biomass to organic solvents. Ethanol and methanol have been the major solvents in the process.[53-55] Organosolv process has advantages compared with the conventional Kraft pulping process. It fractionates biomass into separate streams (cellulose, hemicellulose, and lignin) and is more efficient at removing lignin with minimum lignin condensation.[34] Black and co-workers at the National Renewable Energy Laboratory developed a new organosolv fractionation technology, also known as "Clean Fractionation", which used a mixture of solvents system, composed of methyl isobutyl ketone (MIBK), ethanol, and water with sulfuric acid as catalyst.[56] Lignin and hemicellulose are selectively dissolved in the liquid phase, leaving cellulose as an undissolved solid. The liquid phase is further treated with water, MIBK or a salt resulting in an organic phase containing mainly the lignin fraction and an aqueous phase enriched in hemicellulose and aqueous lignin.[47] The hemicellulose fraction is very difficult to be purified since it is the most chemically complex fraction containing sulfuric acid, organic acids generated during the fractionation, ethanol, MIBK, and lignin fragments of low molecular weight, extractives, ash, and degraded products.

1.6.2 Ionic liquid process

Some solvents with unique properties have been designed to improve the sustainability of various chemical reactions and processes including organic-aqueous tunable solvents, near-critical water, switchable piperylene sulfone, a volatile dimethylsulfoxide substitute, ionic liquids (ILs), and so forth.[57, 58] ILs are generally defined as salts that melt below 100 °C.[49] They are composed entirely of ions, an anion and a cation (Figure 1.10). The term "ionic liquid" has replaced the older name "molten salts" ions. ILs present their potential as "green solvents" to substitute the volatile and unstable organic solvents,[59] due to their distinguished properties such as high thermal stability and nearly complete no-volatility.

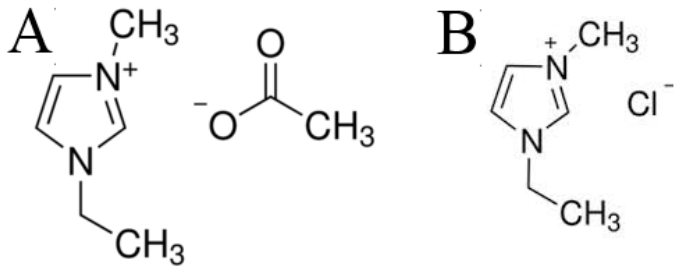

Figure 1.10 Chemical structures of IL examples. (A) 1-ethyl-3-methylimidazolium acetate ([C_2mim][OAc]). (B) 1-ethyl-3-methylimidazolium chloride ([C_2mim]Cl).

Deconstruction of lignocellulosic biomass is hampered by the high recalcitrance of lignocellulosic feedstock to chemicals or enzymes.[33] In the last decade, ILs have been examined and developed as potential solvents to improve the dissolution and deconstruction of cell walls. The dissolving power of certain ILs has been typically attributed to strong hydrogen-bonding interactions between the anion and equatorial hydroxyl group of cellulose.[6] Ludwig et al. reported that the ability of the anion to disrupt

the strong hydrogen bond network in cellulose highly determines the dissolution of cellulose in IL.[60] In addition, some of the cations were reported to have close interactions with the polysaccharides through hydrophobic interactions.[61] For example, Liu et al. revealed that the $[C_2mim]^+$ cation of [C_2mim][OAc] has close contact with cellulose by van der Waals interactions.[61] Besides the dissolution ability for polysaccharides, IL is a good solvent for lignin as well. In 2007, Pu and co-workers first demonstrated that up to 20 wt% of pine Kraft lignin could be dissolved in some imidazolium-based ILs.[62] The computational mechanistic model developed by Casas et al. revealed that the affinity of lignin for ILs highly depends on the anion.[63] Hydrogen bond is the main interaction between lignin and IL. Furthermore, Janesko applied dispersion-corrected density functional theory to simulate the interactions of [C_2mim]Cl with 1-(4-methoxyphenyl)-2-methoxyethanol as the model compound of lignin polyphenol, and revealed that both anions and cations determine the solubility of lignin in IL.[64] The lignin model compound has strong hydrogen bonding and π -stacking interactions with the $[C_2mim]^+$ cation.[64] Overall, these published data demonstrated both IL cation and anion play an important role in the dissolution of carbohydrates and lignin in IL.

The good deconstruction ability of some ILs for lignocellulosic biomass makes it possible to obtain major biopolymers as the starting materials to produce fuels, chemicals, and products. Imidazolium ILs, especially 1-ethyl-3-methylimidazolium acetate, have been applied to solubilize a wide range of lignocellulosic biomass and biopolymers due to its good dissolution abilities (Table 1.4). To produce bioethanol from cellulose, the Joint Bioenergy Institute (JBEI) developed approaches to pretreat lignocellulosic biomass and reduce the recalcitrance of cellulose for enzymes by imidazolium ILs at high temperature

Table 1.4 Biomass pretreatment and solubility in imidazolium ILs.

IL	Feedstock	Dissolution condition		Solubility	Ref.
		Temp. (°C)	Time (h)	(wt%)	
[AMIM]Cl	Norway spruce sawdust	110	8	8	[65]
[AMIM]Cl	Norway spruce sawdust	80	24	5	[65]
[BMIM]Cl	Norway spruce sawdust	110	8	8	[65]
[AMIM]Cl	Norway spruce TMP	130	8	7	[65]
[BMIM]Cl	Norway spruce TMP	130	8	7	[65]
[AMIM]Cl	Southern pine TMP	110	8	2	[65]
[AMIM]Cl	Southern pine TMP	130	8	5	[65]
[BMIM]Cl	Southern pine TMP	130	8	5	[65]
[BzMIM]Cl	Southern pine TMP	130	8	5	[65]
[BzMIM]Cl	Norway spruce TMP	130	8	5	[65]
[BMIM][Ac]	Miscanthus	130	>12	4	[66]
[BPy][Cl]	Miscanthus	130	>15	4	[66]
[BMIM][Cl]	Miscanthus	130	8	3	[66]
[EMIM][Cl]	Miscanthus	130	8-10	4	[66]
[BDMIM][Cl]	Miscanthus	130	10	3	[66]
[HEMIM][Cl]	Miscanthus	130	9	2	[66]
[MMIM][DMP]	Miscanthus	130	>15	4	[66]
[EMIM][DMP]	Miscanthus	130	>15	4	[66]
[BMIM][DMP]	Miscanthus	130	>15	3	[66]
[EMIM][$MeSO_4$]	Miscanthus	130	10-14	1.5	[66]
[EMIM][Ts]	Miscanthus	130	>12	1	[66]
[C_2mim][OAc]	Cellulose pulp	110	>12	15	[67]
[C_2mim][OAc]	Microcrystalline cellulose	25	>12	15	[68]
[C_2mim][OAc]	Xylan	25	>12	5	[68]

[AMIM]Cl: 1-allyl-3-methylimidazolium chloride
[BMIM][Cl]: 1-butyl-3-methylimidazolium
[BMIM][Ac]: 1-butyl-3-methylimidazolium acetate
[BMIM][Cl]: 1-butyl-3-methylimidazolium chloride
[BDMIM][Cl]: 1-butyl-2,3-dimethylimidazolium chloride
[MMIM][DMP]: 1-methyl-3-methylimidazolium dimethylphosphate
[EMIM][$MeSO_4$]: 1-ethyl-3-methylimidazolium methylsulfate
[EMIM][DMP]: 1-ethyl-3-methylimidazolium imethylphosphate
[C_2mim][OAc]: 1-ethyl-3-methylimidazolium acetate
[BMIM][DMP]: 1-butyl-3-methylimidazolium dimethylphosphate
[BzMIM]Cl: 1-benzyl-3-methylimidazolium chloride
[BPy][Cl]: N-butylpyridinium chloride
[EMIM][Cl]: 1-ethyl-3-methylimidazolium chloride
[HEMIM][Cl]: 1-hydroxyethyl-methylimidazolium chloride
[EMIM][Ts]: 1-ethyl-3-methylimidazolium tosylate

conditions.[69-76] A majority of the processes was conducted at the temperature above 100 °C and long reaction time, up to 24 h. These severe conditions contribute to a better dissolution of lignocellulosic biomass by the maximum removal of lignin and hemicellulose, therefore increasing cellulose accessibility (Table 1.4).

Recently, some novel ILs were developed and applied to pretreat lignocellulosic biomass. Jessop et al. of Queen's university first synthesized a switchable IL, $DBUH^+$ by DBU (1,8-diazabicyclo-[5.4.0]-undec-7-ene) and 1-hexanol with the exposure of CO_2.[77] This ionic liquid can be easily converted back to DBU and 1-hexanol by bubbling N_2 or argon. Considering this unique property, switchable IL may facilitate the solvent recovery. Anugwom et al. investigated the dissolution of spruce in $DBUH^+$ and revealed its effect of extracting high amount of hemicellulose and small percentage of lignin at 55 °C for 5 days.[78] More recently, Liszka et al. at JBEI developed another other class of switchable ILs based on di-carboxylic acids.[79] Of all of these new ILs, the pretreatment by choline glutamate (2 Choline : 1 Glutamate) at 120 °C for 3 h had the best pretreatment effect, and the enzymatic saccharification conversion could be achieved 90% by 72 h.[79] In addition, Aaron et al. at JBEI synthesized tertiary amine-based ILs from aromatic aldehydes derived from lignin and hemicellulose.[80] The enzymatic saccharification data showed that pretreated switchgrass with tertiary amine-based ILs had higher recalcitrance than the switchgrass treated with $[C_2mim][OAc]$.[80] While all these results showed the potential of novel ILs for reducing the recalcitrance of cellulose, these processes still could not efficiently utilize all the other major biopolymers, i.e. hemicellulose and lignin, of lignocellulosic biomass. To make biorefineries economically, each biopolymer of lignocellulosic biomass should be used to generate bioproducts.[52, 81]

Table 1.5 Pretreatment and fractionation of lignocellulosic biomass using ILs.

ILs	$[C_2mim][OAc]$	$[C_2mim][OAc]$	TBPH	MEA-DBU-SO_2
Feedstock	Wheat straw	Wheat straw	Poplar	Birch
Temperature (°C)	80	140	110	120
Time (h)	12	6	0.5	24
Cellulose rich fraction (Purity wt %)	64	91	53.1	56
Hemicellulose rich fraction (Purity wt %)	78	96	-	-
Lignin rich fraction (Purity wt %)	67	97	34.8	30.9
Alter lignin structure		Yes	Yes	Yes
Reference	[71]	[71]	[73]	[74]

Tetra-n-butylphosphonium hydroxide: TBPH
Monoethanol amine: MEA 1,8-diazabicyclo-[5.4.0]-undec-7-ene: DBU

To achieve this concept, some fractionation processes have been performed to separate biopolymers from lignocellulosic biomass (Table 1.5). The high severity of these processes resulted in the degradation of the biomass polymers, and a majority of these processes could only generate fractions with low purity. For instance, the fractionation process designed by An et al. showed that the purity of the carbohydrate-rich fraction was less than 70%.[82] Therefore, more investigations still need to be conducted for the complete and efficient ionic liquid fractionation of biomass into the high purity and yield biopolymer streams.

Besides being utilized to deconstruct biomass cell walls, IL has been explored as a chemical platform to convert biomass polymers to high-value materials. Lignocellulosic biomass aerogels were first investigated and prepared by Aaltonen and Jauhiainen in 2009.[83] Spruce wood was dissolved in 1-butyl-3-methylimidazolium chloride, coagulated from the solution by adding ethanol and finally dried and converted to aerogel by releasing supercritical CO_2.[83] Biomass-based aerogels were also prepared from a solution of *Trema*

orientalis wood flour in 1-allyl-3-methylimidazolium chloride and underwent cyclic freeze-thaw treatment.[84] Most recently, Chen et al. prepared biomass aerogels from a solution of bagasse in DMSO/LiCl.[85] The highest Brunauer-Emmett-Teller surface area and total pore volume of the aerogels were 185 m^2 /g and 0.46 cm^3 /g, respectively.[85] Also, lignocellulosic biomass IL solutions have been considered as a good material to spin fibers by wetting spinning, because biomass-IL solution has the advantage of easy acquisition compared with other bio-based materials for producing fibers, such as organosolv lignin and cellulose. Sun et al. reported that lignocellulosic biomass composite fibers were prepared directly from raw biomass/IL solution by a dry-jet wet spinning process.[86] The strength of fibers was correlated with the cellulose content. Higher cellulose content contributed to stronger fibers however the authors concluded that the mechanical properties of the resulting fibers needed to be further improved.

1.6.3 Deep eutectic solvents

Deep eutectic solvents (DESs) are a type of solvent with physical properties similar to ILs. DESs are normally cheaper than ILs since the synthesis and purification of DESs is normally more convenient.[87] Generally, DESs consist of two or more organic compounds that are capable of generating a new single liquid phase by self-association through hydrogen bond interactions between an organic salt (ammonium or phosphonium) and a hydrogen-bond donor such as an alcohol, acid or amide.[88, 89] The melting point of DESs is always much lower than each individual component. DESs have been investigated as potentially green solvents in chemical and biological applications.[90, 91] DESs also have been applied for the pretreatment and fractionation of lignocellulosic biomass. Gunny et al. demonstrated that cellulases can keep more than 90% of their activity in 10% (v/v) for

glycerol based DES and ethylene glycol based DES.[92] Recently, Kumar et al. studied the pretreatment of rice straw using natural DESs (lactic acid/betaine, lactic acid/choline chloride).[88] The best delignification effect was 68±4 mg/g by lactic acid/choline chloride at molar ratio of 5:1 at 60 °C for 12 h. However, the pretreated rice straw showed low cellulose conversion by saccharification (36.0±3.2 %). In addition, Jablonský et al. tested the delignification of wheat straw by choline chloride based DESs at 60 °C for 24 h, and showed that the DESs cannot selectively remove lignin from biomass.[93] Research on lignocellulosic biomass pretreatment by DES is still in its early stage. Much effort is needed to evaluate the feasibility of DES pretreatment on lignocellulosic biomass.

1.7 Introduction of rheological properties of lignocellulosic biomass in ionic liquid

In chemical engineering industry, the characterization and understanding the rheological properties of the polymer solution is very important for identifying processing conditions. Therefore, the characterization of rheological properties of biomass-ionic liquid system is a crucial prerequisite to successfully process biomass-IL solutions.

1.7.1 Rheology

Rheology has been defined as the science of deformation and flow of materials. The study of rheology emphasizes on the measurement of quantitative parameters that define how a material will deform as a function of force, time, and spatial orientation.[94] In Figure 1.11, the two planes are filled with liquid. The bottom one is fixed. The top one moves horizontally at constant speed U ($m \cdot s^{-1}$). F/A is the force per unit area resulting in the motion of the top plate.[95] For Newtonian liquids in simple shear flows we can write:

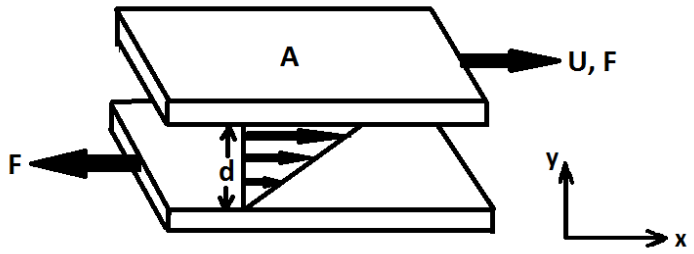

Figure 1.11 The upper plane moves with relative velocity *U*, and the lengths of the arrows between the planes are proportional to the local velocity v_x in the liquid. Reproduced from ref.[95]

$$\sigma = \eta \frac{\partial U}{\partial d} \tag{1.1}$$

where σ is the shear stress, with the unit Pa. The gradient of velocity ($\partial U/\partial d$) is known as the shear rate (sometimes also called velocity gradient or strain rate). The shear rate is calculated by dividing the velocity *U* ($m \cdot s^{-1}$) by the distance between the plates; *d* (m), thus its unit is reciprocal second (s^{-1}). The gradient of velocity makes each layer of fluid moves faster than the one below it. η (Pa·s) is the shear viscosity, which is a measure of the resistance of a fluid to gradual deformation by shear stress. Therefore, high viscosity liquids flow slowly and low viscosity liquids flowed quickly.

Polymer rheology depends on several dominant factors including intermolecular forces, degree of branching, molecular weight distribution, polymer concentration, solvent properties, as well as temperature and pressure.[96] Figure 1.12 shows the relationship between viscosity and shear rate of a polymer solution. In the low shear rate, the viscosity is high as a result of the complete entanglement of polymer chains. The viscosity gradually disappear because the polymers are completely aligned.[96]

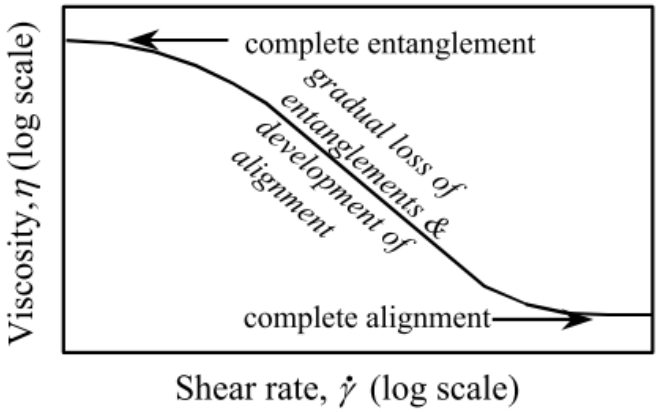

Figure 1.12 A flow curve for a polymer solution. Adapted from ref.[96]

1.7.2 Newtonian and non- Newtonian liquids

Viscosity is the most important rheological property in engineering calculations. If the measured viscosity η does not vary with shear rate or time, the liquid is defined as a Newtonian liquid. A Newtonian liquid is considered as an ideal liquid. A number of liquids have Newtonian behavior under a wide range of shear rates. The Navier–Stokes equation is used to describe the motion of a Newtonian liquid.[97] The general form of Navier–Stokes equation is described as follows:

$$\rho\left(\frac{\partial v}{\partial t} + v \cdot \nabla v\right) = -\nabla p + \nabla \mathbf{T} + f \qquad (1.2)$$

where: $\rho, v, P, \mathbf{T}$ and f are the fluid density, velocity, pressure, stress tensor, and body forces (per unit volume) respectively. The viscosity of Newtonian liquids varies with pressure and temperature. The higher pressure results in the increase of viscosity. In general, the viscosity of simple liquids decreases with increasing temperature. The relationship between viscosity and temperature can be explained by the following Andrade's equation:

$$log_{10}\eta = A + \frac{B}{T} \tag{1.3}$$

where, T is the absolute temperature (K), η is the viscosity (Pa·s), and A and B are structural parameters. Any liquid whose behavior cannot be characterized by the Navier-Stokes equations is called 'non-Newtonian liquid'. The viscosity of non-Newtonian varies with the shear rate. A number of liquids display a non-Newtonian liquid behavior, such as polymer solution, dispersions and emulsions. Non-Newtonian liquids can be summarized as “shear thinning” or “shear thickening” according to the relationship between viscosity and shear rate. Liquids are described as shear thinning if the viscosity decreases with increasing shear rate. For example, although silicone oils are commonly used as Newtonian standards, the viscosity of silicone oils (Figure 1.13) diminished when the shear rate was high enough. All liquids can become non-Newtonian when high sufficiently shear rate is applied.[96] Some liquids can reach 10^{-2} or 10^{-4} of the zero shear rate viscosity. The opposite situation is that the viscosity rises with an increase in shear rate. These liquids are called shear thickening liquids.

The flow curve of non-Newtonian liquids can be described by the Cross model,[96] which is named after Malcolm Cross:

$$\frac{\eta - \eta_\infty}{\eta_0 - \eta_\infty} = \frac{1}{1 + (K\gamma)^m} \tag{1.4}$$

where, K is the time in second (s), m is dimensionless, γ is the shear rate (s^{-1}).

At a very high shear rate, $\eta_0 \gg \eta_\infty$, and $K\gamma \gg 1$, thus the Cross model can be reduced to the Sisko equation:

$$\eta = \eta_\infty + \frac{\eta_0}{(K\gamma)^m} \tag{1.5}$$

In some conditions where $\eta_0 \gg \eta_\infty$, and $K\gamma \gg 1$, the Cross model is simplified to the power law model,

$$\eta = k\gamma^{n-1} \tag{1.6}$$

where, k is the flow consistency index (Pa·s^n); n is the flow behavior index (dimensionless). The power-law model is the most widely used model in engineering calculation since the model can provide good fit for a majority of liquids in the range of 1 to 10^3 s^{-1}.

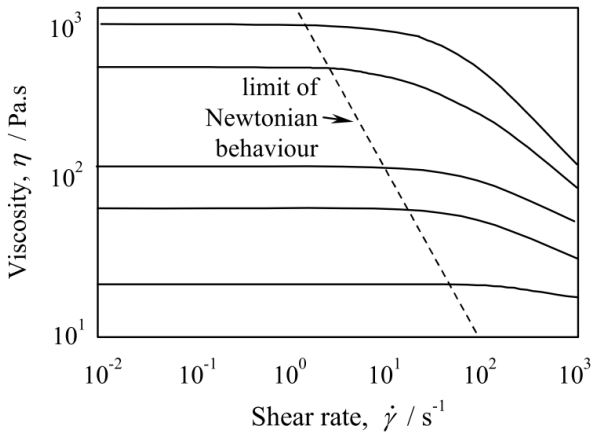

Figure 1.13 Viscosity behavior of a series of silicone oils versus shear rate. Adapted from ref.[96]

Shear thinning must be distinguished from thixotropy. Thixotropy is a decrease of viscosity with increasing time. The difference between the two situations —viscoelastic and thixotropic—is that in the linear viscoelastic region, the microstructure responds over a certain time scale without changing, while in thixotropy, the microstructure does change—by breaking down or building up—and such changes take time.

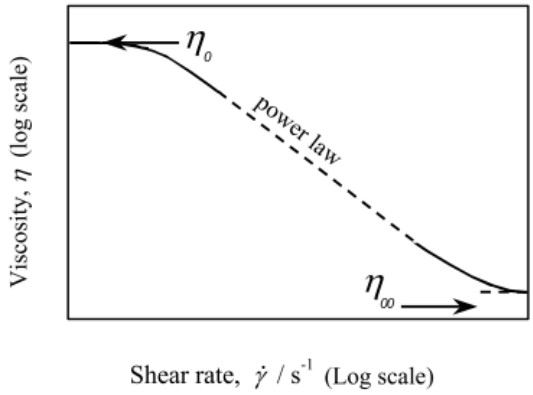

Figure 1.14 Definition diagram of the Cross model. Adapted from ref.[96]

1.7.3 Viscoelasticity

All structured liquids tend to keep their natural rest condition which is the lowest energy state. Therefore, deformed liquids always try to reproduce their rest condition. The phenomenon is like an extended or compressed spring, which was moved from the rest state, unextended length and tries to return to the static status. This kind of energy is the origin of elasticity in structured liquids. The material-generated stress due to any deformation follows Hooke's law:

$$\tau_{ij} = G\gamma_{ij} \tag{1.7}$$

where τ_{ij} is the material-general stress, G is the shear modulus and γ_{ij} is the deformation. Viscoelasticity is the property of materials that exhibit both viscous and elastic characteristics under deformation. The viscoelastic properties reflect structure and strength of polymer solution. If the body of a material is under a deformation as a result of an applied force, the body is said to be strained. In this situation, the chemical and physical structure or properties of the material may have new quantities. These materials properties are called

moduli.

In a simple shear deformation, the elastic modulus, G is calculated by the stress σ divided by the corresponding elastic strain Υ. The solid-like component at any particular frequency is described by the elastic modulus G', and the liquid-like response is characterized by the complementary viscous modulus G''.[98] The units of both these moduli are Pascal (Pa). If the elastic modulus of a material is lower than the viscous modulus, indicating that the material acts as a fluid. In contrast, if the viscous modulus is lower than the elastic modulus, the material behaves like a solid. The material in Figure 1.15 shows typical shear thinning behavior in the range of 0.05 to 10 Hz. In this condition, the elastic modulus is lower than the viscous modulus, indicating that the material behaves like a fluid.

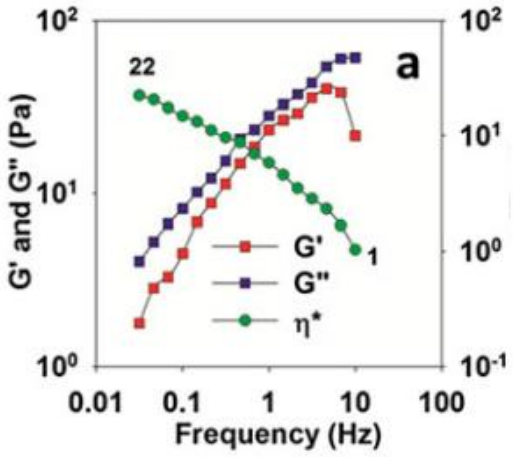

Figure 1.15 Storage modulus (G'), loss modulus (G'') and complex viscosity (η^*) of pretreated switchgrass slurries during frequency sweep from 0.01 to 10 Hz. Adapted from ref.[74]

1.7.4 Yield stress

Yield stress is a critical stress to describe the physical property of materials. The yield stress τ_y of a solid is the applied stress that must be exceeded in order to make the solid to first display a liquid behavior. The meaning of the verb 'to yield' would be 'to give way under pressure', which implies an abrupt and significant change in behavior to a less resistant state.[5] The viscosity of the material has significantly decreased when the shear stress exceeds 1 Pa (Figure 1.16). If the applied stress is below yield stress, only elastic behavior can take place. The yield stress of a liquid can be defined as when decreasing the applied stress, the liquid first shows a solid-like behavior. Yield stress can be obtained by measuring the elastic modulus with increasing strain amplitudes. However, it is difficult to determine exactly the value at which the behavior starts to change.[99]

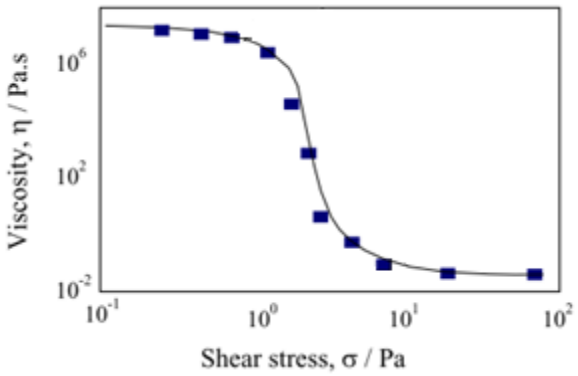

Figure 1.16 Flow curve of 10% suspension of Bentonite. Adapted and reproduced from ref.[96]

1.8 Rheological property of polymers in ILs

Novel applications of polymer-IL solution have been investigated, such as spinning fibers with dissolved biopolymers in IL,[100] formation of membranes,[101, 102] composite materials[103, 104] and synthesis of biopolymer derivatives.[105, 106] The characterization and understanding of rheological properties are a crucial prerequisite to successfully process the solution. Rheological properties, such as the apparent viscosity η and the yield stress τ_y, has been found to strongly depend on the particle size and the insoluble content.[107] The yield stress and the elastic modulus in the linear viscoelastic region increased dramatically with the insoluble polymer concentration.[107] Nunez et al. demonstrated that higher percentage of hyperbranched polymer, replacing linear polymers, reduced the viscosity of polymers in 1-methyl-2-pyrrolidinone solvent.[108]

IL has been recognized as an environmentally benign solvent to increase the dissolution of cellulose. There are a few reports on rheology studies of cellulose/IL solutions.[109-112] Sescousse et al. reported the viscosity of the complete dissolution of cellulose in imidazolium-based IL in 2010.[113] The viscosity of the cellulose-[C_2mim][OAc] solutions increases with cellulose concentration and decreases with temperature as it is expected for classical polymer solutions. 5% of cellulose-[C_2mim][OAc] had a Newtonian behavior at low shear rate from 0 to 100 °C.[101] The properties of a mixture of corn starch and cellulose in [C_2mim][OAc] were investigated in order to produce cellulose-starch films via wet casting.[101] Zero-shear rate viscosity plot indicated that there were no special interactions between the components since the mixture behaved as a simple summary of the two components. Yao et al. studied the rheological behavior of cellulose and silk fibroin blend in [BMIM][Cl].[114] The results revealed that

the viscosity and dynamic modulus of the blend solution decreased with increasing ratio of silk fibroin. The dispersion of cellulose and silk fibroin was improved at high shear rate since the dynamic modulus of the blend solution showed positive deviations for all cellulose/ silk fibroin blend ratios.

A prerequisite for spinning fiber from biomass/IL system is a fundamental understanding of the viscosity behavior and flow properties of lignocellulose in IL. The only publication related to the rheological properties of biomass in IL is from Gruz et al. in 2013.[74] In this paper, the impact of switchgrass loading in [C_2mim][OAc] was evaluated by measuring viscosity, chemical composition, cellulose crystallinity, saccharification kinetics, and sugar yield.[74] The rheological properties of different loading of switchgrass (3, 10, 20 and 30 wt%) in [C_2mim][OAc] were determined. In all loading conditions, the switchgrass/IL slurries displayed shear thinning behavior (the decrease of complex viscosity) in the range of 0.05 to 10 Hz. Higher loading enhanced shear thinning behavior, which can lead to a reduction in the viscosity by a two orders of magnitude. Thus, the shear thinning behavior can decrease the required power to mix the viscous pretreated switchgrass slurries, and also impact the design of the pumps, mixers and other equipment for the biomass pretreatment system.

In conclusion, many pretreatment and fractionation processes have been investigated to deconstruct lignocellulosic biomass, and reduce the recalcitrance of biomass for producing high value-added bioproducts. However, the entire and efficient utilization of lignocellulosic biomass is still challenging. In the following chapters, by improving biopolymer-ionic liquid interaction, a better process was explored to utilize each major lignocellulosic biopolymer. In the second chapter, the interactions of biopolymers of

lignocellulosic biomass with IL were increased through an autohydrolysis step. By the enhanced interactions between biopolymers and IL, the complete dissolution of lignocellulosic biomass was achieved, and biomass films were produced from biomass-IL solution in the third chapter. Considering the low recalcitrance of biomass after autohydrolysis and ionic liquid activation, a biomass fractionation process was designed to produce carbohydrates and lignin fractions with high yield and purity in the fourth chapter.

1.9 References

1. Mosier, N., et al., *Features of promising technologies for pretreatment of lignocellulosic biomass.* Bioresource technology, 2005. 96(6): p. 673-686.
2. Lin, Y. and S. Tanaka, *Ethanol fermentation from biomass resources: current state and prospects.* Appl Microbiol Biotechnol, 2006. 69(6): p. 627-42.
3. EPA, *EPA Proposes Renewable Fuel Standards for 2014, 2015, and 2016, and the Biomass-Based Diesel Volume for 2017.* 2015.
4. Lee, H., S. Hamid, and S. Zain, *Conversion of lignocellulosic biomass to nanocellulose: structure and chemical process.* The Scientific World Journal, 2014. 2014.
5. Barnes, H.A., *The yield stress—a review or 'παντα ρει'—everything flows?* Journal of Non-Newtonian Fluid Mechanics, 1999. 81(1): p. 133-178.
6. Brandt, A., et al., *Deconstruction of lignocellulosic biomass with ionic liquids.* Green Chemistry, 2013.
7. O'SULLIVAN, A.C., *Cellulose: the structure slowly unravels.* Cellulose, 1997(4): p. 173-207.
8. Mariko Ago, T.E.a.T.H., *Crystalline transformation of native cellulose from cellulose I to cellulose II polymorph by a ball-milling method with a specific amount of water.* Cellulose, 2004(11): p. 163-167.
9. Kumar, S., et al., *Cellulose pretreatment in subcritical water: effect of temperature on molecular structure and enzymatic reactivity.* Bioresour Technol, 2010. 101(4): p. 1337-47.
10. Brandt, A., et al., *Deconstruction of lignocellulosic biomass with ionic liquids.* Green chemistry, 2013. 15(3): p. 550-583.
11. Wang, H., G. Gurau, and R.D. Rogers, *Ionic liquid processing of cellulose.* Chemical Society Reviews, 2012. 41(4): p. 1519-1537.
12. Timell, T., *Recent progress in the chemistry of wood hemicelluloses.* Wood Science and Technology, 1967. 1(1): p. 45-70.
13. Hartley, R.D. and C.W. Ford, *Phenolic constituents of plant cell walls and wall biodegradability.* Plant cell wall polymers, biogenesis and biodegradation, 1989. 399: p. 137-145.
14. DOE., U.S., *Breaking the Biological Barriers to Cellulosic Ethanol: A Joint Research Agenda.* DOE/SC/EE-0095, U.S. Department of Energy Office of Science and Office of Energy Efficiency and Renewable Energy, 2006.
15. Wyman, C.E., et al., *Hydrolysis of cellulose and hemicellulose.* Polysaccharides: Structural diversity and functional versatility, 2005. 1: p. 1023-1062.
16. Biely, P., J. Puls, and H. Schneider, *Acetyl xylan esterases in fungal cellulolytic systems.* FEBS letters, 1985. 186(1): p. 80-84.
17. Labbé, N., et al., *Activation of lignocellulosic biomass by ionic liquid for biorefinery fractionation.* Bioresource Technology, 2012. 104: p. 701-707.
18. K. GROHMANN, D.J.M., 1 M. E. HIMMEL, B. E. DALE, AND H. A. SCHROEDER *The Role of Ester Groups in Resistance of Plant Cell Wall Polysaccharides to Enzymatic Hydrolysis* Applied Biochemistry and Biotechnology, 1989. 20: p. 45-61.

19. Boerjan, W., J. Ralph, and M. Baucher, *Lignin biosynthesis.* Annual review of plant biology, 2003. 54(1): p. 519-546.
20. Ralph, J., et al., *Lignins: natural polymers from oxidative coupling of 4-hydroxyphenyl-propanoids.* Phytochemistry Reviews, 2004. 3(1-2): p. 29-60.
21. Björkman, A., *Studies on finely divided wood. Part 1. Extraction of lignin with neutral solvents.* Svensk papperstidning, 1956. 59(13): p. 477-485.
22. Santos, R.B., et al., *Lignin structural variation in hardwood species.* Journal of Agricultural and Food Chemistry, 2012. 60(19): p. 4923-4930.
23. Landucci, L.L., S.A. Ralph, and K.E. Hammel, *13C NMR characterization of guaiacyl, guaiacyl/syringyl and syringyl dehydrogenation polymers.* Holzforschung, 1998. 52(2): p. 160-170.
24. Kanitskaya, L.V., et al., *1H and 13C NMR study of lignin structure.* Polymer Science - Series A, 1997. 39(6): p. 634-640.
25. Holtman, K.M., et al., *Quantitative 13C NMR characterization of milled wood lignins isolated by different milling techniques.* Journal of Wood Chemistry and Technology, 2006. 26(1): p. 21-34.
26. Balakshin, M.Y., et al., *NMR studies on Fraser fir Abies fraseri (Pursh) Poir. lignins.* Holzforschung, 2005. 59(5): p. 488-496.
27. Chen, C.L., *Characterization of Milled Wood Lignins and Dehydrogenative Polymerisates from Monolignols by Carbon-13 NMR Spectroscopy*. 1998. p. 255-275.
28. Nimz, H., et al., *Carbon-13 NMR spectra of lignins, 10.1 Comparison of structural units in spruce and beech lignin.* Journal of wood chemistry and technology, 1984. 4(3): p. 265-284.
29. Ikeda, T., et al., *Studies on the effect of ball milling on lignin structure using a modified DFRC method.* Journal of agricultural and food chemistry, 2002. 50(1): p. 129-135.
30. Mao, J., et al., *Differences between lignin in unprocessed wood, milled wood, mutant wood, and extracted lignin detected by 13C solid-state NMR.* Journal of agricultural and food chemistry, 2006. 54(26): p. 9677-9686.
31. Jeffries, T.W., *Biodegradation of lignin and hemicelluloses,* in *Biochemistry of microbial degradation*. 1994, Springer. p. 233-277.
32. Guerra, A., et al., *Toward a better understanding of the lignin isolation process from wood.* Journal of agricultural and food chemistry, 2006. 54(16): p. 5939-5947.
33. Himmel, M.E., et al., *Biomass recalcitrance: engineering plants and enzymes for biofuels production.* Science, 2007. 315(5813): p. 804-7.
34. Bussemaker, M.J. and D.K. Zhang, *Effect of Ultrasound on Lignocellulosic Biomass as a Pretreatment for Biorefinery and Biofuel Applications.* Industrial & Engineering Chemistry Research, 2013. 52(10): p. 3563-3580.
35. Langan, P., et al., *Common processes drive the thermochemical pretreatment of lignocellulosic biomass.* Green Chemistry, 2014. 16(1): p. 63-68.
36. Kumar, P., et al., *Methods for pretreatment of lignocellulosic biomass for efficient hydrolysis and biofuel production.* Industrial & Engineering Chemistry Research, 2009. 48(8): p. 3713-3729.
37. Freeman, M., *PPI International Fact and Price Book.* Pulp Paper Int.: San Francisco, CA, 1997.

38. Holladay, J., et al., *Top value-added chemicals from biomass.* DOE Report PNNL, 2007. 16983.
39. Chakar, F.S. and A.J. Ragauskas, *Review of current and future softwood kraft lignin process chemistry.* Industrial Crops and Products, 2004. 20(2): p. 131-141.
40. Huber, G.W., S. Iborra, and A. Corma, *Synthesis of transportation fuels from biomass: chemistry, catalysts, and engineering.* Chemical reviews, 2006. 106(9): p. 4044-4098.
41. Gierer, J., *Chemical aspects of kraft pulping.* Wood Science and Technology, 1980. 14(4): p. 241-266.
42. Hu, F. and A. Ragauskas, *Pretreatment and lignocellulosic chemistry.* Bioenergy Research, 2012. 5(4): p. 1043-1066.
43. Yang, B. and C.E. Wyman, *Pretreatment: the key to unlocking low-cost cellulosic ethanol.* Biofuels, Bioproducts and Biorefining, 2008. 2(1): p. 26-40.
44. Shi, J., et al., *Impact of pretreatment technologies on saccharification and isopentenol fermentation of mixed lignocellulosic feedstocks.* BioEnergy Research, 2015. 8(3): p. 1004-1013.
45. Um, B.-H., M.N. Karim, and L.L. Henk, *Effect of sulfuric and phosphoric acid pretreatments on enzymatic hydrolysis of corn stover*, in *Biotechnology for Fuels and Chemicals*. 2003, Springer. p. 115-125.
46. Jönsson, L.J. and C. Martín, *Pretreatment of lignocellulose: Formation of inhibitory by-products and strategies for minimizing their effects.* Bioresource technology, 2016. 199: p. 103-112.
47. Bozell, J.J., et al., *Solvent fractionation of renewable woody feedstocks: Organosolv generation of biorefinery process streams for the production of biobased chemicals.* Biomass and Bioenergy, 2011. 35(10): p. 4197-4208.
48. Varanasi, P., et al., *Survey of renewable chemicals produced from lignocellulosic biomass during ionic liquid pretreatment.* Biotechnology for biofuels, 2013. 6(1): p. 1-9.
49. Sun, N., et al., *Where are ionic liquid strategies most suited in the pursuit of chemicals and energy from lignocellulosic biomass?* Chemical Communications, 2011. 47(5): p. 1405-1421.
50. Bozell, J.J. and G.R. Petersen, *Technology development for the production of biobased products from biorefinery carbohydrates—the US Department of Energy's "Top 10" revisited.* Green Chemistry, 2010. 12(4): p. 539.
51. Bozell, J.J., *Feedstocks for the Future - Biorefinery Production of Chemicals from Renewable Carbon.* CLEAN - Soil, Air, Water, 2008. 36(8): p. 641-647.
52. Bozell, J.J., *An evolution from pretreatment to fractionation will enable successful development of the integrated biorefinery.* BioResources, 2010. 5(3): p. 1326-1327.
53. Pan, X., et al., *Biorefining of softwoods using ethanol organosolv pulping: preliminary evaluation of process streams for manufacture of fuel-grade ethanol and co-products.* Biotechnology and bioengineering, 2005. 90(4): p. 473-481.
54. Zhao, X., K. Cheng, and D. Liu, *Organosolv pretreatment of lignocellulosic biomass for enzymatic hydrolysis.* Applied microbiology and biotechnology, 2009. 82(5): p. 815-827.

55. Holtzapple, M.T. and A.E. Humphrey, *The effect of organosolv pretreatment on the enzymatic hydrolysis of poplar.* Biotechnology and bioengineering, 1984. 26(7): p. 670-676.
56. Black, S.K., B.R. Hames, and M.D. Myers, *Method of separating lignocellulosic material into lignin, cellulose and dissolved sugars*. 1998, Google Patents.
57. Fadhel, A.Z., et al., *Novel solvents for sustainable production of specialty chemicals.* Annual review of chemical and biomolecular engineering, 2011. 2: p. 189-210.
58. Liu, J., G. Jiang, and J.Å. Jönsson, *Application of ionic liquids in analytical chemistry.* TrAC Trends in Analytical Chemistry, 2005. 24(1): p. 20-27.
59. Lee, S.H., et al., *Ionic Liquid-Mediated Selective Extraction of Lignin From Wood Leading to Enhanced Enzymatic Cellulose Hydrolysis.* Biotechnology and Bioengineering, 2009. 102(5): p. 1368-1376.
60. Papanyan, Z., et al., *Understanding the dissolution of polyols by ionic liquids using the example of a well-defined model compound.* Chemphyschem, 2011. 12(13): p. 2400-4.
61. Hanbin Liu, K.L.S., Bradley M. Holmes, Blake A. Simmons,and and S. Singh, *Understanding the Interactions of Cellulose with Ionic Liquids: A Molecular Dynamics Study.* The Journal of Physical Chemistry B, 2010. 114(12): p. 4293-4301.
62. Pu, Y., N. Jiang, and A.J. Ragauskas, *Ionic Liquid as a Green Solvent for Lignin.* Journal of Wood Chemistry and Technology, 2007. 27(1): p. 23-33.
63. Casas, A., et al., *Comparison of lignin and cellulose solubilities in ionic liquids by COSMO-RS analysis and experimental validation.* Industrial Crops and Products, 2012. 37(1): p. 155-163.
64. Janesko, B.G., *Modeling interactions between lignocellulose and ionic liquids using DFT-D.* Phys Chem Chem Phys, 2011. 13(23): p. 11393-401.
65. Kilpelainen, I., et al., *Dissolution of wood in ionic liquids.* Journal of Agricultural and Food Chemistry, 2007. 55(22): p. 9142-9148.
66. Padmanabhan, S., et al., *Solubility and rate of dissolution for Miscanthus in hydrophilic ionic liquids.* Fluid Phase Equilibria, 2011. 309(1): p. 89-96.
67. Zhao, H., et al., *Designing enzyme-compatible ionic liquids that can dissolve carbohydrates.* Green chemistry, 2008. 10(6): p. 696-705.
68. Castro, M.C., et al., *Mixtures of Ethanol and the Ionic Liquid 1-Ethyl-3-methylimidazolium Acetate for the Fractionated Solubility of Biopolymers of Lignocellulosic Biomass.* Industrial & Engineering Chemistry Research, 2014. 53(29): p. 11850-11861.
69. Singh, S., B.A. Simmons, and K.P. Vogel, *Visualization of biomass solubilization and cellulose regeneration during ionic liquid pretreatment of switchgrass.* Biotechnology and Bioengineering, 2009. 104(1): p. 68-75.
70. Li, C., et al., *Comparison of dilute acid and ionic liquid pretreatment of switchgrass: biomass recalcitrance, delignification and enzymatic saccharification.* Bioresource technology, 2010. 101(13): p. 4900-4906.
71. Cheng, G., et al., *Transition of cellulose crystalline structure and surface morphology of biomass as a function of ionic liquid pretreatment and its relation to enzymatic hydrolysis.* Biomacromolecules, 2011. 12(4): p. 933-941.

72. Dibble, D.C., et al., *A facile method for the recovery of ionic liquid and lignin from biomass pretreatment.* Green Chemistry, 2011. 13(11): p. 3255-3264.
73. Cheng, G., et al., *Impact of ionic liquid pretreatment conditions on cellulose crystalline structure using 1-ethyl-3-methylimidazolium acetate.* The Journal of Physical Chemistry B, 2012. 116(33): p. 10049-10054.
74. Cruz, A.G., et al., *Impact of high biomass loading on ionic liquid pretreatment.* Biotechnology for biofuels, 2013. 6(1): p. 1-10.
75. Li, C., et al., *Scale-up and evaluation of high solid ionic liquid pretreatment and enzymatic hydrolysis of switchgrass.* Biotechnology for biofuels, 2013. 6(1): p. 1.
76. Shi, J., et al., *One-pot ionic liquid pretreatment and saccharification of switchgrass.* Green Chemistry, 2013. 15(9): p. 2579-2589.
77. Jessop, P., et al., *A reversible ionic/non-ionic switchable solvent.* Nature, 2005. 436: p. 1102.
78. Anugwom, I., et al., *Switchable Ionic Liquids as Delignification Solvents for Lignocellulosic Materials.* ChemSusChem, 2014. 7(4): p. 1170-1176.
79. Liszka, M.J., et al., *Switchable ionic liquids based on di-carboxylic acids for one-pot conversion of biomass to an advanced biofuel.* Green Chemistry, 2016.
80. Socha, A.M., et al., *Efficient biomass pretreatment using ionic liquids derived from lignin and hemicellulose.* Proceedings of the National Academy of Sciences, 2014. 111(35): p. E3587-E3595.
81. Bozell, J.J., *Feedstocks for the future–biorefinery production of chemicals from renewable carbon.* CLEAN–Soil, Air, Water, 2008. 36(8): p. 641-647.
82. An, Y.-X., et al., *Pretreatment of lignocellulosic biomass with renewable cholinium ionic liquids: Biomass fractionation, enzymatic digestion and ionic liquid reuse.* Bioresource technology, 2015. 192: p. 165-171.
83. Aaltonen, O. and O. Jauhiainen, *The preparation of lignocellulosic aerogels from ionic liquid solutions.* Carbohydrate Polymers, 2009. 75(1): p. 125-129.
84. Li, J., et al., *Lignocellulose aerogel from wood-ionic liquid solution (1-allyl-3-methylimidazolium chloride) under freezing and thawing conditions.* Biomacromolecules, 2011. 12(5): p. 1860-7.
85. Chen, M., et al., *Direct preparation of green and renewable aerogel materials from crude bagasse.* Cellulose, 2016. 23(2): p. 1325-1334.
86. Sun, N., et al., *Composite fibers spun directly from solutions of raw lignocellulosic biomass dissolved in ionic liquids.* Green Chemistry, 2011. 13(5): p. 1158-1161.
87. Vigier, K.D.O., G. Chatel, and F. Jérôme, *Contribution of deep eutectic solvents for biomass processing: Opportunities, challenges, and limitations.* ChemCatChem, 2015. 7(8): p. 1250-1260.
88. Kumar, A.K., B.S. Parikh, and M. Pravakar, *Natural deep eutectic solvent mediated pretreatment of rice straw: bioanalytical characterization of lignin extract and enzymatic hydrolysis of pretreated biomass residue.* Environmental Science and Pollution Research, 2015: p. 1-11.
89. Durand, E., *Deep eutectic solvents.* 2013.
90. Choi, Y.H., et al., *Are natural deep eutectic solvents the missing link in understanding cellular metabolism and physiology?* Plant physiology, 2011. 156(4): p. 1701-1705.

91. Huang, Z.L., et al., *Deep eutectic solvents can be viable enzyme activators and stabilizers.* Journal of Chemical Technology and Biotechnology, 2014. 89(12): p. 1975-1981.
92. Gunny, A.A.N., et al., *Applicability evaluation of Deep Eutectic Solvents–Cellulase system for lignocellulose hydrolysis.* Bioresource technology, 2015. 181: p. 297-302.
93. Jablonský, M., et al., *Deep Eutectic Solvents: Fractionation of Wheat Straw.* BioResources, 2015. 10(4): p. 8039-8047.
94. Janmey, P.A. and M. Schliwa, *Rheology.* Current biology: CB, 2008. 18(15): p. R639.
95. Barnes, H.A., J.F. Hutton, and K. Walters, *An introduction to rheology*. Vol. 3. 1989: Elsevier.
96. Barnes, H.A., *A handbook of elementary rheology.* 2000.
97. Batchelor, G.K., *An introduction to fluid dynamics*. 2000: Cambridge university press.
98. Barnes, H.A., *A Handbook of Elementary Rheology Institute of Non-Newtonian Fluid Mechanics.* University of Wales, 2000.
99. Dullaert, K. and J. Mewis, *A structural kinetics model for thixotropy.* Journal of non-newtonian fluid mechanics, 2006. 139(1): p. 21-30.
100. Yao, Y.B., et al., *Study on the temperature-induced sol-gel transition of cellulose/silk fibroin blends in 1-butyl-3-methylimidazolium chloride via rheological behavior.* Cellulose, 2014. 21(5): p. 3737-3743.
101. Liu, W. and T. Budtova, *Ionic liquid: a powerful solvent for homogeneous starch–cellulose mixing and making films with tuned morphology.* Polymer, 2012. 53(25): p. 5779-5787.
102. Carlin, R.T. and J. Fuller, *Ionic liquid–polymer gel catalytic membrane.* Chemical Communications, 1997(15): p. 1345-1346.
103. Snedden, P., et al., *Cross-linked polymer-ionic liquid composite materials.* Macromolecules, 2003. 36(12): p. 4549-4556.
104. Simmons, T.J., et al., *Preparation of synthetic wood composites using ionic liquids.* Wood Science and Technology, 2011. 45(4): p. 719-733.
105. Kubisa, P., *Application of ionic liquids as solvents for polymerization processes.* Progress in Polymer Science, 2004. 29(1): p. 3-12.
106. Carmichael, A.J., et al., *Copper (I) mediated living radical polymerisation in an ionic liquid.* Chemical Communications, 2000(14): p. 1237-1238.
107. Wiman, M., et al., *Rheological characterization of dilute acid pretreated softwood.* Biotechnology and bioengineering, 2011. 108(5): p. 1031-1041.
108. Chen, X., et al., *Solution rheology of cellulose in 1-butyl-3-methyl imidazolium chloride.* Journal of Rheology, 2011. 55(3): p. 485-494.
109. Sharma, M., et al., *Dissolution of alpha-chitin in deep eutectic solvents.* Rsc Advances, 2013. 3(39): p. 18149-18155.
110. Zhang, Y., et al., *Green chemical preparation of cellulose/high performance elastomer blend fibers by melt-spinning method.* Journal of Polymer Research, 2013. 20(6).
111. Horinaka, J., et al., *Entanglement network of chitin and chitosan in ionic liquid solutions.* Journal of Applied Polymer Science, 2013. 130(4): p. 2439-2443.

112. Trivedi, T.J., K.S. Rao, and A. Kumar, *Facile preparation of agarose-chitosan hybrid materials and nanocomposite ionogels using an ionic liquid via dissolution, regeneration and sol-gel transition.* Green Chemistry, 2014. 16(1): p. 320-330.
113. Sescousse, R., et al., *Viscosity of cellulose− imidazolium-based ionic liquid solutions.* The Journal of Physical Chemistry B, 2010. 114(21): p. 7222-7228.
114. Yao, Y.B., et al., *Rheological behavior of cellulose/silk fibroin blend solutions with ionic liquid as solvent.* Cellulose, 2014. 21(1): p. 675-684.

CHAPTER TWO

IMPACTS OF AUTOHYDROLYSIS ON BIOMASS DISSOLUTION IN IONIC LIQUID

The cell wall architecture of biomass restricts the penetration of chemicals and enzymes into the cellulosic microfibrils. In this chapter, an autohydrolysis step prior to an ionic liquid activation was explored to hydrolyze a portion of hemicellulose, disrupt the lignin-hemicellulose coating on cellulosic fibrils of lignocellulosic biomass, and further improve the interactions between biopolymers with IL.

This chapter entitled "**Impacts of autohydrolysis on biomass dissolution in ionic liquid**" with the co-authors of Jing Wang, Jingming Tao, David Harper, Amit K. Naskar, Timothy Rials, and Nicole Labbé was submitted to the journal of ***Biomass & Bioenergy*** on June 10, 2016. Jing Wang performed the experiment, conducted the data analysis, and drafted the manuscript. Dr. Tao performed the chemical composition analysis of switchgrass samples. Dr. Harper participated in the design and performance of rheological property measurements, and data interpretation. Nicole Labbé designed the experiments, assisted in data analysis and writing the manuscript. All authors contributed to the manuscript revision and approved the final version of the manuscript.

2.1 Abstract

The partial removal of hemicellulose by hot water, i.e. autohydrolysis of biomass was investigated to improve the dissolution of biomass in an IL system. Higher amount of autohydrolyzed switchgrass was found to dissolve in [C_2mim][OAc]. In addition, the dissolution behavior of the biomass samples extracted under various severities was evaluated by monitoring the viscosity of the biomass-IL solutions over time for three different temperatures. The model of the dissolution data evidenced that the autohydrolysis severity was the major contributor for the improved biomass dissolution. Time-dependent viscosity data followed a power law model, which indicated a diffusion controlled

dissolution of the biomass in IL. Autohydrolysis greatly enhanced the dissolution rate as observed by a sharp rise in solution viscosity and led to nearly complete dissolution of the biomass at high severity.

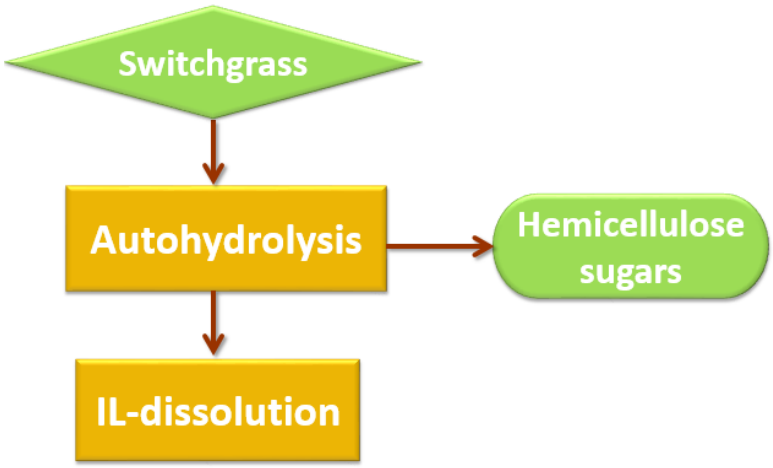

Figure 2.1 Abstract graphic.

2.2 Introduction

Dissolution and further separation of major components of lignocellulosic biomass are hampered by the complex assembly of dissimilar polymers comprising the plant cell wall of lignocellulosic feedstock.[1] In the last decade, ILs have been investigated and developed as potential solvents to improve solubility, pretreatment, and fractionation of lignocellulosic biomass. Fort and co-workers were the first to report that woody biomass such as pine (*Pinus*), poplar (*Populus*), eucalyptus (*Eucalyptus*), and oak (*Quercus*) partially dissolved in 1-n-butyl-3-methylimidazolium chloride.[2] Soon after, Kilpeläinen's group demonstrated that both hardwoods and softwoods, were readily soluble in various

imidazolium-based ILs likely due to improved interaction of the aromatic character of the cation in IL with the lignin in the wood.[3] More recently, Li et al. reported that the synergistic effect of cations and anions of ILs contribute to the decrease of cellulose crystallinity and its dissolution in ionic liquid.[4] Nevertheless, the dissolution ability of certain ILs for lignocellulosic biomass makes it possible to obtain biomass major components as the starting materials to generate fuels, chemicals, and products.

Most IL biomass pretreatments are conducted at temperatures above 100 ^{o}C.[5, 6] High pretreatment temperature and long-time contribute to access to the cellulosic fraction of lignocellulosic biomass by solubilizing and removing part of the lignin and hemicellulose. These high severity pretreatment processes generally focus on maximizing lignin and hemicellulose removal while minimizing cellulose modification/degradation to generate C6 sugars for biofuel production.[6, 7] Under these conditions, the other two major components of lignocellulosic biomass, lignin and hemicellulose, are not fully utilized, as they are partially degraded. In addition, high temperatures processing can result in IL degradation which can inhibit the recovery and reuse of IL. Li et al. estimated that 15% of [C_2mim][OAc] was degraded when heated at 185 °C for 10 min.[8] The dealkylation of the ethyl group occurred.[8] More recently, several studies have proposed new or improved methods to fractionate biomass in an attempt to generate lignin, cellulose, and hemicellulose rich-fractions.[9, 10] However, these methods still have limitations in generating high purity streams of each biomass major component. Access to clean fractions is necessary for biorefineries to be viable and sustainable, allowing the integrated production of high-value chemicals and high volume commodity fuels from each biomass component.[11]

Labbé et al. have shown that under low severities (mild temperature, a few hours), [C_2mim][OAc] activates biomass with minimal degradation and provides a less recalcitrant biomass than raw biomass.[12] However, a complete disruption of the physical entanglements and covalent linkages between the biopolymers was not achieved when dissolving switchgrass in IL without degradation of each biopolymer.[13] On the other hand, xylan (a major component of hemicellulose) has lower solubility than lignin and cellulose in ILs.[14, 15] Therefore, an autohydrolysis step, also called hydrothermal or hot water pretreatment, prior to IL treatment is a plausible approach to improve the dissolution of lignocellulosic biomass in IL by partially extracting hemicellulose and breaking the interconnected network of biopolymers. Autohydrolysis of biomass is a semi-selective extraction process with reported temperatures ranging from 120 to 230 °C.[16] During the process, hydronium ions, generated by water autoionization, act as a catalyst and primarily attack the acetyl groups present in hemicellulose and lignin, generating acetic acid that further hydrolyzes hemicellulose. Under mild conditions, a large fraction of hemicellulose is hydrolyzed into mono- and oligosaccharides without significant degradation of lignin and cellulose.[17] When compared to other approaches such as dilute acid and alkaline pre-hydrolysis which degrade high amount of lignin and cellulose, the approach produces a stream containing mainly hemicellulose-derived sugars.[18] Most recently, Deb et al. reported that autohydrolysis can facilitate wood chips dissolution in IL.[19] However, no kinetic analysis was provided for the dissolution process.

The kinetics of dissolution of biomass components in IL and the rate and magnitude of viscosity development are key factors in assessing the quality and performance of the system. Moreover, the compositional and structural changes that biomass undergoes during

IL pretreatment have been shown to alter the rheology of biomass/IL slurries.[20] The rheological properties of lignocellulosic biomass in IL could be monitored by the viscosity behavior and flow properties of the system.[20] Ultimately, the viscosity of biomass-IL solutions will play an important role during handling, dissolution, and further processing.

Therefore, the aim of our study was to evaluate the impacts of various autohydrolysis severities on the dissolution behavior of switchgrass in [C_2mim][OAc]. In addition to determining the amount of biomass that dissolved in the IL under three different temperatures, Fourier transform infrared (FT-IR) spectroscopy was used to compare the chemical characteristics of the IL-insoluble biomass fraction and estimate if the dissolution was specific to carbohydrates or lignin. The dissolution behavior of the biomass was investigated by rheology and the collected viscosity-time trend lines were fitted by a power law to compare the impacts of autohydrolysis severity on the dissolution rate of switchgrass in [C_2mim][OAc]. To the best of our knowledge, this is the first report on time dependent viscosity to monitor biomass dissolution in an IL. Favorable conditions for enhanced dissolution rate of biomass could increase mass throughput for appropriate processing, end use, and logistics associated with bulk handling of biomass. Results presented in this study will enable development of biomass-derived value-added products and their readymade high density feedstock.

2.3 Materials and Methods

2.3.1 Materials

Switchgrass (Panicum virgatum "*ALAMO*" variety) was obtained from a Tennessee farm managed by the University of Tennessee Biofuels Initiative. The biomass was

harvested in May 2013, air-dried, chopped, and milled with a Wiley mill (Thomas Scientific, Model # 3383-L10, Swedesboro, NJ) to a particle size of 40 mesh (0.425 mm). The biomass powder was extracted in an Accelerated Solvent Extractor (ASE 350, Dionex, Sunnyvale, CA) to remove non-structural compounds (i.e. extractives) according to the method described in the National Renewable Energy Laboratory (NREL) Analytical Procedure "Determination of Extractives in Biomass". In brief, powdered biomass (approximatively 7 g) and glass beads (3 mm diameter, 40 g) were added to a 66 mL extraction cell and sequentially extracted with water and ethanol under 1500 psi, at 100 °C, for 7 min static time, and three static cycles. The wet extractives-free switchgrass was then oven dried at 40 °C until constant moisture content (less than 10% by weight).

The IL [C_2mim][OAc] (purum≥95%) was purchased from Iolitec Inc. (Tuscaloosa, AL) and used without further purification. Dimethyl sulfoxide (DMSO) (99.9%) was purchased from Sigma-Aldrich (St. Louis, MO). Deionized (DI) water was employed throughout the experiments.

2.3.2 Autohydrolysis

Autohydrolysis was carried out in a Dionex ASE 350 accelerated solvent extractor (approximately 8.5:1 water-to-dry biomass ratio) at two temperature levels (140 and 160 °C) and three static time levels (20, 40, and 60 min). Extractives-free switchgrass (5 g) and glass beads (3 mm diameter, 40 g) were placed in a 66 mL extraction cell and autohydrolysis extraction was performed with DI water at 1500 psi, at selected temperature and time. Each extraction condition was performed in triplicate. The hydrolyzate was drained from the cell and the remaining solid switchgrass was rinsed with 100% cell volume DI water to displace the extract in the cell after autohydrolysis. The final mass ratio

of hydrolyzate to dry biomass was about 22:1. The extracted switchgrass was oven dried at 40 °C until a constant moisture content was reached (less than 10% by weight). The chemical composition of the biomass after autohydrolysis and extractives-free switchgrass (the control), was determined in three replicates according to the method described in NREL Analytical Procedure "Determination of Structural Carbohydrates and Lignin in Biomass".[21] The acid-soluble lignin content in the hydrolyzates was measured at 205 nm using a dual-beam Lambda 650 series spectrophotometer (PerkinElmer). The hydrolyzates were also analyzed for hydrolyzed sugars by high performance liquid chromatography using the NREL protocol "Determination of Sugars, By-products, and Degradation Products in Liquid Fraction Process Samples".[22] The severity of the autohydrolysis was determined by the extraction temperature and time. These parameters can be combined to a single factor, R_0, to allow comparison of the various extractions[23]:

$$R_0 = t \times \exp\left(\frac{T_H - T_R}{14.75}\right) \tag{2.1}$$

where *t* represents extraction time in minutes; T_H is the extraction temperature in °C; T_R is the reference temperature (100 °C); $\log R_0$ is used to describe the autohydrolysis severity.[24, 25]

2.3.3 Dissolution of switchgrass in [C_2mim][OAc]

The effect of autohydrolysis on the dissolution of switchgrass in [C_2mim][OAc] was assessed by measuring the percentage of dissolution of switchgrass in [C_2mim][OAc] at 60, 80, and 100 °C after 3 h following a published method.[26] In each dissolution trial, biomass powder (0.35 g) was added to ionic liquid (9.65 g) in a 20 mL vial. The vial was placed on a heating/mixing plate at specific temperature for 3 h with a 600 rpm magnetic

stirring. After three hours, 10 mL of DMSO were added to each vial to decrease the viscosity of the mixture and facilitate the filtration step. The solution was well mixed by vigorous vortexing for about 1 min. The remaining solid residue, insoluble fraction, was separated from the solution by centrifuge and vacuum filtration, washed with DMSO (at least 30 mL) to remove any dissolved substances, and further washed with DI water to remove any IL traces, then dried at 105 °C for 24 h. The percent of biomass dissolved was calculated according to the following equation:

$$\text{Biomass dissolved (\%)} = \frac{m_{original} - m_{residue}}{m_{original}} \times 100 \qquad (2.2)$$

where $m_{original}$ represents the oven-dry weight of switchgrass sample prior to the dissolution, and $m_{residue}$ is the oven-dry weight of remaining solid residue after 3 h. Each experiment was performed in duplicate.

2.3.4 FT-IR characterization of the IL-insoluble fraction

FT-IR spectra were collected on the IL-insoluble fraction using a Perkin–Elmer Spectrum One FT-IR spectrometer (Waltham, MA) equipped with an attenuated total reflectance (ATR) accessory with 8 scans at 4 cm^{-1} resolution over the range of 4000-650 cm^{-1}. The samples included switchgrass after autohydrolysis and remaining solid residues (insoluble fraction) after the IL dissolution experiment. Three spectra were collected for each replicate. ATR correction and normalization procedures were performed in the Spectrum One software.

In order to estimate the ratio of lignin to carbohydrates, the ratio of intensity of characteristic absorbance of lignin (1509 cm^{-1}) against a carbohydrates band (1375 cm^{-1})

was calculated.[27] The peak at 1509 cm^{-1} is attributed to aromatic skeletal vibration (C=C stretching vibration) in lignin while the band at 1375 cm^{-1} (C-H bending vibration in cellulose and hemicellulose) is purely due to carbohydrates.

To clearly delineate the effects of autohydrolysis severity and dissolution conditions on the chemical features of the remaining solid switchgrass residues, principal component analysis (PCA), a multivariate technique, was performed on the FT-IR spectra using The Unscrambler statistical software 9.0 (CAMO Software Inc., Woodbridge, NJ). A full multiplicative scatter correction prior to PCA was performed to compensate for additive and/or multiplicative effects in the spectral data, thus reducing interference effects. More detailed information about PCA principle has been reported in our previous published paper.[12]

2.3.5 X-ray Diffraction of IL-insoluble fraction

Autohydrolyzed switchgrass (160 °C for 60 min) and the remaining solid residues treated in [C_2mim][OAc] at 60, 80 and 100 °C were placed on a low-background quartz holder and measured using a PANalytical Empyrean X-ray diffractometer (PANalytical Inc., Westborough, MA) with a Cu tube (λ ¼ 1.5405 Å). The radiation was generated at 40 mA and 45 kV. A step size of 0.01° exposure was used for measuring the scattering angle 2θ in the range 9–41°. Cellulose I appears with at main peak at 22.5° and a secondary peak at 16°.[28] Cellulose I can be converted into cellulose II by IL treatment and regeneration processes with a main peak as a doublet around at 20.0° and 21.9°, and a secondary peak at 12.1°.[28] According to the Scherrer equation, the full width at half-maximum (FWHM) is inversely proportional to crystallite size.[29] FWHM of the peak at 22.5° calculated by

PANalytical Data Viewer Software was used to reveal the impact of dissolution temperature on the crystallite size or misalignment of crystals of the remaining residuals.

2.3.6 Rheological property measurements

The viscosity of the autohydrolyzed switchgrass samples in IL at 60, 80, and 100 °C was monitored over a three hours period. These conditions were the same as those used for the dissolution of switchgrass in [C_2mim][OAc]. Biomass powder (0.09 g) was added to [C_2mim][OAc] (2.41 g) in 20 mL vial. The vial was placed on a mixing plate for 1 min with magnetic stirring at 1000 rpm. The 3.5 wt% biomass-IL mixture was then loaded onto a Peltier temperature-controlled plate of a controlled stress rheometer (TA Instruments AR-G2). Silicon oil and a plate cover were used to avoid biomass-IL absorbing water during the measurement. The viscosity of each sample was measured at shear rate of 100 s^{-1}, determined by finding the linear region in a variable rate experiment, using 40 mm diameter cylindrical plates with a gap of 1000 μm. This testing methodology was employed to simulate the shear mixing used to homogenize the biomass and IL solution. The viscosity data were collected every 10 s for 3 h at selected temperature to monitor the viscosity changes during the dissolution process. Duplicate experiments were performed for each sample and condition.

Microsoft Excel was used to fit a power law regression to the viscosity-time data. This analysis allows the dependence of switchgrass/IL viscosity on temperature and time to be evaluated.

2.4 Results and Discussion

2.4.1 Autohydrolysis of lignocellulosic biomass

A severity factor which encompasses for the temperature and the time that the autohydrolysis was performed was used to evaluate the level of the treatment. As reported in the literature, adequate severity of hot water extraction is an effective way to produce high sugars yields from various lignocellulosic biomass types.[30] Extractives-free switchgrass was extracted with severity varying from 2.48 to 3.54 with the expectation that more hemicellulose will be released in the form of monosugars with higher severity. Mass recovery of switchgrass after autohydrolysis, chemical composition of the extracted switchgrass, and soluble lignin content in the hydrolyzates are presented in Table 2.1. Predictably, the percentage of recovered biomass decreased as the severity increased. The lowest mass recovery was about 72% at the highest severity of 3.54 (160 °C for 60 min). The amount of soluble lignin in the hydrolyzates increased with severity from 2.4 to 22.6% of the total lignin (20.8%) present in the starting material (i.e. extractives-free switchgrass). More acid soluble lignin was extracted and solubilized at higher severity, confirming that high temperature not only induces the hydrolysis of hemicellulose, but also partially delignifies the biomass. The high performance liquid chromatography analysis of the hydrolyzates confirmed the removal of hemicellulose with high concentration of xylose (4.0 mg/mL) and arabinose (2.0 mg/mL) under high severity 3.54 (160 °C for 60 min); however, cellobiose and glucose were not detected (data not shown) indicating that cellulose was not hydrolyzed during the extraction.

The chemical composition of switchgrass after the hot water treatment did not change dramatically until the severity reached 3.37. Hemicellulose content then decreased from

32.4 to 27.7% at severity 3.37 (160 °C for 40 min) and to 23.7% at the highest severity 3.54 (160 °C for 60 min). Cellulose content increased from 41.8 to 47.7% with severity (from 2.48 to 3.54). Lignin content in all autohydrolyzed samples was essentially constant, while hemicellulose and cellulose content was inversely correlated as severity increased above 3.

Table 2.1 Chemical composition (% on dry basis) of switchgrass, mass recovery, and soluble lignin content in hydrolyzates in function of autohydrolysis severity.

Temp. [˚C]	Time [min]	Severity	Chemical composition [%]				Mass Recovery	Soluble lignin
			[C]	[H]	[L]	[A]	[%]	[%]
Extractives free		-	41.8 (0.5)	32.4 (0.3)	20.8 (0.3)	1.4 (0.1)	–	–
140	20	2.48	39.9 (0.3)	31.2 (0.2)	22.6 (0.2)	1.0 (0.1)	96.1 (0.1)	2.4 (0.1)
140	40	2.78	41.1 (0.4)	31.7 (0.1)	22.6 (0.5)	0.8 (0.1)	94.9 (0.1)	5.3 (0.0)
140	60	2.96	40.4 (0.3)	30.6 (0.1)	22.3 (0.7)	0.7 (0.1)	93.1 (1.0)	6.3 (0.2)
160	20	3.07	40.8 (0.2)	30.4 (0.1)	22.1 (0.2)	0.8 (0.0)	90.2 (0.1)	9.1 (0.1)
160	40	3.37	45.9 (0.7)	27.7 (0.2)	22.4 (0.4)	0.7 (0.0)	80.3 (0.6)	14.4 (0.2)
160	60	3.54	47.7 (0.1)	23.7 (0.1)	22.6 (0.2)	0.7 (0.1)	71.9 (0.1)	22.6 (0.0)

[C]: cellulose. [H]: hemicellulose. [L]; lignin. [A]: Ash.

As expected, the mild autohydrolysis conditions employed in this study partially hydrolyzed the hemicellulose present in switchgrass with minor to no removal of lignin and cellulose, respectively.

2.4.2 Dissolution of autohydrolyzed biomass in [C_2mim][OAc]

Recent studies have shown that high temperature (e.g. above 110 °C) contributes to greater dissolution of biomass in IL; however, high temperature often results in the

degradation of biomass components and IL.[31] Previous work by Labbé et. al. demonstrated that biomass can be activated in [C_2mim][OAc] with minimal degradation under mild conditions (60 °C and 80 °C).[12] Wang and co-workers have reported that switchgrass was completely dissolved in [C_2mim][OAc] without degradation of IL and biomass components at 110 °C for 44 h.[13] Based on these findings, mild temperatures (60, 80, and 100 °C) were chosen to evaluate the dissolution of autohydrolyzed switchgrass in [C_2mim][OAc]. In our previous work, we also demonstrated that 3 hours were sufficient to significantly reduce the recalcitrance of lignocellulosic biomass in [C_2mim][OAc], therefore our dissolution experiments were performed for 3 hours.[12] Short dissolution time also minimizes the degradation of lignocellulosic biomass components.

The dissolution data and profile at a specific temperature versus the autohydrolysis severity are presented in Figure 2.2. Higher dissolution was achieved with elevated severity and IL dissolution temperature. At dissolution temperature of 60 °C, the amount of biomass dissolved was 29.2% for switchgrass autohydrolyzed at a severity of 3.54 (160 °C for 60 min), increasing the percentage of dissolution by a factor of 8 when compared to that of the control (3.8% at 60 °C). Similar trends were obtained at higher IL dissolution temperatures (80 and 100 °C). The highest dissolution (73.3%) was reached with switchgrass autohydrolyzed at severity of 3.54 (160 °C for 60 min) under IL dissolution temperature of 100 °C. The largest increment in dissolution occurred for switchgrass samples that were autohydrolyzed at severity between 3.07 (160 °C for 20 min) and 3.37 (160 °C for 40 min). Overall, these data showed that the dissolution of switchgrass significantly improved in [C_2mim][OAc] when the biomass was subjected to a mild autohydrolysis prior to the IL dissolution step.

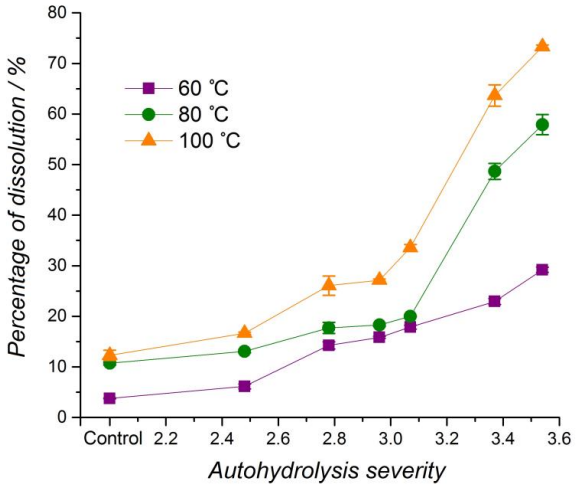

Figure 2.2 Dissolution of switchgrass autohydrolyzed under different autohydrolysis severities in [C_2mim][OAc] at 60, 80, and 100 °C for 3 h. The ″Control″ is the starting extractives-free switchgrass material.

The improved dissolution is mainly attributed to reasons associated with the chemical, physical, and architectural changes that the biomass underwent during autohydrolysis. First, the lower hemicellulose content of biomass after the treatment may contribute to enhanced dissolution because xylan has lower solubility than lignin and cellulose in ILs.[14, 15] Secondly, the partial removal of hemicellulose cleaves lignin-carbohydrates bonds and changes the architecture of cell walls, which subsequently improves the accessibility of biomass components to IL. By reducing the amount of hemicellulose, IL interactions with cellulose and lignin are improved. Third, the biomass surface area is increased during autohydrolysis. Indeed, Xiao et al. demonstrated that the surface of biomass particles suffered serious structural breakdown and had some apparent cracks with hot water pretreatment at 120 °C for 3 h, positively impacting the diffusion of IL and dissolution of biomass.[17] By removing a fraction of hemicellulose, autohydrolysis disrupts the integration of cellulose, hemicellulose, and lignin within the cell wall and their associations

with one another, which effectively contributed to switchgrass dissolution in [C_2mim][OAc].

2.4.3 FT-IR characterization of IL-insoluble fraction

The solid fraction of autohydrolyzed switchgrass (160 °C for 60 min) that remained after the 3 hour IL dissolution step was isolated and characterized by FT-IR. FT-IR spectra indicated that all residues still contained functional groups associated with the three constituents of the initial biomass (Figure 2.3a). While the band at 1030 cm^{-1} arises from C-O-C stretching vibration in cellulose, hemicellulose, and lignin, the band at 1160 cm^{-1} is due to C-O-C asymmetric valence vibration in cellulose and hemicellulose and the bands 1509 and 1610 cm^{-1} are associated to C=C stretching vibration of benzene ring in lignin, respectively. The ratio of lignin and carbohydrates (L/C) was calculated from the intensity of two bands (1509/1375 cm^{-1}; 1375 cm^{-1} originates from CH bending vibration in cellulose and hemicellulose). As shown in Table 2.2, little variation existed in L/C (1.1-1.3) in the material (control) after autohydrolysis (prior to IL dissolution), which was consistent with the chemical composition data (Table 2.1). Interestingly, it is worth noticing that L/C increased in the residues that were autohydrolyzed at high severity conditions, particularly for dissolution study at lower temperature. For example, after 3 hours in IL at 60 °C, the L/C ratio of autohydrolyzed switchgrass at severity of 2.48 was 1.2 and 1.6 for severity of 3.54, respectively. At higher temperature dissolution, all residues showed similar L/C although slightly higher than that was observed in residues from low temperature dissolution. This suggests solvation of relative fraction of cellulose increased with higher autohydrolysis severity and IL dissolution temperature. Although at higher temperature fewer residues were left, relative higher L/C dominated in those residues (even for the

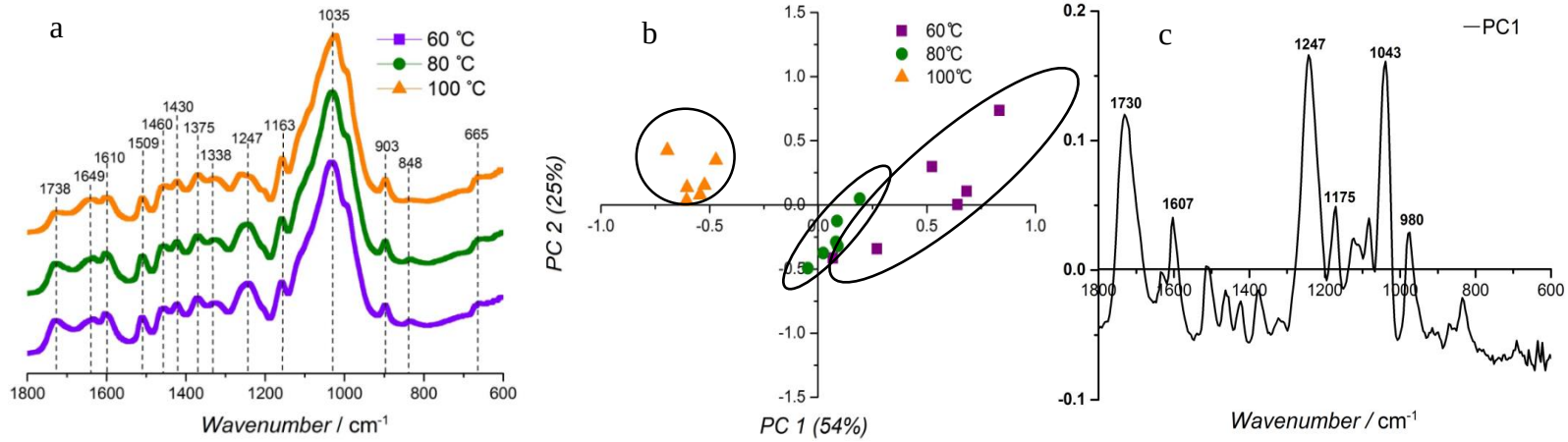

Figure 2.3 (a): FT-IR spectra of remaining solid residues of switchgrass after autohydrolysis at 160 °C for 60 min from 60, 80, and 100 °C (b): PCA scores plot of remaining solid residues of switchgrass after autohydrolysis at 160 °C for 60 min from 60, 80, and 100 °C (c): Loadings plots for PC1.

control; 1.5 at 100 °C versus 1.2 at 60 °C). This particular observation was further substantiated using the rheology data on the switchgrass solution in IL.

To estimate the overall impacts of IL dissolution temperature, principal component analysis (PCA) was performed on the FT-IR spectra collected on the solid residues. The resulting scores and loadings plots are shown in Figure 2.3b and c, respectively. While the 60 and 80 °C samples overlapped in the positive quadrant of PC1, the 100 °C samples clustered in the negative quadrant of PC1. The loadings plot of PC1 (Figure 2.3c) indicated three positive intense bands at 1730 cm^{-1} (C=O stretching vibration in acetyl groups in hemicellulose and lignin), 1247 cm^{-1} (C-O stretch in xylan), 1043 cm^{-1} (C-O stretching vibration in cellulose and hemicellulose), that were mostly responsible for the separation. The classification demonstrated that IL temperature impacted the dissolution of each component and that the residues of samples subjected to high dissolution temperature contained lower amount of carbohydrates.

Table 2.2 Lignin carbohydrates ratio of switchgrass samples and IL-insoluble fraction.

Temp. [°C]	Time [min]	Autohydrolysis severity	Lignin/ Carbohydrates Ratio			
			Control[a]	60 °C	80 °C	100 °C
Extractives free		–	1.2 (0.0)	1.2 (0.1)	1.3 (0.0)	1.5 (0.0)
140	20	2.48	1.2 (0.1)	1.2 (0.1)	1.3 (0.1)	1.5 (0.1)
140	40	2.78	1.1 (0.1)	1.2 (0.0)	1.3 (0.0)	1.5 (0.1)
140	60	2.96	1.2 (0.1)	1.3 (0.0)	1.4 (0.0)	1.6 (0.0)
160	20	3.07	1.2 (0.0)	1.3 (0.0)	1.3 (0.0)	1.6 (0.1)
160	40	3.37	1.3 (0.1)	1.4 (0.0)	1.5 (0.0)	1.6 (0.0)
160	60	3.54	1.3 (0.1)	1.6 (0.1)	1.7 (0.1)	1.6 (0.0)

[a] "Control" Lignin/carbohydrates ratio of switchgrass after autohydrolysis before IL treatment.

[b] ( ): Standard deviation

2.4.4 XRD measurements of IL-insoluble fraction

To visualize the changes of cellulose structure in the remaining solid residues of switchgrass, the XRD patterns are plotted in Figure 2.4. Autohydrolyzed switchgrass has a main peak at 22.3°. For residues generated at 60, 80 and 100 °C, the main peak at 22.3° disappeared and shifted to 20.8°. The shift of the peak towards lower 2θ angles suggests the swelling of cellulose I lattice through the biomass dissolution of regeneration processes.[28, 32] Moreover, the secondary peak at 16° became a broad shoulder and the small peak at 34.8° appeared vanishingly small. The reduction of peak intensity indicates that the arrangement of cellulose chains was disturbed by [C_2mim][OAc].[28, 32] There is no evident peak at 12.1° (the secondary peak of cellulose II), suggesting that the low content or the

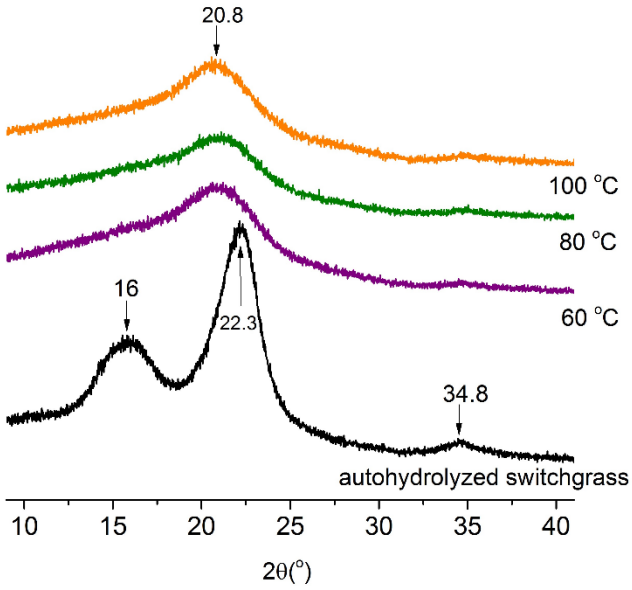

Figure 2.4 XRD patterns of autohydrolyzed switchgrass (160 °C for 60 min) and the remaining solid residues (IL-insoluble fraction) treated in [C_2mim][OAc] at 60, 80 and 100 °C.

nonexistence of cellulose II. In addition to the changes of peak positions, the main peak width changes as well. The FWHM of the main peak (at 20.8°) of all residues decreases from 6.6 (60 °C), 6.5 (80 °C) to 5.9 (100 °C). This indicates that residues treated at 100 °C have higher crystalline order of cellulose lattice than those residues treated at 60 and 80 °C. The phenomenon can be explained by the assumption that higher IL treatment temperature depolymerizes cellulose chains with lower molecular weight and those smaller chains are more easily recrystallized by adding water as anti-solvent.[28, 32]

2.4.5 Rheological properties of autohydrolyzed switchgrass in [C_2mim][OAc]

The viscosity-time curves of autohydrolyzed switchgrass samples were collected at 60, 80 and 100 °C as shown in Figure 2.5. Viscosity increased with time and temperature. The cell wall polymers were assumed to be all in the glassy state at the start of the rheology experiment.[33] Thus, it was hypothesized that the dissolution of the biomass was dominated by diffusion of the IL solvent into the cell wall prior to swelling of polymer chains followed by disentanglement and dissolution in the bulk of IL. A clear response difference existed in viscosity between samples that were subjected to low and high severity. For all biomass samples, the viscosity increased as more polymer went into solution. Figure 2.5a, c and e show the viscosity profiles for switchgrass samples extracted at low severities while Figure 2.5 b, d and f represent samples generated under higher severity. Visual comparison of the profiles suggests that the differences may result from an inherent increase in the porosity with treatment severity. After 3 h, the viscosity of samples dissolved at 60 °C ranged from 0.0755 to 2.6105 Pa·s. After the same dissolution time, the viscosity increased from 0.0927 to 2.7070 Pa·s and from 0.1417 to 3.1740 Pa·s, at 80 °C, and 100 °C, respectively. At each of these three temperatures, the viscosity of switchgrass after autohydrolysis at

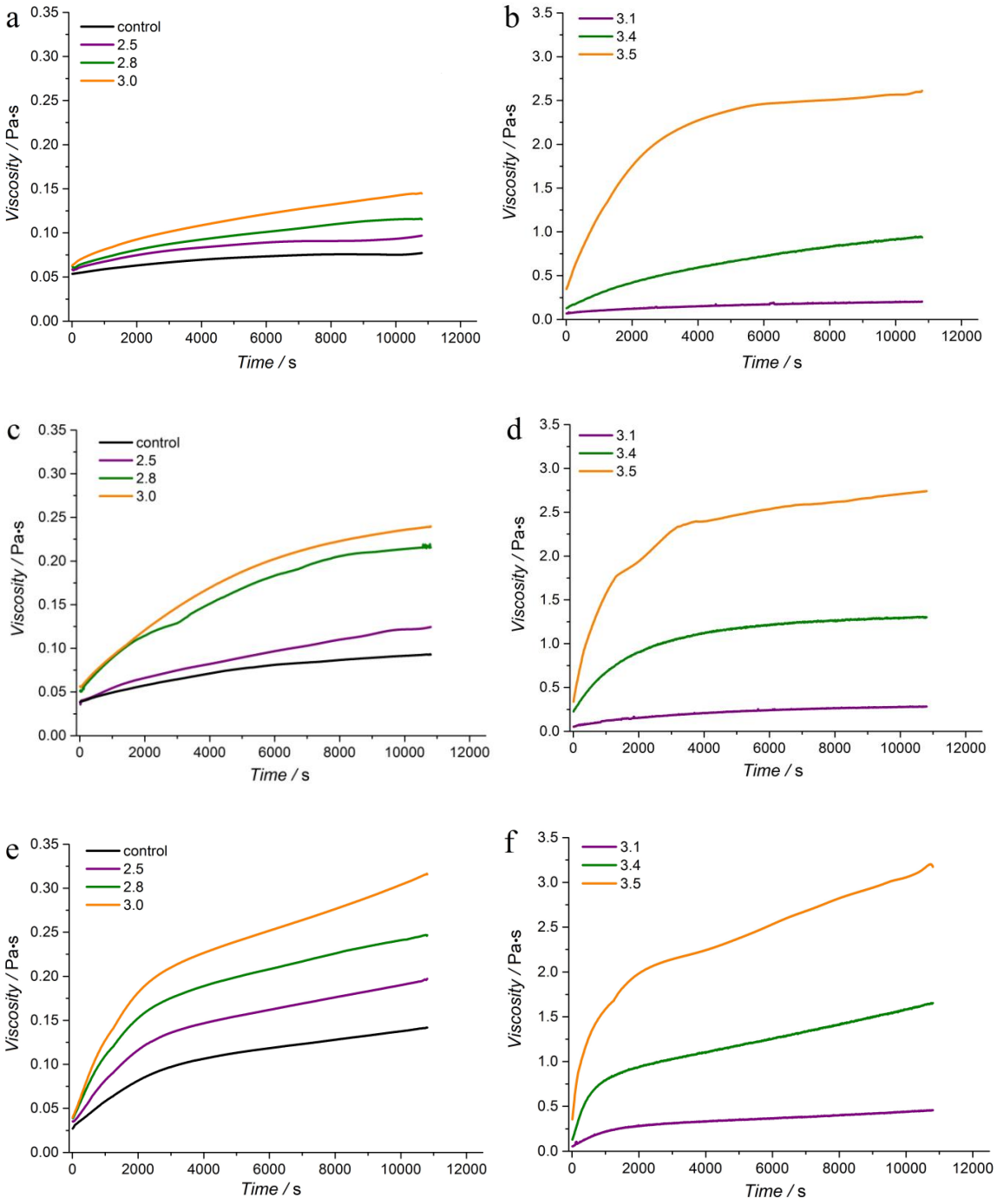

Figure 2.5 The rheological behavior of switchgrass after autohydrolysis at varying severity in [C_2mim][OAc] during 3 h and temperature (a), (b): 60 °C (c), (d): 80 °C (e), (f): 100 °C. [a] ″Control″ is extractives-free switchgrass.

highest severity 3.54 (160 °C for 60 min) was at least 15 times higher than that of switchgrass extracted at the mildest severity 2.48 (140 °C for 20 min). The control (with no hot water treatment) had the lowest viscosity and highest amount of undissolved material. As previously observed, these results confirmed that autohydrolysis enhanced the dissolution of switchgrass in [C_2mim][OAc].

A phenomenological approach was adopted to model the dissolution process as described by Ueberreiter.[34] In this case, the polymer(s) is infiltrated by a solvent resulting in its swelling, which creates a gel layer of the polymer in the rubbery state. The polymer in this gel layer is then able to disentangle and go into solution resulting in an increase in viscosity. Thus, the measured viscosity rise is a secondary result of IL diffusion that is only feasible if cell wall polymers are accessible and then soluble. A power law regression $\eta = Kt^n$ was used to fit the viscosity-time data by minimization of the sum of squares (R-squared), which describes the goodness of fit. Most R^2 values (Table 2.3) were higher than 0.9 indicating that the power law regression accurately described the viscosity data. Moreover, the regression for higher temperature conditions was consistently better, as reflected by the higher correlation coefficient.

The solute (lignocellulosic biomass after autohydrolysis) was assumed as a spherical rigid body as a simple approximation. Therefore, a first order Huggins equation describes the impact of solute concentration (φ) on the solution viscosity (η) [35]:

$$\eta = \eta_s(1 + [\eta]\varphi) \tag{2.3}$$

where φ here is the mass concentration with units of gram per deciliter (g/dL), $[\eta]$ is the intrinsic viscosity with units of deciliter per gram (dL/g) and η_s is the solvent viscosity (Pa·s). The value of η is proportional to the concentration of polymer in IL. Both the

Table 2.3 Power regression for rheological behavior at 60, 80, and 100 °C.

Temp	Time	Severity	60 °C			80 °C			100 °C		
[°C]	[min]		*K*	*n*	R^2	*K*	*n*	R^2	*K*	*n*	R^2
Extractives free		-	0.0320	0.0941	0.924	0.0115	0.2224	0.931	0.0061	0.3405	0.969
140	20	2.48	0.0314	0.1181	0.949	0.0079	0.2886	0.927	0.0078	0.3497	0.964
140	40	2.78	0.0245	0.1637	0.927	0.0087	0.3462	0.950	0.0109	0.3401	0.968
140	60	2.96	0.0227	0.1935	0.925	0.0087	0.3581	0.959	0.0101	0.3719	0.969
160	20	3.07	0.0194	0.2499	0.958	0.0107	0.3552	0.980	0.0197	0.3390	0.972
160	40	3.37	0.0155	0.4404	0.976	0.0784	0.3126	0.958	0.0675	0.3403	0.971
160	60	3.54	0.1160	0.3480	0.923	0.1984	0.2922	0.926	0.2292	0.2796	0.972

Fickian and non-Fickian diffusion process could be described by a power law approximation as follows[36]:

$$\frac{M_t}{M_\infty} = kt^n \tag{2.4}$$

M_t and M_∞ here are the mass that dissolved into the solvent at time t and infinite time, respectively. Equation 4 also holds for mass concentration, because of the fixed solvent volume:

$$\frac{M_t}{M_\infty} = \frac{[\eta]\varphi_t}{[\eta]\varphi_\infty} = kt^n \tag{2.5}$$

Thus we have:

$$1 + [\eta]\varphi_t = kt^n[\eta]\varphi_\infty + 1 \tag{2.6}$$

The viscosity of the system could be calculated via combining equation 3 and equation 6:

$$\eta = \eta_s(1 + [\eta]\varphi) = \eta_s(kt^n[\eta]\varphi_\infty + 1) \tag{2.7}$$

At a very early the first term on the right ($kt^n[\eta]\varphi_\infty$) can be ignored, where the startup viscosity is the solvent viscosity. After a threshold is reached, concentration and time dominate the system viscosity. The factor k is given by the Fickian diffusion: $k = (4D/\pi L^2)^{1/2}$, where D is the diffusion coefficient and L is the time dependent, therefore, equation 2.7 can be simplified into $\eta = Kt^n$, where $K = \eta_s \cdot k[\eta]\varphi_\infty$.

The *K*-values were quite similar for the "140 °C" series for 60 °C, 80 °C, and 100 °C treatment, but changed significantly in the "160 °C" series (see Table 2.3 and Figure 2.6) a dramatic increase in *K* and thus *D* was observed for the samples that were subjected to an autohydrolysis at severity 3.37 (160 °C for 40 min) or 3.54 (160 °C for 60 min). The results indicated that the cell wall architecture of lignocellulosic biomass was not

significantly disrupted under low autohydrolysis severity. The temperature at which the viscosity was measured also impacted *K* to a lesser extent. Nevertheless, switchgrass after autohydrolysis at severity 3.54 (160 ^{o}C for 60 min) had the viscosity of 0.1160 Pa·s at 60 °C, 0.1984 Pa·s at 80 °C, and 0.2292 Pa·s at 100 °C. The benefit of higher dissolution temperature was only achieved after prior autohydrolysis at high severity.

The exponent *n* was not significantly affected by the severity of the pretreatment, as observed in Figure 2.6 where it remained below 0.5 indicating that it is influenced mainly by geometry. The control system showed the lowest n value at each dissolution temperature, suggesting a large difference in surface area between the samples. The largest increase of biomass dissolution in IL was achieved by enhancing the autohydrolysis severity, not by increasing dissolution temperature. Simple viscosity data at different time (Figure 2.5) shows that viscosity rise nearly levels off at 4000 s of dissolution time at lower dissolution temperature. At higher dissolution temperature, viscosities for all samples show marching curve irrespective of degree of autohydrolysis severity. This indicates accelerated swelling, disentanglement and dissolution of biomass at higher temperatures. Compared to crystalline cellulose segments, amorphous lignin phase likely undergoes rapid dissolution at early stage and at longer time and higher temperature dissolution of cellulose dominates. Autohydrolysis pretreatment severity further enhances dissolution of cellulose component.

In the future higher loadings of biomass after autohydrolysis in IL will be tested since higher loadings would be an attractive route to decrease pretreatment cost and improve the profitability of biorefineries.[20] The higher loadings of biomass and increase in dissolution produced a concentrated polymer in the gel state. A comprehensive rheological characterization of biomass after autohydrolysis in IL coupled with light scattering to

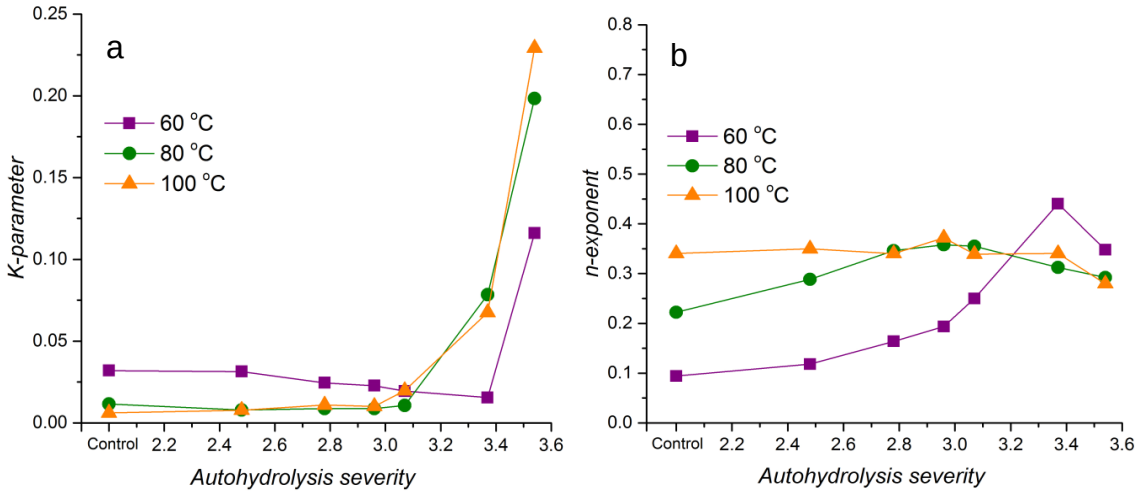

Figure 2.6 (a): *K* parameter of power regression for rheological behavior at 60, 80, and 100 °C vs. autohydrolysis severity (b): *n*-exponent of power regression for rheological behavior at 60, 80, and 100 °C vs. autohydrolysis severity. [a] ″Control″ is extractives-free switchgrass.

observe the effect of hot water extraction and x-ray diffraction on the architecture of biomass in solution will be carried out to develop a better understanding of biomass dissolution in IL.

2.5 Conclusion

A mild autohydrolysis enhanced the dissolution of the resulting switchgrass in [C_2mim][OAc]. The amount of dissolved biomass increased by a factor of 8 with the highest severity treatment (160 °C for 60 min). The power law regression provided an accurate description of the viscosity-time trend lines. The pre-exponential *K*-value strongly correlated with dissolution rate in [C_2mim][OAc] and disruption of cell wall architecture. For this system, the largest benefit to dissolution of biomass was achieved by increasing the severity of autohydrolysis.

2.6 References

1. Himmel, M.E., et al., *Biomass recalcitrance: engineering plants and enzymes for biofuels production.* science, 2007. 315(5813): p. 804-807.
2. Fort, D.A., et al., *Can ionic liquids dissolve wood? Processing and analysis of lignocellulosic materials with 1-n-butyl-3-methylimidazolium chloride.* Green Chemistry, 2007. 9(1): p. 63-69.
3. Kilpeläinen, I., et al., *Dissolution of wood in ionic liquids.* Journal of Agricultural and Food Chemistry, 2007. 55(22): p. 9142-9148.
4. Li, Y., et al., *Dissolving process of a cellulose bunch in ionic liquids: a molecular dynamics study.* Physical Chemistry Chemical Physics, 2015. 17(27): p. 17894-17905.
5. Hauru, L.K., et al., *Enhancement of ionic liquid-aided fractionation of birchwood. Part 1: autohydrolysis pretreatment.* RSC Advances, 2013. 3(37): p. 16365-16373.
6. Singh, S., B.A. Simmons, and K.P. Vogel, *Visualization of biomass solubilization and cellulose regeneration during ionic liquid pretreatment of switchgrass.* Biotechnology and Bioengineering, 2009. 104(1): p. 68-75.
7. Zhang, J., et al., *Understanding changes in cellulose crystalline structure of lignocellulosic biomass during ionic liquid pretreatment by XRD.* Bioresource technology, 2014. 151: p. 402-405.
8. Li, W., et al., *Rapid dissolution of lignocellulosic biomass in ionic liquids using temperatures above the glass transition of lignin.* Green Chemistry, 2011. 13(8): p. 2038-2047.
9. da Silva, S.P.M., et al., *Novel pre-treatment and fractionation method for lignocellulosic biomass using ionic liquids.* RSC Advances, 2013. 3(36): p. 16040-16050.
10. Hamada, Y., et al., *A possible means of realizing a sacrifice-free three component separation of lignocellulose from wood biomass using an amino acid ionic liquid.* Green Chemistry, 2013. 15(7): p. 1863-1868.
11. Bozell, J.J., et al., *Solvent fractionation of renewable woody feedstocks: Organosolv generation of biorefinery process streams for the production of biobased chemicals.* biomass and bioenergy, 2011. 35(10): p. 4197-4208.
12. Labbé, N., et al., *Activation of lignocellulosic biomass by ionic liquid for biorefinery fractionation.* Bioresource technology, 2012. 104: p. 701-707.
13. Wang, H., et al., *Physical Insight into Switchgrass Dissolution in Ionic Liquid 1-Ethyl-3-methylimidazolium Acetate.* ACS Sustainable Chemistry & Engineering, 2014. 2(5): p. 1264-1269.
14. Castro, M.C., et al., *Mixtures of ethanol and the ionic liquid 1-ethyl-3-methylimidazolium acetate for the fractionated solubility of biopolymers of lignocellulosic biomass.* Industrial & Engineering Chemistry Research, 2014. 53(29): p. 11850-11861.
15. Achinivu, E.C., et al., *Lignin extraction from biomass with protic ionic liquids.* Green Chemistry, 2014. 16(3): p. 1114-1119.
16. Garrote, G. and J.C. Parajó, *Autohydrolysis of corncob: study of non-isothermal operation for xylooligosaccharide production.* Journal of Food Engineering, 2002. 52(3): p. 211-218.

17. Xiao, X., et al., *Autohydrolysis of bamboo (Dendrocalamus giganteus Munro) culm for the production of xylo-oligosaccharides.* Bioresource technology, 2013. 138: p. 63-70.
18. Chen, X., M. Lawoko, and A. van Heiningen, *Kinetics and mechanism of autohydrolysis of hardwoods.* Bioresource technology, 2010. 101(20): p. 7812-7819.
19. Deb, S., et al., *Application of mild autohydrolysis to facilitate the dissolution of wood chips in direct-dissolution solvents.* Green Chemistry, 2016.
20. Cruz, A.G., et al., *Impact of high biomass loading on ionic liquid pretreatment.* Biotechnology for biofuels, 2013. 6(1): p. 1-10.
21. A. Sluiter, B.H., R. Ruiz, C. Scarlata, J. Sluiter, D. Templeton, and D. Crocker, *Determination of Structural Carbohydrates and Lignin in Biomass.* NREL Biomass Analysis Technology Team Laboratory Analytical Procedure, 2011.
22. A. Sluiter, B.H., R. Ruiz, C. Scarlata, J. Sluiter, D. Templeton, *Determination of Sugars, Byproducts, and Degradation Products in Liquid Fraction Process Samples* NREL Biomass Analysis Technology Team Laboratory Analytical Procedure, 2008.
23. Overend, R.P., E. Chornet, and J. Gascoigne, *Fractionation of lignocellulosics by steam-aqueous pretreatments [and discussion]*. Philosophical Transactions of the Royal Society of London. Series A, Mathematical and Physical Sciences, 1987. 321(1561): p. 523-536.
24. Egüés, I., et al., *Effect of alkaline and autohydrolysis processes on the purity of obtained hemicelluloses from corn stalks.* Bioresource technology, 2012. 103(1): p. 239-248.
25. Lloyd, T.A. and C.E. Wyman, *Combined sugar yields for dilute sulfuric acid pretreatment of corn stover followed by enzymatic hydrolysis of the remaining solids.* Bioresource Technology, 2005. 96(18): p. 1967-1977.
26. Sun, N., et al., *Complete dissolution and partial delignification of wood in the ionic liquid 1-ethyl-3-methylimidazolium acetate.* Green Chemistry, 2009. 11(5): p. 646-655.
27. Pandey, K.K., *A note on the influence of extractives on the photo-discoloration and photo-degradation of wood.* Polymer degradation and stability, 2005. 87(2): p. 375-379.
28. Cheng, G., et al., *Transition of cellulose crystalline structure and surface morphology of biomass as a function of ionic liquid pretreatment and its relation to enzymatic hydrolysis.* Biomacromolecules, 2011. 12(4): p. 933-941.
29. Langford, J.I. and A. Wilson, *Scherrer after sixty years: a survey and some new results in the determination of crystallite size.* Journal of Applied Crystallography, 1978. 11(2): p. 102-113.
30. Pu, Y., et al., *Assessing the molecular structure basis for biomass recalcitrance during dilute acid and hydrothermal pretreatments.* Biotechnol Biofuels, 2013. 6(1): p. 1-13.
31. Gladden, J.M., et al., *Glycoside hydrolase activities of thermophilic bacterial consortia adapted to switchgrass.* Applied and environmental microbiology, 2011. 77(16): p. 5804-5812.

32. Cheng, G., et al., *Impact of ionic liquid pretreatment conditions on cellulose crystalline structure using 1-ethyl-3-methylimidazolium acetate.* J Phys Chem B, 2012. 116(33): p. 10049-54.
33. Shigematsu, M., et al., *Enhancement of miscibility between hemicellulose and lignin by addition of their copolymer, the lignin-carbohydrate complex.* Macromolecular Chemistry and Physics, 1994. 195(8): p. 2827-2837.
34. Ueberreiter, K., *The solution process*. 1968, Academic Press: New York. p. 219-257.
35. Sudduth, R.D., *Development of Huggins' and Kraemer's equations for polymer solution evaluations from the generalized viscosity model for suspensions.* Journal of applied polymer science, 1997. 66(12): p. 2319-2332.
36. Korsmeyer, R.W. and N.A. Peppas, *Effect of the morphology of hydrophilic polymeric matrices on the diffusion and release of water soluble drugs.* Journal of Membrane Science, 1981. 9(3): p. 211-227.

CHAPTER THREE

DIRECT PRODUCTION OF MATERIALS FROM LIGNOCELLULOSIC BIOMASS-IONIC LIQUID SYSTEM

In the previous chapter, we demonstrated that the diffusion of IL to biomass cell walls was much improved by the partial removal of hemicellulose. The best dissolution ability of biomass in IL was achieved at 100 °C with biomass autohydrolyzed at 160 °C for 60 min. In this chapter, autohydrolysis and IL dissolution steps were applied to achieve the complete dissolution of biomass in IL. A solution of the autohydrolyzed biomass/IL was prepared to directly produce a high-value biomaterial, biomass film.

A manuscript entitled **"Direct Production of Lignocellulosic Films from Ionic Liquid System"** with the following authors of Jing Wang, Ramiz Boy, Amit K. Naskar, David Harper, Mikhael Soliman, Laurene Tetard, Timothy Rials, and Nicole Labbé is in preparation for submission to the journal of ***ACS sustainable chemistry & Engineering***. Jing Wang designed and performed the experiment, conducted the data analysis, and drafted the manuscript. Dr. Ramiz Boy assisted with film preparation and collected the film images by scanning electron microscopy, and conducted the dynamic mechanical property measurements. Dr. Laurene Tetard and Mr. Mikhael Soliman provided the film surface maps by atomic force microscopy. Drs. Amit Naskar, David Harper, Timothy Rials, assisted in interpreting the data and revising the manuscript. Dr. Labbé assisted in designing the experiment, analysing the data, and writing the manuscript.

3.1 Abstract

The direct conversion of lignocellulosic biomass into high value-added materials remains a challenge mainly due to biomass poor solubility in common organic solvents. In this study, ionic liquids (ILs) have been investigated as a media to dissolve and process lignocellulosic biomass. We therefore report an approach to directly convert lignocellulosic biomass-ionic liquid solution to biomass films without additives. To obtain

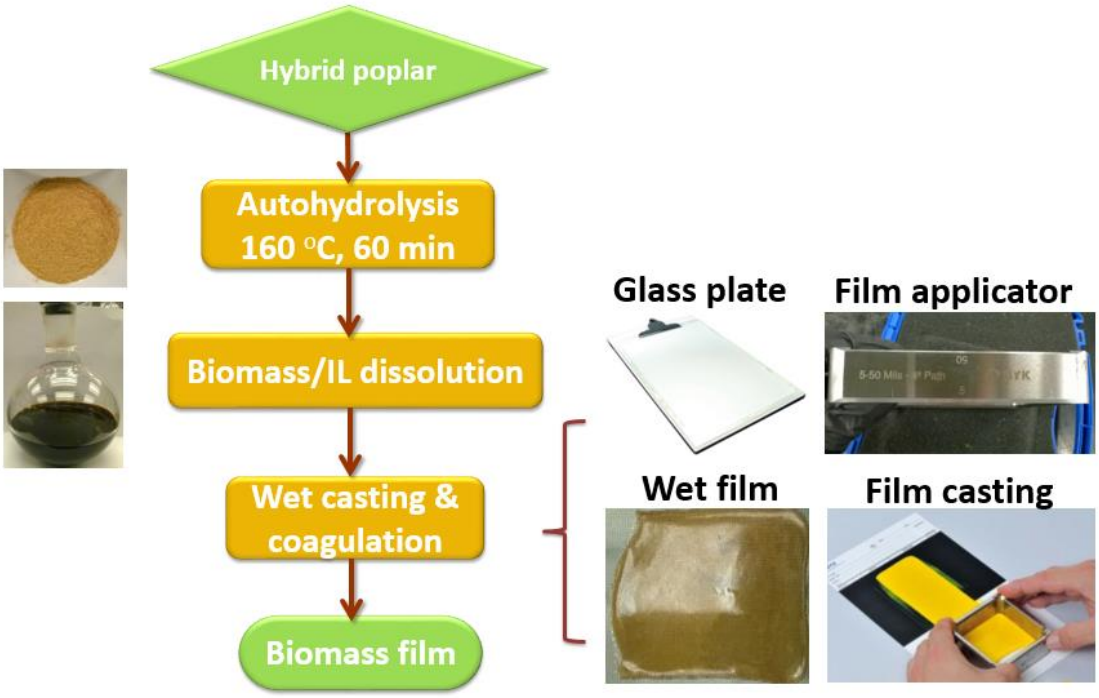

Figure 3.1 Abstract graphic.

an adequate biomass-IL system, an autohydrolysis step was conducted on the biomass prior to the IL dissolution step. The biomass/1-ethyl-3-methyl imidazolium acetate ([C_2mim][OAc]) solution was then used to directly cast films which were coagulated in either methanol, N,N-Dimethylacetamide (DMAc/water) mixture or water. The properties of the films were found to be highly dependent on the polarity of coagulants. The carbohydrates to lignin ratio of methanol, DMAc/water and water films was 4.0, 7.7 and 2.1, respectively. Methanol film exhibited more homogeneous structure than DMAc/water or water films. Moreover, methanol film had the highest decomposition temperature, mainly resulting from lignin with high molecular weight. In addition, the tensile stress of biomass films was between 37-70 MPa. The optimum ratio of carbohydrates to lignin, the

high cross-link density between carbohydrates and lignin, and uniform structure contributed to the better mechanical properties of the methanol films.

3.2 Introduction

Lignocellulosic biomass is being explored as resources for fuels, chemicals, and materials such as plastics, films and other bioproducts.[1, 2] One attractive aspect of biomass-based materials is their biodegradability and renewability, which are not attainable with synthetic polymers produced from fossil resource.

The complexity of the physical and chemical structure of lignocellulosic biomass, for example the high crystallinity of cellulose, the lignin and carbohydrate complex, results in its low dissolution in commonly used organic solvents.[3] This characteristic has limited the processability of lignocellulosic biomass and inhibited its direct and efficient conversion to produce bio-based materials. Recently, a number of novel biomass-based materials have been developed from individual biomass polymers (i.e. cellulose, hemicellulose, and lignin).[4, 5] These biopolymers were isolated from biomass through a fractionation method using a strong base or an organosolv process.[6, 7] However, these processes always required strong and toxic solvents. They also produce a large amount of by-products, which negatively impact their applications.[7] To overcome these limitations, novel solvents in which biomass has high solubility are needed.

Ionic liquid (IL) processes are a promising technology for biochemicals and biomaterials production.[8] ILs are organic salts composed of cations and anions with melting points lower than 100 °C. Most ILs exhibit high thermal stability and nearly no emission of volatile organic compounds, which is an advantage compared to organic solvents. Rogers and co-workers first demonstrated that imidazolium based ILs can

dissolve cellulose in 2002.[9] Later, a number of studies have showed that ILs can dissolve biomass partially above 100 °C. When the temperature is higher than the glass transition temperature of lignin, the dissolution process is usually more efficient.[10] As of now, biopolymer-based fibers and films have been produced from blends of isolated cellulose and lignin/IL solution.[11, 12] Only a few studies have explored the direct transformation of biomass/IL solutions to biomass-based materials. In 2007, Fort et al. attempted to cast membranes directly from a 1-n-butyl-3-methyimidazolium chloride-wood solution and concluded that hemicellulose and/or lignin were responsible for their failure because they inhibited the formation of structured cellulose hydrogels.[13] Sun et al. reported that through an IL treatment at 110 °C for 16 h, fibers could be spun from bagasse /IL solution but not from pine/IL solution.[14] Most recently, Abdulkhani et al. demonstrated that cellulose composite films can be produced from an 1-butyl-3-methylimidazolium chloride solution of extracted cellulose from woody materials.[15] This approach did not utilize hemicellulose and lignin of the biomass and thus could not achieve the direct conversion strategy of biomass. To the best of our knowledge, there is no reported literature about the direct casting of films from lignocellulosic biomass/IL solution.

The main goal of this study was to develop a process that allows the direct conversion of lignocellulosic biomass/IL solution to high value-added materials, biomass films. To evaluate the films, their chemical, physical and mechanical properties were characterized by ultraviolet-visible spectrophotometry (UV-Vis), Fourier transform infrared spectroscopy (FT-IR), scanning electron microscopy (SEM), atomic force microscopy (AFM), x-ray diffractometry (XRD), thermogravimetric analysis (TGA), dynamic mechanical analysis (DMA) and tensile testing.

3.3 Materials and Methods

3.3.1 Materials

Air dried hybrid poplar (*Populus*×*Deltoides*) wood chips (particle size smaller than 1 cm^3) were used for this study. The ionic liquid 1-ethyl-3-methylimidazolium acetate ([C_2mim][OAc], purum≥95%) was purchased from Iolitec Inc. (Tuscaloosa, AL) and used without further purification. Methanol and N,N-Dimethylacetamide (DMAc) of analytical reagent grade were purchased from Sigma-Aldrich (St. Louis, MO). Deionized water (DI water) was employed throughout the experiments.

3.3.2 Autohydrolyzed-hybrid poplar/[C_2mim][OAc] solution and film preparation.

Autohydrolyzed-hybrid poplar (HP) was generated by extracting the raw biomass (187 g) with DI water at 160 °C for 60 min in a Hastelloy C276 pressure reactor with solid/liquid ratio of 1:20. The extracted-HP was dried at 40 °C until a constant moisture content was reached (less than 10% by weight), and then milled with a Wiley mill through a 40-mesh screen (0.425 mm). Then the biomass-IL solution was prepared by mixing 9.8 g of autohydrolyzed-HP with [C_2mim][OAc] (140.2 g) and mechanically stirring at 75 rpm at 100 °C in a 500 mL round bottle until complete dissolution. This was determined by optical microscopy with a 10×magnification.

After the complete dissolution, the wet film was directly cast from the HP/[C_2mim][OAc] at 100 °C, which was higher than the cross-over point (66 °C) of storage modulus and loss modulus of the HP/[C_2mim][OAc]. The solution behaves as liquid-like material while its temperature is higher than 66 °C. For the film preparation process, the

HP/[C_2mim][OAc] needed to be transferred onto glass plate and cast into very thin layer. So, the solution temperature should be higher than 66 °C.

The HP/[C_2mim][OAc] solution (100 °C) was poured onto a glass plate and cast by a 30 mil square frame applicator (from BYK Additives & Instruments). The glass plate with the thin film was then submerged in three subsequent solvent baths in order to entirely remove [C_2mim][OAc]: the first bath (1000 mL coagulant) for 60 min, the second and third bath for 30 min (250 mL of coagulant) each to completely remove IL from the films. Three different coagulants were tested for the solvent baths: methanol, DMAc/water (50/50, v/v), and water. Duplicates of the films were prepared for each coagulation condition. The coagulated films were then covered by a stainless steel screen mesh, fixed by plastic binder clips, and gradually dried at around 25 °C in a seal container over a sequence of saturated saline solutions (KNO_3, KCl, NaCl and $Mg(NO_3)_2$) to prevent shrinkage and wrinkles. The saturated solutions provided relative humidity ranging from around 94 to 54%.[16] The films were exposed to each relative humidity condition for 2 days. The length and width of the dried films were measured using a ruler (precision 1 mm), and the thickness by a micrometer (Marathon, precision 0.01 mm). Film thicknesses were calculated from an average of five measurements.

3.3.3 Morphological characterization of the films

The morphology of the films was determined by SEM and AFM. The microstructure of the cross sections of the films was observed using a Hitachi S-4800 field emission SEM with an acceleration voltage of 5 kV after sputter coating with a thin layer of carbon while the stiffness of film surface was characterized by AFM topography and pulsed-force-microscopy (PFM).

3.3.4 FT-IR characterization of the films

FT-IR spectra were collected on the methanol, DMAc/water and water films using a Perkin–Elmer Spectrum One FT-IR spectrometer (Waltham, MA) equipped with an attenuated total reflectance (ATR) accessory with 8 scans at 4 cm^{-1} resolution over 4000-650 cm^{-1} range. Five spectra were collected for each film. In order to clearly delineate the impacts of coagulating solvents on the chemical features of the biomass films, principal component analysis (PCA), was conducted on the FT-IR spectra using The Unscrambler statistical software 9.0 (CAMO Software Inc., Woodbridge, NJ).[17]

3.3.5 Chemical composition of the films

The films were first cut to small pieces, and the chemical composition of the films was determined according to the National Renewable Energy Laboratory (NREL) Analytical Procedure "Determination of Structural Carbohydrates and Lignin in Biomass".[18]

3.3.6 Optical property of the films

To measure the percentage of transmittance of radiation, UV-Vis spectra of films were collected at the scan speed of 240 nm/min on a Perkin–Elmer Lambda 35 spectrometer in the wavelength range of 200 to 700 nm.

3.3.7 Crystallinity and orientation of cellulose in the films

To visualize the effects of coagulating solvents on the cellulose structure, the films (about length 3 cm × width 3 cm) were mounted on a low-background quartz holder and measured using a PANalytical Empyrean X-ray diffractometer (PANalytical Inc.,

Westborough, MA) with a Cu tube (λ ¼ 1.5405 Å). The radiation was generated at 40 mA and 45 kV. A step size of 0.01º exposure was used for measuring the scattering angle 2θ in the range 9–41º.

3.3.8 Thermal property of the films

Thermogravimetric analysis was conducted using a thermogravimetric analyzer (Pyris 1 TGA, Perkin Elmer, Shelton, CT). Approximately, 3 mg of each film was initially heated from 50 to 105 °C with the rate of 10 °C /min under nitrogen (10 mL/min). The temperature was hold at 105 °C for 10 min to ensure that the moisture was completely removed. Subsequently, the sample was heated to 900 °C at 10 °C /min under nitrogen (10 mL/min) and finally kept at 900 °C for 60 min under air (10 mL/min). Thermograms were differentiated into weight loss rates for differential thermogravimetric (DTG) peaks. The temperature at 2.5% weight loss of the sample ($T_{initial}$) and the temperature at the maximum decomposition derivative peak (T_{peak}) were calculated in accordance with the method reported by Grønli et al.[19]

3.3.9 Dynamic mechanical property of the films

Dynamic mechanical analysis was used to measure the storage modulus (E') and loss modulus (E") of the films using a RSA3 Dynamic Mechanical Analyzer (TA Instruments). The film was cut into a strip of 35 mm length and 5 mm width. The thickness was calculated from the average of five measurements by a micrometer (Marathon, precision 0.01 mm). To reduce the interference from moisture on the measurement, the film was first kept in the chamber without loading to the grips at 105 °C for 15 min. The samples were then

placed in the grips with an approximate distance of 20 mm and tested from 25 to 300 °C with 3 °C/min at 1 Hz.

3.3.10 Tensile strength testing

The films were subjected to tensile testing on an Instron 5943, with Bluehill 3 software for test-control, data acquisition and results analysis. Measurements were carried out following the standard protocol ASTM D882-12 (2012). Briefly, the films were conditioned for two days at around 25 °C and 54% relative humidity (saturated $Mg(NO_3)_2$ solution). Before testing, 10 to 20 strips of width 12.7 mm and length 70 mm were prepared, providing a 30 mm testing length. Young's modulus, maximum tensile strain, and tensile stress at maximum load were calculated as the average of 6 individual specimens.

3.4 Results and Discussion

3.4.1 Morphological features of the films

After being dried under gradual relative humidity, the biomass films exhibited very smooth and uniform surface (Figure 3.2). Several studies have reported that biopolymer films severely cracked when exposed to environment with large decrease in relative humidity.[5, 20, 21] In lower relative humidity and constant temperature, cellulose and biomass films lose moisture and shrink. Our observations are in agreement with previously reported severe cracks in biopolymer films exposed to large decreases in relative humidity. To solve the problems, we implemented a drying process with saturated salts to create a sequence of humidity variations for gentle drying of the films. The results suggest that a gradual decrease in environmental humidity can minimize the degree of shrinkage and

cracks in biomass-based films produced. The conditions were optimized to produce biomass films without any cracks or wrinkles. As a result, the biomass films was produced free of wrinkles or cracks (Figure 3.2). Biomass films have lateral dimensions (length 14 cm× width 8.5 cm) and their thicknesses in the range 25 to 33 μm (Table 3.3).

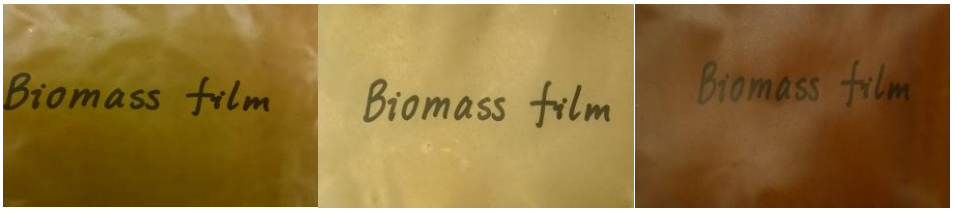

Figure 3.2 Pictures of dried methanol, DMAc/water and water biomass-films (from left to right) with the dimension of length 14 cm × width 8.5 cm.

The cross section and surface of the films were investigated by SEM and AFM, respectively. The SEM image of the films cross section reveal a significantly different morphology of the methanol film compared to DMAc/water and water films (Figure 3.3, top row). Methanol film had quite dense, homogeneous, and smooth cross section. DMAc/water and water films displayed disordered, rough, and sheet-like aggregation structure. The non-uniform cross section of DMAc/water and water films resulted in larger thickness and higher standard deviation of thickness than the methanol film. Furthermore, AFM measurements were conducted to characterize the texture of the films surfaces. The stiffness analysis of the film surface showed more variation in the water film than in the other two films. Water film had obviously phase-separated structure. Methanol film exhibited the most consistent stiffness and the lowest stiffness (darker regions). The morphological characterization by SEM and AFM revealed that methanol film had the

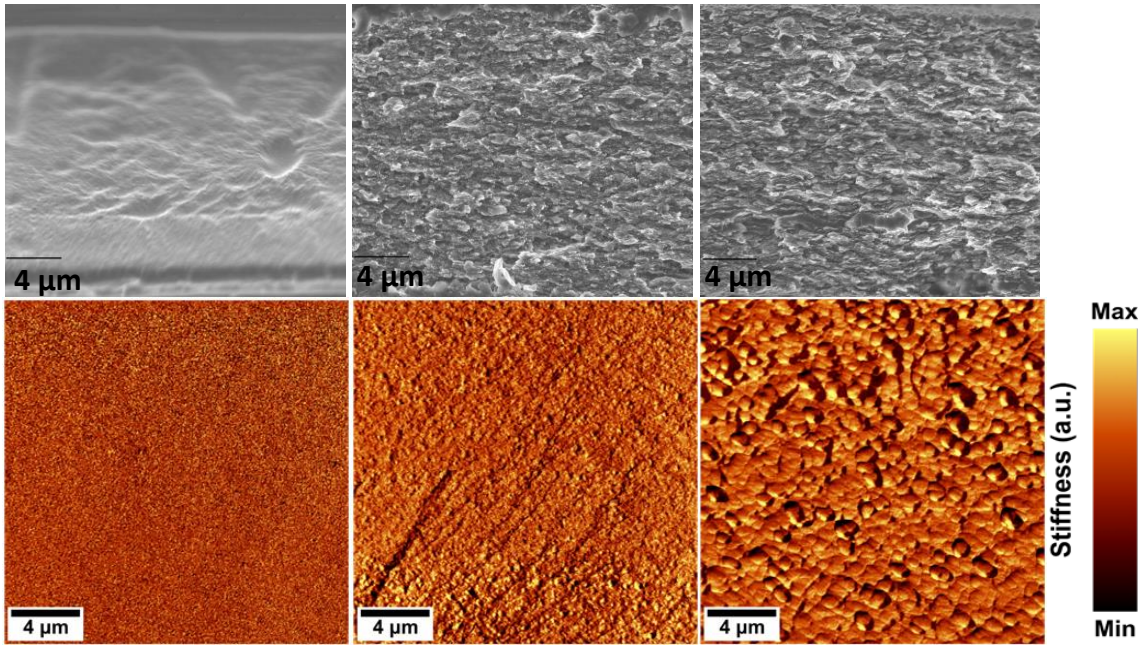

Figure 3.3 SEM images of cross sections (the first row) and AFM maps of the stiffness of surface (the second row) of dried biomass films coagulated in methanol, DMAc/water film, and water (from left to right).

most homogenous physical surface than DMAc/water or water film.

These morphological characteristics were clearly influenced by the polarity of the coagulating solvent, which varied from high (water), intermediate (DMAc/water) to low (methanol). First, during the film coagulation process, we observed that the film was coagulated faster in water than in DMAc/water or methanol. The diffusion process of the lower polarity coagulating solvent to the biomass phase could be gentler and further resulted in smoother film surface and cross section. Second, carbohydrates and lignin in methanol film could have better miscibility than in DMAc/water and water films. The high-polar solvents, especially water may have very different interaction strengths with carbohydrates and lignin, which caused the micro-phase separation. The phase separation could result in cellulose- and lignin- isolated domains with different molecular densities, chemical compositions and physical properties. Therefore, the surfaces of DMAc/water

and water films showed more variations than methanol film. In addition, the different features of the cross section of the films can be interpreted by the orientation of cellulose II crystal planes (see the results and discussion of XRD patterns).

3.4.2 Chemical features of the films.

FT-IR spectra were collected to determine possible variations in the bonds formed in the films obtained from different coagulants, and identify the chemical features of the three films. The data were mined to determine the potential traces of coagulating solvent or IL remaining in the films. The absence of the characteristic bands at 1392 cm^{-1} ($N-CH_3$ deformation); 1186 cm^{-1} (C-N stretching) demonstrate that DMAc was completely removed from the DMAc/water-coagulated film (Figure 3.4). The complete removal of $[C_2mim][OAc]$ was confirmed by the nonappearance of characteristic peak of $[C_2mim][OAc]$ (C=N band at 1565 cm^{-1}).

To clearly identify the differences in the FT-IR spectra of the three films, principal component analysis (PCA) was performed. The scores plot of PCA showed that the three films presented different chemical signature and therefore clustered separately. The water film displayed a more scattered data in Figure 3.4b in agreement with its non-uniform structure. The water film clearly separated from methanol and DMAc/water films by PC 1 (60%) (Figure 3.4b), while the later separated by PC 2 (30%). From the loadings of PC 1, the major positive bands contributing to the separation were at 1159 cm^{-1} (C-O-C antisymmetric bridge stretching vibration in cellulose and hemicellulose), 1035 cm^{-1} (C-O, C=C, C-C-O stretching vibration) and 898 cm^{-1} (C-H deformation vibration in cellulose), and the negative bands were at 1607 and 1511 cm^{-1} (aromatic skeletal vibration of lignin). Water film displayed scatter data as seen in Figure 3.4b confirming its nonuniform

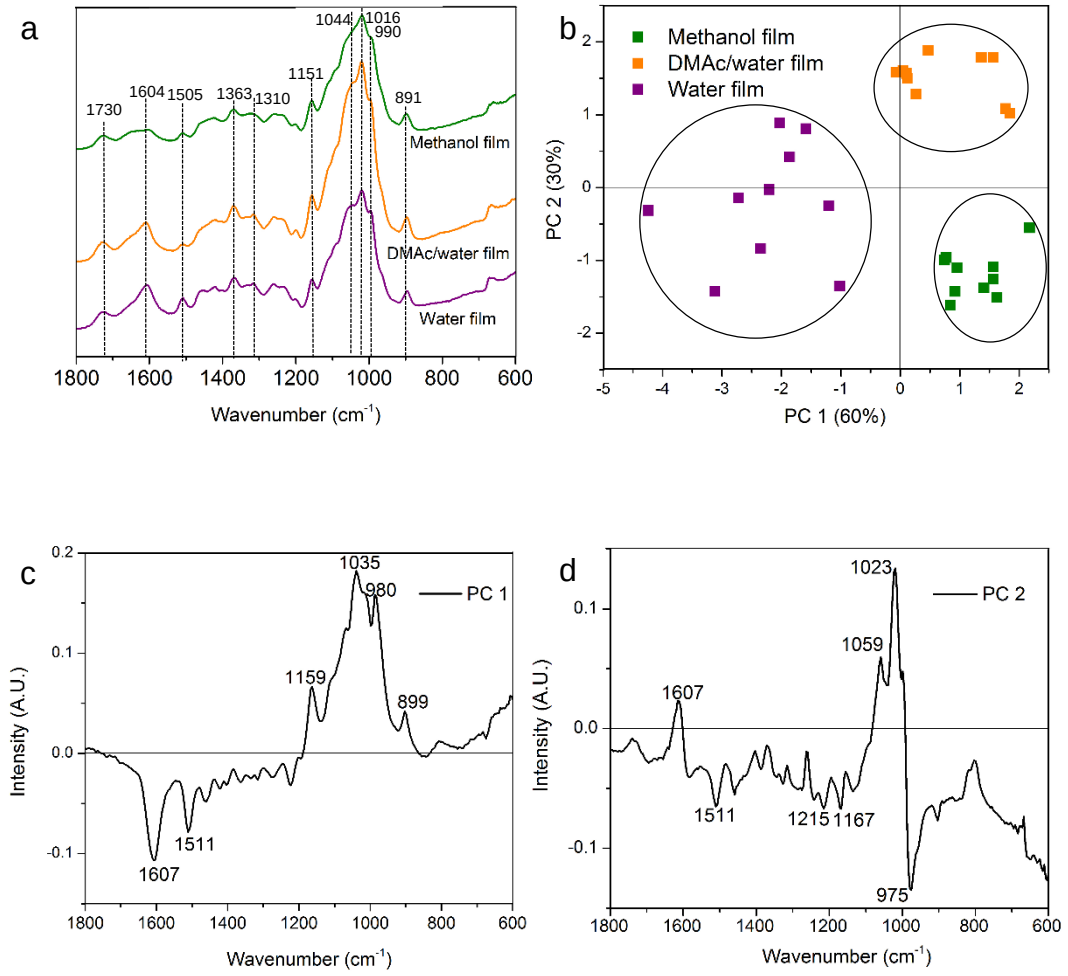

Figure 3.4 FT-IR and PCA analysis of biomass films (a) FTIR spectra of films (b) PCA scores plot (c) Loadings plot for PC 1 (d) Loadings plot for PC 2.

structure. The PCA results revealed that methanol and DMAc/water films contained a higher amount of carbohydrates and a lower content of lignin than the water film. In addition, the major bands of 1023 cm^{-1} (C-H in-plane deformation) and 975 cm^{-1} in the loadings plot of PC 2 (Figure 3.4d) indicated that DMAc/water film was richer in carbohydrates than the methanol film.

Table 3.1 Chemical composition of biomass films.

Material	Cellulose [%]	Hemicellulose [%]	Lignin [%]	C/L[a] ratio
Autohydrolyzed hybrid poplar	55.4	12.5	27.7	2.5
Film coagulated in methanol	68.8	4.3	18.4	4.0
Film coagulated in DMAc/water	82.5	3.9	11.2	7.7
Film coagulated in water	58.5	0.9	28.4	2.1

Chemical composition was calculated based on dry basis of the sample.

[a] C/L ratio is carbohydrates to lignin ratio.

To confirm the FT-IR findings, the carbohydrates and lignin content of the films were determined (Table 3.1) following the NREL protocol. The results confirmed that coagulating solvents had significant impact on the carbohydrates and lignin contents of the films. Water film had the lowest carbohydrates content (59.4%), highest content of lignin (28.4%) and lowest carbohydrate to lignin ratio (C/L ratio) of the films. This can be first explained by the high solubility of monosaccharides, oligosaccharides and even some polysaccharides in water. During the coagulation step, the high polarity of water leads to strong hydrogen bonding interactions with these carbohydrates[22] and therefore induced the partial dissolution of carbohydrates, which in turn generated water film with a lower level of carbohydrates. Lignin has been shown to have weaker dissolution ability in water

than in organic solvents, which can explain the higher percentage of lignin in the water film than in the films coagulated in DMAc/water or methanol.

3.4.3 Physical and mechanical properties of the films

The optical transmittance of the films analyzed by UV-vis spectrophotometer (Figure 3.5) revealed that the three films had very different light transmittance value in the wavelength ranging from 200 to 700 nm. Water film absorbed the radiation close to 100% from UV to ~ 450 nm while DMAc/water film absorbed only in UV up to ~ 300 nm. According to the analysis of the chemical content, the DMAc/water film contains the highest cellulose and lowest lignin content, which is in accordance with previous reports of cellulose and lignin materials films obtained with ILs.[15] Strong light absorbance is directly related to the lignin content. The transparency of DMAc/water and methanol films in the visible suggests high-value added films for applications such as coatings and food packaging, while the absorbance of lignin rich layers such as in the water films could be of interest as protection packaging of UV sensitive materials, such as organic chemicals and cosmetics.[21]

XRD analysis revealed the cellulose structure of films. Two broad peaks at around 20.0^{o} and 12.0^{o} were observed in the XRD patterns for the three films (Figure 3.6). These peaks were indicative of cellulose II structure.[23] Cellulose I (the native state of cellulose in biomass) was transformed to cellulose II via the IL dissolution step. For water and DMAc/water films, the intensity of crystal plane (1-10) at 12.0^{o} was very strong, and higher than the crystal plane (110) at 20.0^{o}. This reveals that the crystal plane (1-10) is oriented parallel to the surface of DMAc/water or water film.[24] The parallel orientation of the

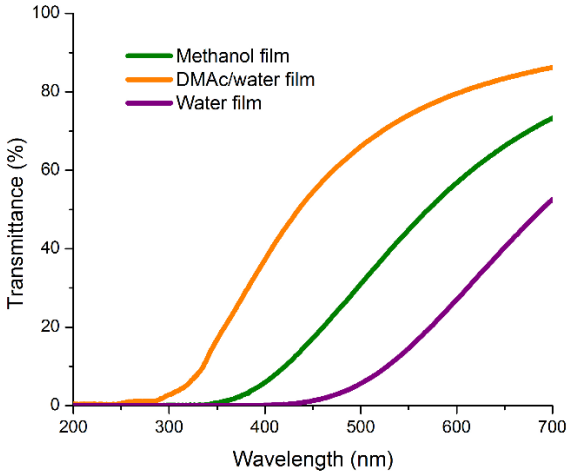

Figure 3.5 The UV-Vis spectra of the percentage of transmittance of biomass films for wavelength range of 200-700 nm.

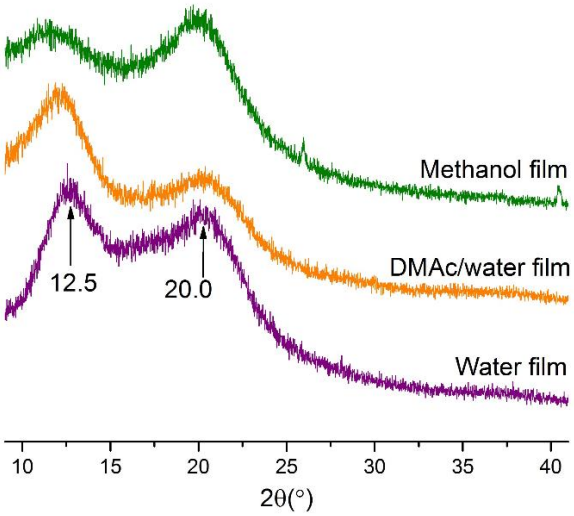

Figure 3.6 XRD patterns of biomass films.

crystal plane (1-10) to the film surface in cellulose films has been reported in a few research.[24, 25] It is noteworthy that the intensity of crystal plane (1-10) was lower than the crystal plane (110) in the XRD patterns of methanol film, which indicates that the crystal plane (1-10) is not parallel to the surface of methanol film.

These differences in cellulose chains orientation could be explained by the polarity of the coagulant baths. The higher polarity of the coagulant (DMAc/water, water) has stronger the interaction with hydroxyl groups of glucopyranose ring and further induces the hydrophilic surface of DMAc/water and water films,[24, 26] while the lower polarity of methanol causes less hydrophilic surface. Hydrophilicity made it easier for water film to absorb water and thus exhibited larger thicknesses. Furthermore, the orientation of cellulose II crystal planes support the observation of the sheet-like aggregation in the SEM images of the cross section of DMAc/water and water films as they can be caused by the stacking of layers of cellulose crystal planes (1-10).[24, 26]

The thermal properties of the films were characterized by thermogravimetric analysis (TGA). The water film decomposed the at the smallest $T_{initial}$ with 2.5 wt% weight loss achieved at 237 °C, compared to 252 °C for DMAc/water film and 272 °C for the methanol film (Table 3.2). Water and DMAc/water films showed maximum decomposition derivative peak T_{peak} around 338 °C, which is much lower than the temperature found for the methanol film at 354 °C. The alteration of degradation temperature suggests that the methanol film has a higher thermal stability than the two other films. This property could result from the dissolution ability of lignin in methanol. Methanol has been used in solvent fractionation of lignin since it can extract low-molecular-weight lignin.[27] Therefore, methanol film may contain a lignin with higher molecular weight than the DMAc/water

and water films. Hence, the good thermal property of methanol film could be attributed to its lignin with high molecular weight. At the end of the heating process, the water film exhibited a char yield (carbonization yield) of 25.5% at 900 °C. Since lignin has higher carbon content than carbohydrates, the higher amount of lignin in the water film explains the production of a higher amount of char than what was measurements with the other two films.

Table 3.2 TGA results of biomass films.

Material	$T_{initial}$ [a] (°C)	T_{peak} [b] (°C)	Char % [c]
Methanol film	272 (1)	354 (1)	19.7 (0.5)
DMAc/water film	252 (1)	339 (3)	24.1 (0.0)
Water film	237 (0)	338 (3)	25.2 (1.3)

[a] $T_{initial}$ is the temperature of 2.5% weight loss of the dry solid.

[b] T_{peak} is the temperature of the maximum decomposition derivative peak.

[c] Char% is the percentage of carbonization yield at 900 °C.

The storage modulus of the films decreased considerably with increasing temperature due to the softening of films (Figure 3.7). The methanol film had the highest storage modulus from 25 to 300 °C. At low temperature below 75 °C, water film had relatively higher storage modulus than DMAc/water film, which was consistent with the tensile strength data. Above 80 °C, DMAc/water film showed much elevated storage modulus than that of water film, indicating the reinforcement by cellulose in films. In addition, Saito reported that the storage modulus can be enhanced by adding lignin as a way to increase cross-link density. However, adding too much lignin can also decrease the modulus as lignin can make the material very brittle.[27] Here, although the high lignin content in the

water film may have increased the cross-link density, the methanol film had higher storage modulus than DMAc/water and water films, suggesting a better carbohydrates to lignin ratio (Figure 3.7) in terms of mechanical properties.

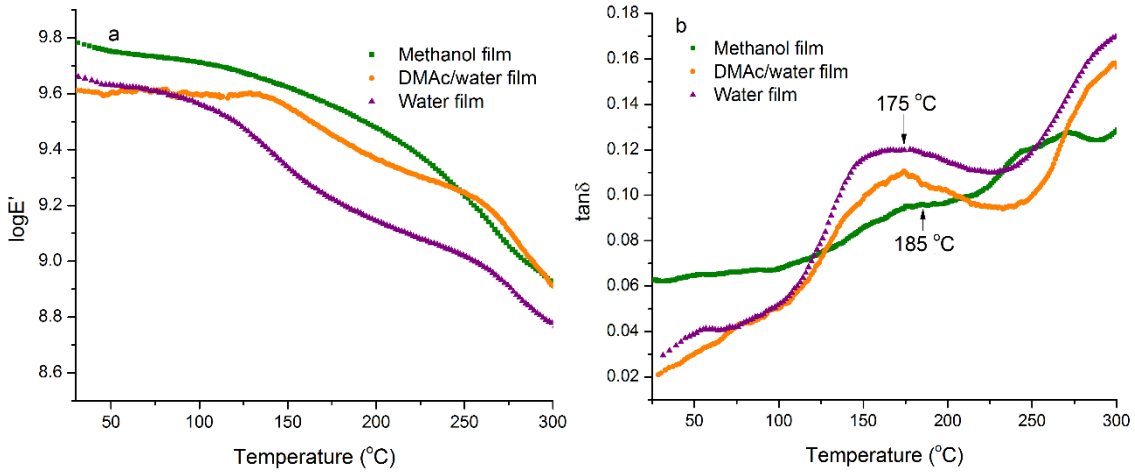

Figure 3.7 DMA data for biomass films (a) log storage modulus as a function of temperature (b) tan δ as a function of temperature.

The water and DMAc/water films exhibited an obvious transition about 175 °C (Figure 3.7b), which corresponds to the Tg of lignin. Methanol film showed a shoulder at approximately 185 °C. The higher Tg value of methanol film was mainly due to a high-molecular-weight lignin. These results demonstrate the assumption proposed in the characterization of the thermal properties that lignin with low molecular weight was extracted by methanol, that the resulting methanol film is composed of lignin with high molecular weight.

Among all the three films, the methanol film had the highest Young's modulus (5.9 GPa) and tensile stress (70 MPa) (Table 3.3). These results also indicated that the methanol film had the most appropriate ratio of carbohydrates to lignin. These three films exhibited

significantly higher modulus and tensile stress compared to other biopolymer films reported in the literature.[15, 21] For example, Chen et al. prepared biomass films with 2.3 GPa Young's modulus and 38 MPa tensile stress.[21] Methanol and DMAc/water films had better tensile strain than water film (Table 3.3 and Figure 3.8). Moreover, both methanol and DMAc/water films had the elongation after yield. Water film did not exhibit a yield point showing that water film was not able to deform plastically. Compared to the methanol film, the lower tensile strength of DMAc/water and water films may be due to the nonuniform structure and improper cellulose to lignin ratio. SEM and AFM images showed that the surfaces of the DMAc/water and water films were less uniform than the methanol film. The heterogeneity of the surface structure had been demonstrated to have negative impact on tensile strength.[28, 29] In addition, the plasticity of methanol and DMAc/water films was likely due to their high cellulose content varying between 69 and 83% since cellulose is known to substantially improve the plasticity of films.[15]

Table 3.3 Tensile testing results of biomass films.

Material	Thickness (mm)	Young's modulus (GPa)	Maximum tensile strain (%)	Tensile stress at Yield (MPa)	Tensile strain at Yield (%)
Methanol film	0.025 (0.001)	5.9 (0.3)	1.6 (0.4)	70 (5)	1.6 (0.4)
DMAc/water film	0.029 (0.002)	3.9 (0.7)	1.4 (0.3)	37 (6)	1.1 (0.2)
Water film	0.033 (0.002)	4.5 (0.9)	0.6 (0.1)	22 (7)	0.6 (0.4)

( ): Standard deviation

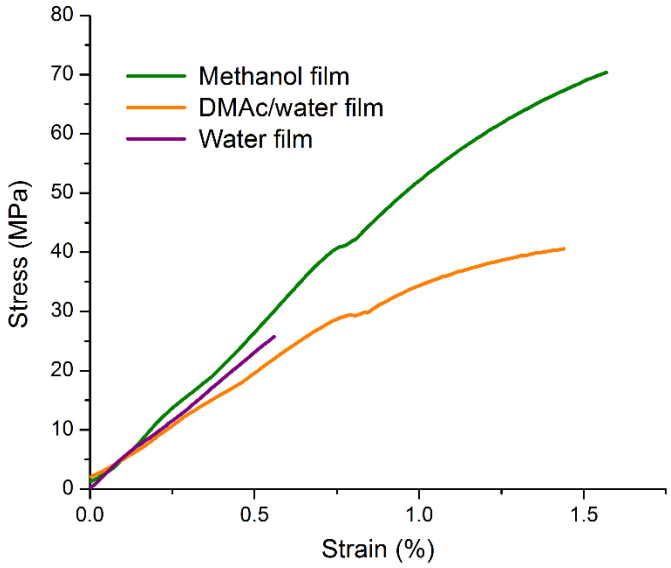

Figure 3.8 Stress-strain curves of biomass films.

3.5 Conclusion

Hybrid poplar was investigated to directly produce biomass films using an ionic liquid system. The biomass was subjected to a mild autohydrolysis to remove a portion of the hemicellulose and generate an adequate biomass-IL solution for film casting. Biomass films were then regenerated from the hybrid poplar/ [C_2mim][OAc] solution using different coagulating solvents (methanol, DMAc/water and water). The dried biomass films were semi-transparent with yellow or brown color, free of cracks or wrinkles. We showed that the coagulating solvents had a strong effect on the physicochemical properties of the coagulated films. Methanol film had a more uniform texture than DMAc/water or water films, which could be due to the gentle diffusion of methanol during coagulation, the good miscibility of carbohydrates and lignin, and the unparalleled orientation of cellulose planes to the surface of methanol film. Moreover, the good thermal property of methanol film could be attributed to its high-molecular-weight lignin. In addition, a ratio of carbohydrates

to lignin of methanol film resulted in the methanol film having the best mechanical properties. Lignin has dual effect on film properties. On one hand, the presence of lignin can increase the cross-links between the biopolymers and enhance the tensile strength. On the other hand, too much lignin has negative effect on tensile strength. Further study will be investigated to improve biomass film quality by investigating “the optimum point” of carbohydrates to lignin ratio.

3.6 References

1. Isikgor, F.H. and C.R. Becer, *Lignocellulosic biomass: a sustainable platform for the production of bio-based chemicals and polymers.* Polymer Chemistry, 2015. 6(25): p. 4497-4559.
2. Binder, J.B. and R.T. Raines, *Simple chemical transformation of lignocellulosic biomass into furans for fuels and chemicals.* Journal of the American Chemical Society, 2009. 131(5): p. 1979-1985.
3. Brandt, A., et al., *Deconstruction of lignocellulosic biomass with ionic liquids.* Green chemistry, 2013. 15(3): p. 550-583.
4. Sun, L., et al., *Crystalline characteristics of cellulose fiber and film regenerated from ionic liquid solution.* Carbohydr Polym, 2015. 118: p. 150-5.
5. Svard, A., E. Brannvall, and U. Edlund, *Rapeseed straw as a renewable source of hemicelluloses: Extraction, characterization and film formation.* Carbohydr Polym, 2015. 133: p. 179-86.
6. Bozell, J.J., et al., *Solvent fractionation of renewable woody feedstocks: Organosolv generation of biorefinery process streams for the production of biobased chemicals.* Biomass and Bioenergy, 2011. 35(10): p. 4197-4208.
7. Mosier, N., et al., *Features of promising technologies for pretreatment of lignocellulosic biomass.* Bioresource technology, 2005. 96(6): p. 673-686.
8. Sun, N., et al., *Where are ionic liquid strategies most suited in the pursuit of chemicals and energy from lignocellulosic biomass?* Chemical Communications, 2011. 47(5): p. 1405-1421.
9. Swatloski, R.P., et al., *Dissolution of cellose with ionic liquids.* Journal of the American Chemical Society, 2002. 124(18): p. 4974-4975.
10. Li, W., et al., *Rapid dissolution of lignocellulosic biomass in ionic liquids using temperatures above the glass transition of lignin.* Green Chemistry, 2011. 13(8): p. 2038-2047.
11. Wu, R.-L., et al., *Green composite films prepared from cellulose, starch and lignin in room-temperature ionic liquid.* Bioresource Technology, 2009. 100(9): p. 2569-2574.
12. Ma, Y., et al., *High-Strength Composite Fibers from Cellulose–Lignin Blends Regenerated from Ionic Liquid Solution.* ChemSusChem, 2015. 8(23): p. 4030-4039.
13. Fort, D.A., et al., *Can ionic liquids dissolve wood? Processing and analysis of lignocellulosic materials with 1-n-butyl-3-methylimidazolium chloride.* Green Chemistry, 2007. 9(1): p. 63-69.
14. Sun, N., et al., *Composite fibers spun directly from solutions of raw lignocellulosic biomass dissolved in ionic liquids.* Green Chemistry, 2011. 13(5): p. 1158-1161.
15. Abdulkhani, A., et al., *Effects of dissolution of some lignocellulosic materials with ionic liquids as green solvents on mechanical and physical properties of composite films.* Carbohydr Polym, 2013. 95(1): p. 57-63.
16. Winston, P.W. and D.H. Bates, *Saturated solutions for the control of humidity in biological research.* Ecology, 1960. 41(1): p. 232-237.
17. Labbé, N., et al., *Activation of lignocellulosic biomass by ionic liquid for biorefinery fractionation.* Bioresource technology, 2012. 104: p. 701-707.

18. A. Sluiter, B.H., R. Ruiz, C. Scarlata, J. Sluiter, D. Templeton, and D. Crocker, *Determination of Structural Carbohydrates and Lignin in Biomass.* NREL Biomass Analysis Technology Team Laboratory Analytical Procedure, 2011.
19. Grønli, M.G., G. Varhegyi, and C. Di Blasi, *Thermogravimetric analysis and devolatilization kinetics of wood.* Industrial & Engineering Chemistry Research, 2002. 41(17): p. 4201-4208.
20. Sundberg, J., G. Toriz, and P. Gatenholm, *Effect of xylan content on mechanical properties in regenerated cellulose/xylan blend films from ionic liquid.* Cellulose, 2015. 22(3): p. 1943-1953.
21. Chen, M., et al., *Approach to renewable lignocellulosic biomass film directly from bagasse.* ACS Sustainable Chemistry & Engineering, 2014. 2(5): p. 1164-1168.
22. Dibble, D.C., et al., *A facile method for the recovery of ionic liquid and lignin from biomass pretreatment.* Green Chemistry, 2011. 13(11): p. 3255-3264.
23. Cheng, G., et al., *Transition of cellulose crystalline structure and surface morphology of biomass as a function of ionic liquid pretreatment and its relation to enzymatic hydrolysis.* Biomacromolecules, 2011. 12(4): p. 933-941.
24. Yamane, C., et al., *Two different surface properties of regenerated cellulose due to structural anisotropy.* Polymer journal, 2006. 38(8): p. 819-826.
25. Tammelin, T., et al., *Method to prepare smooth and even cellulose-lignophenol films.* BioResources, 2011. 6(3): p. 2386-2398.
26. Isobe, N., et al., *Internal surface polarity of regenerated cellulose gel depends on the species used as coagulant.* Journal of colloid and interface science, 2011. 359(1): p. 194-201.
27. Saito, T., et al., *Development of lignin-based polyurethane thermoplastics.* RSC Advances, 2013. 3(44): p. 21832-21840.
28. Hassan, A., P. Hornsby, and M. Folkes, *Structure–property relationship of injection-molded carbon fibre-reinforced polyamide 6, 6 composites: the effect of compounding routes.* Polymer testing, 2003. 22(2): p. 185-189.
29. Morris, E.A., et al., *High performance carbon fibers from very high molecular weight polyacrylonitrile precursors.* Carbon, 2016. 101: p. 245-252.

CHAPTER FOUR

BIOMASS FRACTIONATION AND ISOLATION OF LIGNIN THROUGH AN AUTOHYDROLYSIS-IONIC LIQUID PROCESS

By removing a portion of hemicellulose, the interactions of biopolymers with IL, and the dissolution of biomass in IL can be much enhanced (the second chapter). The complete dissolution of biomass in IL paved the way for the direct conversion of the whole biomass to biomass films (the third chapter). The other approach for lignocellulosic biomass utilization is the isolation of biopolymers for downstream processing. The increased interaction of autohydrolyzed biomass with IL reduces the recalcitrance and improves the hydrolyzability of biomass. In this chapter, a biomass fractionation process was designed to isolate lignocellulosic biomass into high yield and purity carbohydrates and lignin streams.

The manuscript of this chapter entitled "**Biomass fractionation and isolation of lignin through an autohydrolysis-ionic liquid process**" has been submitted to the journal of ***ACS Sustainable Chemistry & Engineering*** with the following authors Jing Wang, Stephen C. Chmely, Timothy G. Rials and Nicole Labbé on June 8, 2016. Jing Wang performed the experiments, conducted the data analysis, and drafted the manuscript. Dr. Stephen Chmely assisted with plotting and interpreting the NMR spectra. Dr. Nicole Labbé designed the experiment, and participated in thethe data analysis and interpretation, and the writing of the manuscript. Drs. Stephen Chmely, Timothy Rials and Nicole Labbé contributed to the revision of the manuscript. All authors approved the final version of the manuscript.

4.1 Abstract

Although various IL processes have been designed to pretreat and/or fractionate lignocellulosic biomass, one major goal of these processes yet to be achieved is to produce high yield and purity lignin and hemicellulose fractions. In this study, a fractionation

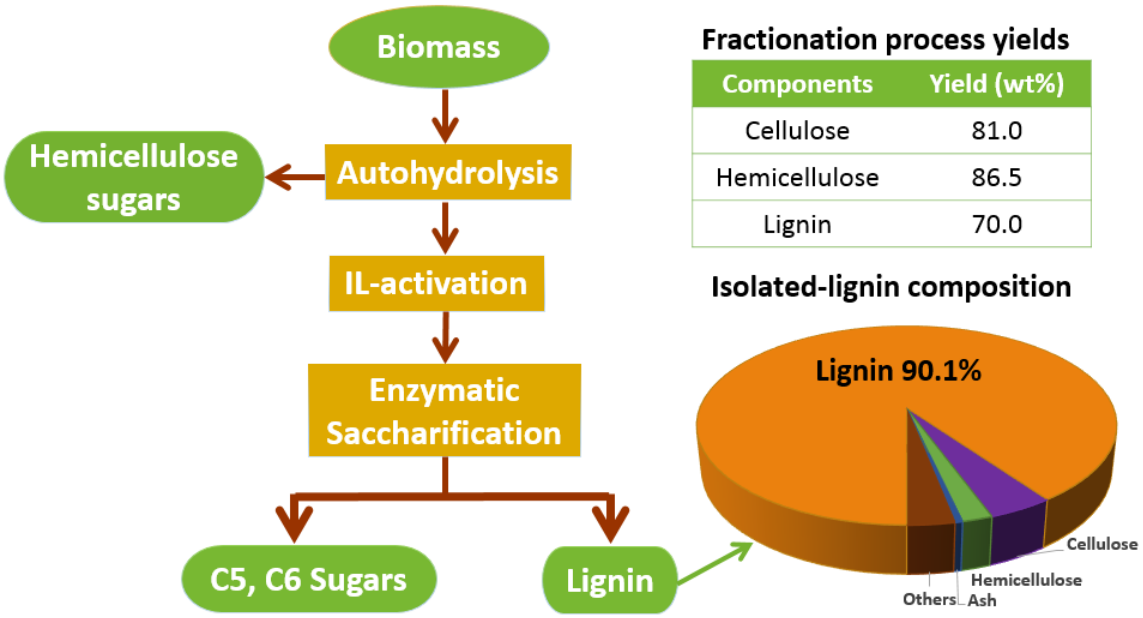

Figure 4.1 Abstract graphic.

process with [C_2mim][OAc] was designed to fractionate hybrid poplar to high purity fractions with minor degradation and modification. First, approximately 55% of hemicellulose was extracted by autohydrolysis at 160 °C for 60 min with minimal loss of lignin and cellulose. The extracted biomass was then activated with [C_2mim][OAc] at 60 °C for 3 h followed by an enzymatic saccharification to hydrolyze the carbohydrates into monosugars and generate the lignin fraction. The saccharification kinetics and carbohydrates conversion yields revealed that a combination of autohydrolysis and IL activation significantly reduced the recalcitrance of the IL-regenerated autohydrolyzed biomass, making it more susceptible to enzymatic hydrolysis than each treatment separately. Quantitative analyses showed that the fractionation process isolated 87 wt% of cellulose and 81 wt% of hemicellulose in the carbohydrates fraction, and 70 wt% of the lignin with a 90.1% purity. Two dimensional ^{1}H-^{13}C HSQC NMR spectroscopy indicated

that the main linkages of lignin in hybrid poplar were preserved during the fractionation process.

4.2 Introduction

Lignocellulosic biomass has been investigated as a renewable resource to generate fuels, chemicals, and other bioproducts. Lignocellulosic biomass has complex structural and chemical properties that make it highly resistant to release sugars by chemicals and/or enzymes.[1] To overcome this recalcitrance, a wide variety of pretreatment processes have been developed to deconstruct plant cell walls, such as, dilute acid, steam explosion, and ammonia pretreatments.[2] These approaches are able to improve enzyme accessibility and increase yields of fermentable sugars from cellulose.[2, 3] However, lignin and hemicellulose were not easily separated and recovered from these pretreatment processes, which results in a large amount of by-products with low value. A practical pretreatment process should maximize the profit of biorefineries while minimizing environmental impacts.

A new generation of biorefineries has been proposed to follow the model of the petrochemical industry by integrating low value fuel with the production of high value chemicals derived from each primary component of lignocellulose.[4] Novel processes that satisfy the requirements of integrated biorefineries must exhibit the ability to selectively separate each primary component of lignocellulosic biomass, while offering easy access to the isolation of the components after separation.[4] IL processes have received significant attention as a potential technology to meet these requirements.

ILs are a type of molten salts with melting points below 100 °C,[5] although a majority of IL biomass pretreatment processes have been accomplished using severe conditions

(above 100 °C).[6, 7] The removal of lignin and hemicellulose, which generates a cellulose-rich fraction,[6, 7] contributes to the rapid dissolution of biomass at high pretreatment temperatures, especially above 150 °C (near the glass transition temperature of lignin).[8] However, in these pretreatments, lignin and hemicellulose were not fully utilized, mostly due to their degradation and distribution in the product streams.[8-10] Labbé et al. have reported that the recalcitrance of biomass was significantly reduced with minimum degradation of the major biopolymers by [C_2mim][OAc] under mild conditions (60 °C for a few hours).[11]

Recently, a few investigations have proposed new or improved methods with ILs to fractionate biomass in an attempt to generate lignin-, cellulose-, and hemicellulose-rich fractions.[12-17] However many of these methods have limitations pertaining to generating high purity streams of each major component. For example, a one-pot ionic liquid system fractionated a majority of lignin into a solid stream with low purity <70%.[9] To maximize the recovery of biomass and IL, Bogel-Łukasik and co-workers et al. successfully applied a polymer resins and CO_2 extraction technology and extracted phenolic compounds of lignin from IL.[18] Therefore, the direct and complete deconstruction of biomass into fractions with high purity and yield remains a challenge and more integrated technologies are still needed to effectively fractionate lignocellulosic biomass with ILs.

The main goal of this study was to develop a novel ionic liquid process to fractionate hybrid poplar (HP) into a carbohydrate fraction and a lignin fraction (IL-lignin) with high purity and yield. The IL-lignin was characterized by differential scanning calorimetry (DSC) and ^{1}H-^{13}C HSQC NMR (2D NMR) spectroscopy. Powder x-ray diffractometry (XRD) was applied to measure the cellulose crystalline structure changes through the

fractionation process. To evaluate the effect of autohydrolysis and IL treatment on the recalcitrance of biomass, enzymatic hydrolysis of autohydrolyzed hybrid poplar (autohydrolyzed HP), regenerated HP and regenerated autohydrolyzed HP was performed.

4.3 Materials and Methods

Hybrid poplar (*Populus*×*Deltoides*) was obtained from the Center for Renewable Carbon of the University of Tennessee. The biomass was air-dried and chopped to less than 1 cm^3 particle size.

The ionic liquid 1-ethyl-3-methylimidazolium acetate ([C_2mim][OAc], purum≥95%) used in this study was purchased from Iolitec Inc. (Tuscaloosa, AL) and used without further purification. Dimethyl sulfoxide (DMSO)-d_6 (99.9%) and pyridine-d_5 (99.5%) were purchased from Sigma-Aldrich (St. Louis, MO). Deionized water (DI water) was employed throughout the experiments.

4.3.1 Autohydrolysis of biomass

The autohydrolysis was carried out in a Hastelloy C276 pressure reactor heated by band heaters and the system conditions were monitored and controlled using Lab-VIEW 8.6 software. Hybrid poplar (HP) chips (187 g) were transferred into a Teflon basket and then inserted into the reactor. Subsequently, the reactor was sealed and placed under vacuum for 20 min. Afterwards, DI water (3470 mL) was pulled into the reactor under vacuum and heated for 60 min to achieve 160 °C. The extraction was performed at 160 °C for 60 min under an autogenous equilibrium pressure of 0.717 MPa. By the completion of the run, the reactor was cooled down to 50 °C in 120 min then the hydrolysate was carefully drained into a collection tank. The reactor was opened, and the Teflon basket containing the solid

(autohydrolyzed HP) was removed. The material was air dried at 40 °C until a constant moisture content was reached (less than 10% by weight). The dried material was then milled with a Wiley mill (Thomas Scientific, Model # 3383-L10, Swedesboro, NJ) through a 40-mesh screen (0.425 mm).

The severity factor, $\log R_0$ of the autohydrolysis reaction was calculated by the reaction temperature and time to describe the severity of the reaction[19]:

$$logR_0 = \log(t \times \exp\left(\frac{T_H - T_R}{14.75}\right)) \quad (3.1)$$

where t represents reaction time (60 min); T_H is the reaction temperature (160 °C); T_R is the reference temperature (100 °C).

The carbohydrates content of the hydrolysate was quantified according to a standard protocol developed by the National Renewable Energy Laboratory (NREL).[20] The hydrolysate sample was post-hydrolyzed with by 4% sulfuric acid at 121 °C for 60 min to convert oligomeric sugars into the monomeric sugars. The concentration of the monomeric sugars was determined by high-performance liquid chromatography (HPLC) with a refractive index detector equipped with a Bio-Rad Aminex HPX-87P carbohydrate analysis column (Richmond, CA) with deashing guard column (Biorad, Hercules, CA) at 85 °C, and water as the mobile phase at a flow rate of 0.25 mL/min.

The amount of soluble lignin in the hydrolysate (over the total lignin of the starting material) was calculated by the following equation:

$$Soluble\ lignin\ (\%) = \frac{m_{lignin,HP} - m_{lignin,autohydrolyzed\ HP}}{m_{lignin,HP}} \quad (3.2)$$

where $m_{lignin,HP}$ represents the oven-dry weight of lignin of the starting material, HP; $m_{lignin,autohydrolyzed\ HP}$ is the oven-dry weight of lignin of autohydrolyzed HP.

4.3.2 Activation and regeneration of biomass in [C_2mim][OAc]

The moisture content of HP and autohydrolyzed HP was about 5% and 3%, respectively, which was measured according to the standard NREL protocol.[21] [C_2mim][OAc] was first heated to 100 °C for 20 min to remove water and then cooled down to 60 °C. Approximately, 10 % HP or autohydrolyzed HP (40 g) were added to [C_2mim][OAc] (360 g) and mechanically mixed in 0.9 L glass reactor at 600 rpm at 60 °C for 3 h. At the end of IL treatment, room temperature DI water (400 g) was quickly added to the biomass-IL system as an anti-solvent and the mixture was stirred for three additional minutes. The regenerated biomass was filtered and washed with room temperature DI water to remove any traces of IL, and finally recovered by centrifugation. The sample was then dried at 40 °C for 5 days. The complete removal of IL was confirmed by monitoring a characteristic infrared band of [C_2mim][OAc] ($\nu_{C=N}$ = 1565 cm^{-1}) of the regenerated biomass using a Perkin–Elmer Spectrum One FT-IR spectrometer (Waltham, MA).

4.3.3 Cellulose structure of biomass samples by XRD

Powder XRD was used to determine the impact of autohydrolysis and IL treatment on cellulose structure, a small amount of HP, regenerated HP, autohydrolyzed HP, regenerated autohydrolyzed HP. Each sample was mounted on a low-background quartz holder and a PANalytical Empyrean X-ray diffractometer (PANalytical Inc., Westborough, MA) with a Cu tube (λ ¼ 1.5405 Å) was used to collect the XRD data. The radiation was generated at 40 mA and 45 kV. A step size of 0.01° exposure was used for measuring the scattering angle 2θ in the range 9–41°. The index of crystallinity (CrI) of each sample was determined using Segal's method.[22]

4.3.4 Enzymatic saccharification of biomass samples

Enzymatic hydrolysis of regenerated HP, autohydrolyzed HP, and regenerated autohydrolyzed HP was carried out in duplicate according to the NREL Laboratory Analytical Procedure.[23] Briefly, about 2% (w/w) of biomass sample (10 g) was hydrolyzed using a mixture of multicomponent cellulases (CTec 2) and hemicellulases (HTec 2) from Novozymes. The saccharification was performed at 50 °C in a 0.9 L fermenter with constant stirring (140 rpm) with 50 mM citrate buffer (pH 5.5). The carbohydrates conversion was monitored by the monomeric sugar concentrations in aliquots of the saccharification hydrolysate. Aliquots (1.5 mL) taken at 0, 1, 2, 3, 6, 24, 48 and 72 h, were boiled for several minutes to denature the enzymes, and centrifuged to separate the solid residues. The aliquots were then filtered with a 0.45 micron nylon membrane filter from Milli-pore (Billerica, MA) and analyzed by HPLC. After 72 h hydrolysis, the solid residues (IL-lignin) were recovered from the saccharification hydrolysate by centrifugation and further washed with DI water to remove enzymes. IL-lignin was dried at 40 °C for 5 days prior to characterizations.

4.3.5 Quantitative analysis of the fractionation process

The oven-dry weight and chemical composition of HP, autohydrolyzed HP, regenerated autohydrolyzed HP and regenerated autohydrolyzed HP after saccharification (IL-lignin) were determined with three replicates in accordance with the standard NREL protocol.[21]

4.3.6 Thermal analysis of IL-isolated lignin by DSC

Thermal analysis was conducted using a PerkinElmer PYRIS Diamond DSC. The system uses two 1-gram furnaces, which allow the fastest heating and cooling rate up to 500 °C/min and also provide an improved baseline and a better resolution of heat capacity transition.[24] In brief, IL-lignin (~2.5 mg) was placed in a hermetically sealed DSC pan. The top of each pan was punctured in order to allow volatiles to escape. Samples were equilibrated at 25 ºC, heated to 250 ºC with the rate of 100 ºC/min, cooled to 25 ºC at 100 ºC/min. The heating and cooling process was repeated two times to eliminate any unsealed thermal history. The glass transition temperature (Tg) was determined at the midpoint temperature of the heat capacity change during the third heating run.

4.3.7 Thermal analysis of IL-isolated lignin by TGA

Thermogravimetric analysis was conducted by a TGA (Pyris 1 TGA, Perkin Elmer, Shelton, CT). IL-lignin (~5 mg) was first heated from 50 to 105 °C at a rate of 10 °C/min under 10 mL/min of nitrogen and kept at 105 °C for 10 min to remove moisture. To collect the thermal decomposition curve, IL-lignin was subsequently heated to 900 °C at 10 °C/min under 10 mL/min of nitrogen and held at 900 °C for 60 min under 10 mL/min of air. The thermal properties were described by both TG and differential TG (DTG) curves.

4.3.8 2D-NMR spectroscopy of biomass and IL-lignin

HP powder (40 mesh) was extracted in an Accelerated Solvent Extractor (ASE 350, Dionex, Sunnyvale, CA) to remove non-structural compounds (extractives) following the approach in the NREL analytical procedure.[25] Afterwards, the extractives-free HP was

ball milled according to a published protocol.[26] The sample (40 mg) was transferred into 5 mm NMR tubes. Subsequently, 500 µL of DMSO-d_6/pyridine-d_5 (4:1, v/v) was carefully injected on the side of the NMR tube using a syringe. The tube was then sonicated for ~1 h until the formed gel appeared to be homogeneous. Two-dimensional ^{1}H-^{13}C HSQC NMR spectra of the extractives-free HP and IL-lignin were acquired using a Bruker AV-II spectrometer operating at 600.13 MHz.

4.4 Results and Discussion

4.4.1 Quantitative analysis of autohydrolysis and IL activation process

The study on autohydrolysis (chapter 2) has demonstrated that a large amount of biomass hemicellulose was able to be hydrolyzed into soluble sugars with minor degradation of lignin and cellulose at 160 °C for 60 min. Therefore, these conditions were used to perform the autohydrolysis of HP in this study to partially extract hemicellulose and generate a high-purity hemicellulose fraction. The severity factor ($logR_0$) of the autohydrolysis is 3.54. pH of hydrolysate was 3.5. Sugar quantification of the hydrolysate revealed that 54.7% hemicellulose was hydrolyzed. A large amount of xylan (54.1%) and a majority of galactan (95.7%) and arabinan (82.7%) were extracted during this step (Figure 4.4). Small amount of glucose was also detected.

The chemical composition and mass balance of the HP and autohydrolyzed HP are shown in Table 4.1. Calculated based on the total solid weight difference between HP and autohydrolyzed HP, the mass recovery after hot water extraction was 74%. The hemicellulose content decreased from 23.6% to 12.5%. Lignin and cellulose content slightly increased with the extraction. In addition, a significant amount of ash (72%) was

removed as well. It is worth noting that biomass with lower ash content is desirable feedstock for biorefineries, since inorganics present in the biomass can cause problems with reactor equipment, such as slagging, fouling, and even corrosion.[27] In summary, the first step in our fractionation process efficiently hydrolyzed a large portion of hemicellulose and generated biomass with increased cellulose and lignin content and decreased ash content. In the following step, the autohydrolyzed biomass was subjected to an IL activation and regeneration step in order to reduce its recalcitrance. The chemical composition of the IL-regenerated material is given in Table 4.1.

Table 4.1 Chemical composition of streams in fractionation process.

Materials	Cellulose [%]	Hemicellulose [%]	Lignin [%]	Ash [%]
Extractives-free HP	47.0 (0.2)	23.6 (0.1)	25.8 (0.2)	1.1 (0.0)
Autohydrolyzed HP	55.4 (0.7)	12.5 (0.3)	27.7 (0.1)	0.3 (0.1)
Regenerated autohydrolyzed HP	59.6 (0.3)	9.4 (0.2)	29.1 (2.0)	0.4 (0.0)
IL-lignin	4.3 (0.0)	2.0 (0.1)	90.1 (0.0)	0.5 (0.0)

Chemical composition was calculated based on dry basis of the sample. ( ): Standard deviation

Mostly, hemicellulose content declined from 12.5% for the autohydrolyzed HP to 9.4% for the IL-regenerated autohydrolyzed HP, demonstrating that the IL treatment induced some additional hemicellulose loss. This decrease in hemicellulose during IL treatment can be explained by the decrease of the bonding between hemicellulose and lignin or cellulose, which further induced dissolution of hemicellulose in water during the regeneration and washing step.[28] Consequently, the IL-regenerated autohydrolyzed HP had a lower amount of hemicellulose and higher content of cellulose and lignin.

The used IL exhibited good recyclability. First, the IL was applied at mild condition (60 °C for 3 h). We expected the non-degradation and the high yield of the recovered IL. Second, the recovered IL could have very small amount of impurities from biomass, because the mid condition maximized the recovery of the biomass as high as 90% (36 g of regenerated autohydrolyzed HP was recovered from 40 g autohydrolyzed HP, see Figure 4.3). In addition, there should not be any impurity from the ash in biomass. Autohydrolysis step removed a large portion of ash (72%, see Table 4.1). IL-regenerated autohydrolyzed HP had very similar ash content (0.4%) as autohydrolyzed HP (0.3%). Therefore, the recovered IL should have high yield and purity.

4.4.2 Changes of cellulose crystalline structure measured by XRD.

HP, IL-regenerated HP, and autohydrolyzed HP exhibited very similar diffraction patterns (Figure 4.2). The major peak for these three samples was at $2\theta = 22.3°$ and the secondary peak was at $2\theta = 16°$. These peaks indicate the existence of cellulose I crystal structure.[29] The index of crystallinity (CrI) calculated using Segal's method, was 62%, 51% and 70% for HP, IL-regenerated HP, and autohydrolyzed HP, respectively. The lower CrI of IL-regenerated HP indicates that the IL activation decreased cellulose crystallinity in the sample when compared the starting material (HP). However, evidently the autohydrolysis step had the opposite effect, since the CrI was enhanced by autohydrolysis. The higher CrI was mainly due to the partial removal of the amorphous fraction of biomass (hemicellulose (54.7%) and a small portion of lignin (20%)). The removal of these components has been reported to increase cellulose crystallinity by reducing the amorphous background of autohydrolyzed HP.[30]

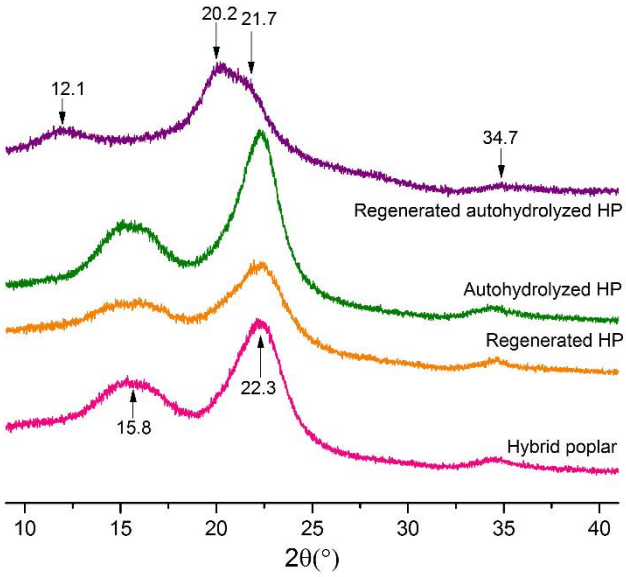

Figure 4.2 XRD patterns of hybrid poplar (HP), autohydrolyzed HP and regenerated autohydrolyzed HP.

IL-regenerated autohydrolyzed HP displayed different diffraction patterns than HP, IL-regenerated HP, and autohydrolyzed HP (Figure 4.2). After the IL activation and regeneration step, the main peak at 22.3° disappeared, and a broad asymmetric peak consisting of a doublet at 20.2 and 21.5° appeared. Moreover, the broad peak at 15.8° vanished, and a new peak emerged at ~12.1°. These changes demonstrated that cellulose I was transformed to cellulose II in the IL-regenerated autohydrolyzed HP. This type of structure changes has been reported in the literature.[29, 31] Cheng and co-workers showed that cellulose I was transformed into cellulose II in switchgrass when treated with [C_2mim][OAc] at 120 °C for 12 h[29] while there was no evidence of transformation for Eucalyptus, a hardwood species under the same conditions. Compared with these published data, the cellulose crystallinity of autohydrolyzed HP was readily reduced by IL at lower temperature (60 °C) and shorter time (3 h) demonstrating that the partial removal of

hemicellulose dismantled the hemicellulose-lignin coating on the cellulosic fibrils and distinctly improved the accessibility of IL to the cellulose of the autohydrolyzed HP.

4.4.3 Saccharification of treated biomass

The final step in our fractionation process is an enzymatic saccharification step that generates a monosugar sugar stream and a lignin-rich fraction. Enzymatic hydrolysis was carried out for autohydrolyzed HP, IL-regenerated HP, and IL-regenerated autohydrolyzed HP. Of these, the IL-regenerated autohydrolyzed HP had the best performance regarding carbohydrates conversion (Figure 4.3). This material displayed the fastest kinetic rate of cellulose conversion from 0 to 3 h, during which 87% of cellulose were hydrolyzed to glucose. At 6 h, cellulose conversion reached 93%. Over the same reaction period, much lower cellulose conversion was observed for the autohydrolyzed HP (25%) and the IL-regenerated HP (18%). By 72 h, about 94% of cellulose of the IL-regenerated autohydrolyzed HP was hydrolyzed while only 68% of cellulose were converted in the autohydrolyzed HP and 32% in the IL-regenerated HP.

It is worth noted that the IL-regenerated autohydrolyzed HP also had the best hemicellulose conversion behavior of the group. However, its hemicellulose conversion was lower than its cellulose, with a mere 43% hydrolyzed after 6 h. Still, this conversion was higher than that for the autohydrolyzed HP (30%) and the IL-regenerated HP (8%) over the same reaction period. After 72 h, the IL-regenerated autohydrolyzed HP reached 68% of hemicellulose conversion, whereas that of autohydrolyzed HP and IL-regenerated HP were 64% and 22%, respectively.

These data demonstrated that the partial removal of the hemicellulose by autohydrolysis and the change that cellulose structure underwent during the IL treatment are responsible

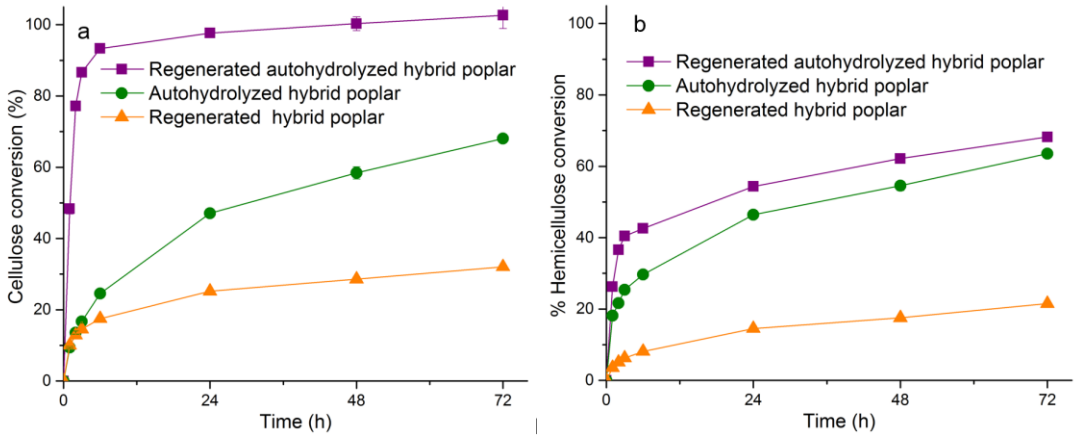

Figure 4.3 Carbohydrate conversion (%) of pretreated hybrid poplar samples as a function of time. (a): cellulose conversion (b): hemicellulose conversion. Standard errors were shown in the profile.

for the higher saccharification conversion of the IL-regenerated autohydrolyzed HP. Indeed, cellulose structure has a significant impact on enzymatic saccharification kinetics and yield of biomass.[29] Cellulose II has been shown to be more easily digested than cellulose I.[29] Accordingly, IL-regenerated autohydrolyzed HP with a cellulose II structure exhibited better hydrolyzability than autohydrolyzed HP and IL-regenerated HP (Figure 4.3a). Although XRD patterns revealed that autohydrolyzed HP had higher CrI than that of IL-regenerated HP, enzymatic saccharification kinetics and carbohydrates conversion yields showed that the former had better hydrolyzability than the latter. Evidently, this indicates that cellulose accessibility is not only affected by crystallinity, but also influenced by the presence of hemicellulose. The partial removal of this amorphous substance reduces the physical protection of cellulose and enhances the access of enzymes to carbohydrates.

The combination of both autohydrolysis and IL activation was much more efficient to reduce the recalcitrance and increase hydrolyzability of biomass than either autohydrolysis or IL treatment. Compared with other IL processes, our approach exhibited superior sugar

conversion rate. Most reported enzymatic saccharification still took at least 2-3 days to achieve 80%-90% of polysaccharides conversion to monosaccharides.[32] For example, , da Costa et al. reported that 90.6% of glucose yield from [C_2mim][OAc] pretreated wheat straw was obtained around 72 h.[33] Recent published data indicate that IL-pretreated corn stover released about 82% of cellulose at 12 h and 47% of hemicellulose at 72 h.[34] In summary, IL-regenerated autohydrolyzed HP has significantly faster saccharification kinetics and much more complete conversion than autohydrolyzed HP and IL-regenerated HP generating a liquid fraction rich in monosugars and a solid fraction containing low carbohydrates.

4.4.4 Quantitative analysis of IL-lignin yield and purity

After saccharification, the solid fraction was isolated by filtration and characterized. The yield of this fraction was 69.9%. The chemical composition analysis showed that it was a lignin-rich fraction with a purity of 90.1% containing a small fraction of cellulose (4.3%) and hemicellulose (2.0%) (Table 4.1).

Overall, the combined autohydrolysis-IL process was able to fractionate hybrid poplar into a carbohydrates fraction and lignin fraction with high yield and purity. The process afforded 54.8% of hemicellulose with mono- and oligosaccharides in the autohydrolysis step, 26.2% of hemicellulose and 86.5% of cellulose in the form of monomers, and 69.9% of lignin with a purity of 90.1% (Figure 4.4) by enzymatic saccharification. Mismatched balances of samples through the fractionation process was mainly due to the mass loss in washing and transferring steps.

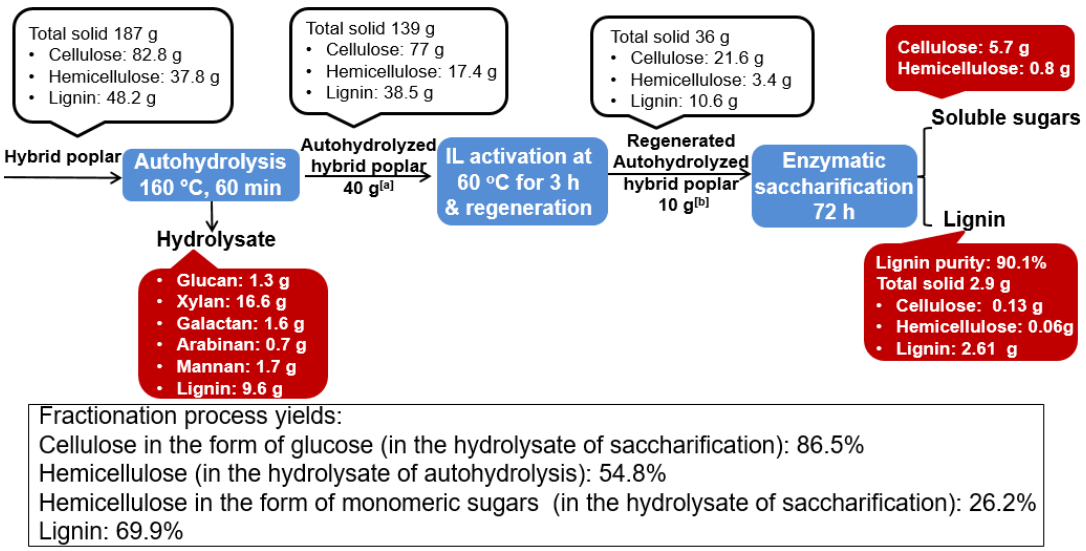

Figure 4.4 Quantitative analysis of the fractionation process. Total solid is on percent dry basis. [a]40 g of total 139 g of autohydrolyzed hybrid poplar was used for IL activation and regeneration step. [b]10 g of total 36 g of IL-regenerated autohydrolyzed hybrid poplar was used for enzymatic saccharification step.

4.4.5 Thermal analysis of IL-isolated lignin

The IL-lignin was analyzed by DSC. The endothermic peak between 170 and 192 °C (Figure 4.5) corresponds to the glass transition temperature (Tg) of the material. The value, taken as the midpoint of this transition, was 181 °C. This value was higher than the Tg of ball-milled lignin (148 °C) and organosolv lignin (135 °C) produced from the same feedstock. This high Tg was likely due to the high molecular weight of the IL-lignin. However, the molecular weight of our IL-lignin could not be measured since it was still not completely soluble after the acetylation or acetobromination method. We postulate that our IL-lignin has a structure similar to native lignin (lignin in hybrid poplar) due to the low severity of each step involved in the fractionation process. Our autohydrolysis-IL fractionation process yield and 10% was lost during the IL activation/regeneration/isolation

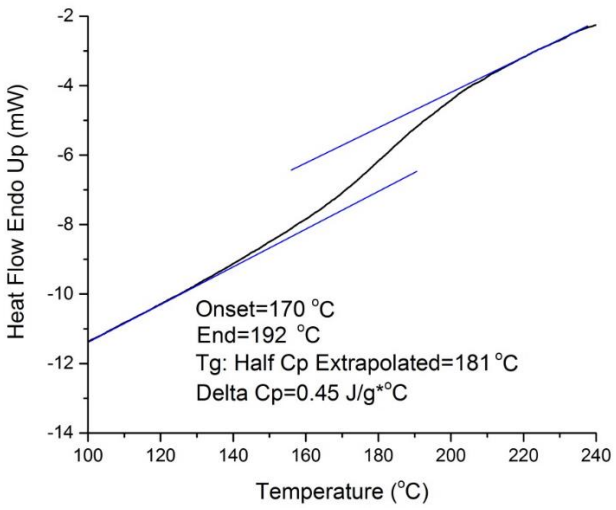

Figure 4.5 DSC profile of IL-lignin.

step.

TG and DTG profiles (Figure 4.6) show the temperature corresponding to the 5% weight loss (T_5) 210 °C, the temperature corresponding to the 10% weight loss (T_{10}) 236 °C, the onset degradation temperature (T_{onset}) 211 °C, and the maximum degradation temperature (T_{max}) is 908 °C. The percentage of char is 31%. The deconvoluted pseudo-component peak occurs at 317 °C, which is the maximum rate of weight loss.

4.4.6 2D-NMR spectroscopy

Many pretreatment and fractionation processes had obvious influence on the isolated lignin structure. For instance, Sathitsuksanoh et al. reported that ionic liquid pretreatment had the distinct cleavage of interunit linkages, especially β-O-4 linkages.[35] Zhu et al. demonstrated that an organosolv process induced severe delignification and almost complete destruction of the β-O-4 linkages.[36] We used ^{1}H-^{13}C HSQC NMR to compare the structure of the isolated lignin (IL-lignin) to in-situ lignin (lignin in HP). In Figure 4.7,

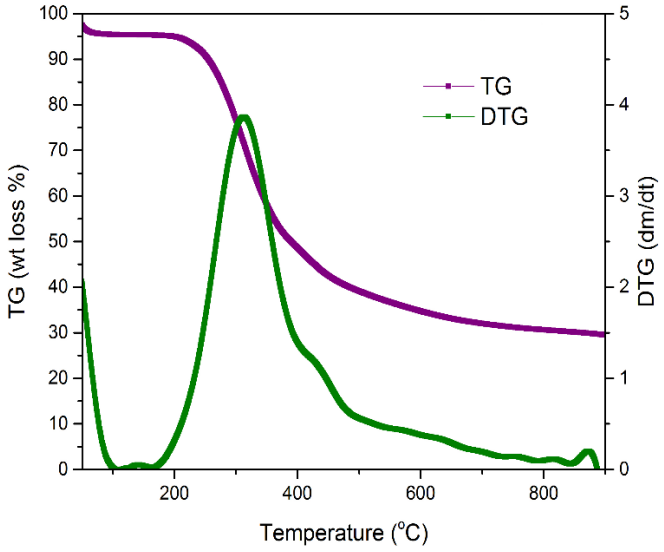

Figure 4.6 TG and DTG profiles of IL-lignin.

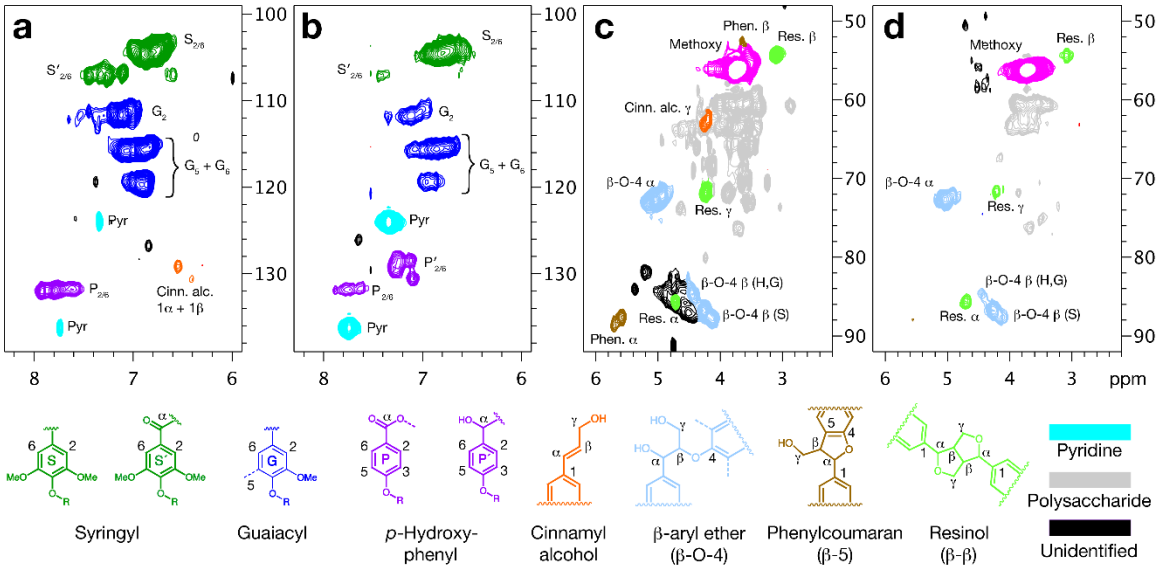

Figure 4.7 2D NMR spectra of hybrid poplar and IL-lignin. (a) aromatic region of HP. (b) aromatic region of IL-lignin. (c) side-chain region of HP. (d) side-chain region of IL-lignin.

Table 4.2 HSQC NMR assignments and annotations for IL-lignin.

δ ^{13}C, ^{1}H	Assignment
	aromatic region
131.8, 7.7	$C_{2,6}/H_{2,6}$ in P(H) benzoate
131.7, 7.6	
130.6, 7.1	$C_{2,6}/H_{2,6}$ in P(H) with α-OH
128.9, 7.2	
128.5, 7.1	
120.7, 7.5	C_6/H_6 in G with α-C=O
119.4, 6.9	C_6/H_6 in G
115.6, 7.1	$C_{3,5}/H_{3,5}$ in P(H)
115.6, 6.9	C_5/H_5 in G
112.1, 7.3	C_5/H_5 in G with 4-ether
112.0, 7.1	C_2/H_2 in G
107.1, 7.4	$C_{2,6}/H_{2.6}$ in S with α-C=O
104.3, 6.8	$C_{2,6}/H_{2.6}$ in S
	side-chain region
87.3, 4.2	C_β/H_β in β-O-4 in S
86.8, 4.3	C_β/H_β in β-O-4 in G
85.7, 4.7	C_α/H_α in resinol (β-β)
84.7, 4.4	C_β/H_β in β-O-4 in P(H)
72.7, 5.0	C_α/H_α in β-O-4
71.6, 4.2	C_γ/H_γ in resinol (β-β)
56.2, 3.7	methoxy
54.3, 3.1	C_β/H_β in resinol (β-β)

the NMR spectra of HP and the IL-lignin were divided into two regions: the aromatic region and side chain region.

In the aromatic region, the spectrum of HP showed syringyl and guaiacyl units with p-hydroxybenzoate and cinnamyl alcohol (Figure 4.7a and Table 4.2) As it can be observed in Figure 4.7b, the signals of syringyl, guaiacyl, and p-hydroxybenzoate units were not distinctly affected by the fractionation process. However, the cinnamyl alcohol end groups in the IL-lignin were not detected which is mostly due to their degradation during the autohydrolysis step.[36]

In the side chain region, β-aryl ether, phenylcoumaran, and resinol were the interunit linkages in the HP (Figure 4.7c and Table 4.2). Strong peak intensities of β-aryl ether and resinol were observed in IL-lignin (Figure 4.7d). The cleavage of β-5 bonds resulted in the

very weak intensity of β-5 linkages in IL-lignin and the appearance of *p*-hydroxyphenyl with α-OH group in the aromatic region of IL-lignin. The comparison between 2D NMR spectra of HP and IL-lignin shows that the main linkages of lignin in hybrid poplar were preserved during the fractionation process and therefore suggests that our IL-lignin had a structure similar to native lignin of HP. Therefore, our fractionation process is able to generate lignin without substantial degradation and modification.

4.5 Conclusion

Lignocellulosic biomass was successfully fractionated into a carbohydrates fraction and a lignin fraction with high yield by an autohydrolysis-mild IL assisted fractionation process. Each component was isolated with high mass recovery and purity. Approximately, 87% of cellulose, 81% of hemicellulose, and 70% of lignin were produced through the process. The autohydrolysis step significantly improved the accessibility of IL to cellulose which was transformed to cellulose II during the IL activation step. The combination of both steps, autohydrolysis and IL activation improves the hydrolyzability of the biomass, and enables the IL-regenerated autohydrolyzed hybrid poplar to have superior enzymatic saccharification kinetics and carbohydrates conversion. In addition, the generated high purity lignin-rich fraction (90.1%) had a high glass transition temperature and chemical features similar to native lignin demonstrating that the fractionation process has minimal impact on lignin structure and chemistry.

4.6 References

1. Himmel, M.E., et al., *Biomass recalcitrance: engineering plants and enzymes for biofuels production.* Science, 2007. 315(5813): p. 804-7.
2. Mosier, N., et al., *Features of promising technologies for pretreatment of lignocellulosic biomass.* Bioresource technology, 2005. 96(6): p. 673-686.
3. Bussemaker, M.J. and D.K. Zhang, *Effect of Ultrasound on Lignocellulosic Biomass as a Pretreatment for Biorefinery and Biofuel Applications.* Industrial & Engineering Chemistry Research, 2013. 52(10): p. 3563-3580.
4. Bozell, J.J., *An evolution from pretreatment to fractionation will enable successful development of the integrated biorefinery.* BioResources, 2010. 5(3): p. 1326-1327.
5. Sun, N., et al., *Where are ionic liquid strategies most suited in the pursuit of chemicals and energy from lignocellulosic biomass?* Chemical Communications, 2011. 47(5): p. 1405-1421.
6. Sathitsuksanoh, N., et al., *Lignin fate and characterization during ionic liquid biomass pretreatment for renewable chemicals and fuels production.* Green Chemistry, 2014.
7. Hauru, L.K., et al., *Enhancement of ionic liquid-aided fractionation of birchwood. Part 1: autohydrolysis pretreatment.* RSC Advances, 2013. 3(37): p. 16365-16373.
8. Hossain, M.M. and L. Aldous, *Ionic liquids for lignin processing: Dissolution, isolation, and conversion.* Australian Journal of Chemistry, 2012. 65(11): p. 1465-1477.
9. Shi, J., et al., *One-pot ionic liquid pretreatment and saccharification of switchgrass.* Green Chemistry, 2013. 15(9): p. 2579-2589.
10. An, Y.-X., et al., *Pretreatment of lignocellulosic biomass with renewable cholinium ionic liquids: Biomass fractionation, enzymatic digestion and ionic liquid reuse.* Bioresource technology, 2015. 192: p. 165-171.
11. Labbé, N., et al., *Activation of lignocellulosic biomass by ionic liquid for biorefinery fractionation.* Bioresource technology, 2012. 104: p. 701-707.
12. Ninomiya, K., et al., *Characterization of fractionated biomass component and recovered ionic liquid during repeated process of cholinium ionic liquid-assisted pretreatment and fractionation.* Chemical Engineering Journal, 2015. 259: p. 323-329.
13. Abe, M., T. Yamada, and H. Ohno, *Dissolution of wet wood biomass without heating.* RSC Advances, 2014. 4(33): p. 17136-17140.
14. Anugwom, I., et al., *Switchable ionic liquids as delignification solvents for lignocellulosic materials.* ChemSusChem, 2014. 7(4): p. 1170-1176.
15. Hamada, Y., et al., *A possible means of realizing a sacrifice-free three component separation of lignocellulose from wood biomass using an amino acid ionic liquid.* Green Chemistry, 2013. 15(7): p. 1863-1868.
16. Lopes, A.M., et al., *Pretreatment and fractionation of wheat straw using various ionic liquids.* J Agric Food Chem, 2013. 61(33): p. 7874-82.
17. da Costa Lopes, A.M., et al., *Pre-treatment of lignocellulosic biomass using ionic liquids: wheat straw fractionation.* Bioresour Technol, 2013. 142: p. 198-208.
18. da Costa Lopes, A.M., et al., *Extraction and Purification of Phenolic Compounds from Lignocellulosic Biomass Assisted by Ionic Liquid, Polymeric Resins, and*

Supercritical CO2. ACS Sustainable Chemistry & Engineering, 2016. 4(6): p. 3357-3367.
19. Overend, R.P., E. Chornet, and J. Gascoigne, *Fractionation of lignocellulosics by steam-aqueous pretreatments [and discussion]*. Philosophical Transactions of the Royal Society of London A: Mathematical, Physical and Engineering Sciences, 1987. 321(1561): p. 523-536.
20. A. Sluiter, B.H., R. Ruiz, C. Scarlata, J. Sluiter, D. Templeton, *Determination of Sugars, Byproducts, and Degradation Products in Liquid Fraction Process Samples* NREL Biomass Analysis Technology Team Laboratory Analytical Procedure, 2008.
21. A. Sluiter, B.H., R. Ruiz, C. Scarlata, J. Sluiter, D. Templeton, and D. Crocker *Determination of structural carbohydrates and lignin in biomass*. 2008, NREL/TP-510-42618 NREL Laboratory Analytical Procedure. National Renewable Energy Laboratory, Golden. http://www. nrel. gov/biomass/pdfs/42618. pdf.
22. Segal, L., et al., *An empirical method for estimating the degree of crystallinity of native cellulose using the X-ray diffractometer.* Textile Research Journal, 1959. 29(10): p. 786-794.
23. Selig, M., N. Weiss, and Y. Ji, *Enzymatic Saccharification of Lignocellulosic Biomass: Laboratory Analytical Procedure (LAP): Issue Date, 3/21/2008*. 2008: National Renewable Energy Laboratory.
24. *PYRIS diamond DSC.* PerkinElmer Instruments: Shelton, CT, 2001; http://www-omcs.materials.ox.ac.uk/uploads/diamond%20dsc%20tech%20sheet.pdf.
25. Sluiter, A., et al., *Determination of extractives in biomass.* Laboratory Analytical Procedure (LAP), 2005. 1617.
26. Mansfield, S.D., et al., *Whole plant cell wall characterization using solution-state 2D NMR.* Nature protocols, 2012. 7(9): p. 1579-1589.
27. Bryers, R.W., *Fireside slagging, fouling, and high-temperature corrosion of heat-transfer surface due to impurities in steam-raising fuels.* Progress in energy and combustion science, 1996. 22(1): p. 29-120.
28. Li, C., et al., *Scale-up and evaluation of high solid ionic liquid pretreatment and enzymatic hydrolysis of switchgrass.* Biotechnology for biofuels, 2013. 6(1): p. 1.
29. Cheng, G., et al., *Transition of cellulose crystalline structure and surface morphology of biomass as a function of ionic liquid pretreatment and its relation to enzymatic hydrolysis.* Biomacromolecules, 2011. 12(4): p. 933-941.
30. Ruiz, H.A., et al., *Development and characterization of an environmentally friendly process sequence (autohydrolysis and organosolv) for wheat straw delignification.* Applied biochemistry and biotechnology, 2011. 164(5): p. 629-641.
31. Cheng, G., et al., *Impact of ionic liquid pretreatment conditions on cellulose crystalline structure using 1-ethyl-3-methylimidazolium acetate.* The Journal of Physical Chemistry B, 2012. 116(33): p. 10049-10054.
32. Li, C., et al., *Comparison of dilute acid and ionic liquid pretreatment of switchgrass: biomass recalcitrance, delignification and enzymatic saccharification.* Bioresource technology, 2010. 101(13): p. 4900-4906.
33. da Silva, S.P.M., et al., *Novel pre-treatment and fractionation method for lignocellulosic biomass using ionic liquids.* RSC Advances, 2013. 3(36): p. 16040-16050.

34. Sun, N., et al., *Blending municipal solid waste with corn stover for sugar production using ionic liquid process.* Bioresource technology, 2015. 186: p. 200-206.
35. Sathitsuksanoh, N., et al., *Lignin fate and characterization during ionic liquid biomass pretreatment for renewable chemicals and fuels production.* Green Chemistry, 2014. 16(3): p. 1236-1247.
36. Zhu, M.-Q., et al., *Effect of structural changes of lignin during the autohydrolysis and organosolv pretreatment on Eucommia ulmoides Oliver for an effective enzymatic hydrolysis.* Bioresource technology, 2015. 185: p. 378-385.

CHAPTER FIVE

CONCLUSIONS AND FUTURE PERSPECTIVES

5.1 Conclusions

The complex physical structure and chemical properties of lignocellulosic biomass highly inhibit the interactions between these biopolymers and IL, and limit the processability of lignocellulosic biomass in biorefineries. This research explored the impacts of the interactions between biopolymers and an ionic liquid on the utilization of lignocellulosic biomass (Figure 5.1). This research reveals that the physical obstacle of hemicellulose is the major inhibitor for IL diffusion to lignocellulosic biomass. The efficient interactions between lignocellulosic biopolymers and IL were achieved by very mild pretreatment (autohydrolysis at 160 °C for 60 min) and IL activation (60 °C for 3 h). By removing about 50% of hemicellulose through hot water extraction, the complex architecture of cell walls was disrupted, and biopolymer-IL interaction and consequently the dissolution of biomass in IL were much greatly improved. Through the proposed process, the whole biomass was directly converted into a high-value biomaterial, biomass film; all biopolymers of lignocellulosic biomass, i.e. hemicellulose, lignin and cellulose, were generated with minimum degradation, high yield and purity.

In the first section, by removing a large percentage of hemicellulose from biomass through an autohydrolysis step, the obstacle of lignocellulosic biomass for [C_2mim][OAc] diffusion was greatly reduced. A mild hemicellulose extraction under various severities was investigated to enhance the interaction between autohydrolyzed switchgrass and IL, and increase the dissolution of the biomass in [C_2mim][OAc]. The autohydrolysis at 160 °C for 60 min was the optimum condition, at which the maximum amount of hemicellulose

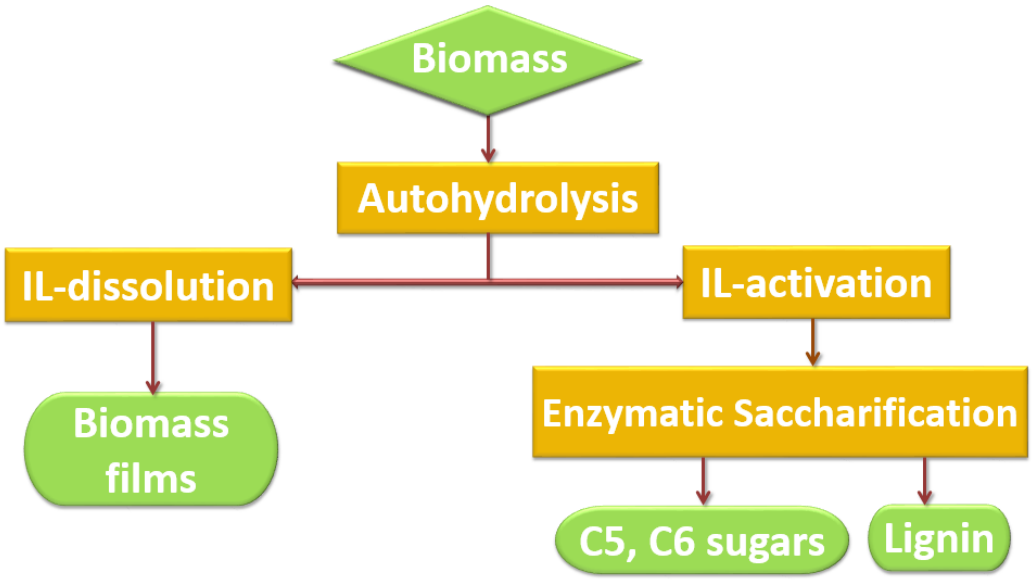

Figure 5.1 The process for lignocellulosic biomass utilization.

can be extracted with minor degradation of lignin and cellulose. After the pretreatment, the amount of dissolved biomass in [C_2mim][OAc] increased by a factor of 8 at 60 °C for 3 h. The highest dissolution (73.3%) was reached at an IL temperature of 100 °C and a residence time of 3 h. The IL dissolution temperature (60, 80 and 100 °C) impacted the dissolution of each biopolymer. The undissolved biomass residues that were subjected to high dissolution temperature contained lower amount of carbohydrates. Moreover, the dissolution behavior of the biomass autohydrolyzed under various severities was evaluated by monitoring the viscosity of the biomass-IL solutions over time for three different temperatures. The modelling of the dissolution data evidenced that the autohydrolysis severity was the major contributor for the improved biopolymer-ionic liquid interaction and biomass dissolution. Time-dependent viscosity data followed a power law model, which indicated the diffusion rate of IL to cell walls. Partial removal of hemicellulose

greatly enhanced the dissolution rate as observed by a sharp rise in solution viscosity and led to nearly complete dissolution of the biomass.

In the next section, through the improved interactions between biopolymers of lignocellulosic biomass and IL, lignocellulosic biomass was completely dissolved in IL, and IL-biomass solution was directly converted into films. Hybrid poplar biomass after autohydrolysis at 160 °C for 60 min entirely dissolved in [C_2mim][OAc] at 100 °C. Biomass films were directly cast from the autohydrolyzed-biomass/[C_2mim][OAc] solution and coagulated by either methanol, N,N-Dimethylacetamide (DMAc/water) mixture, or water. The biomass films were gradually dried over a sequence of humidity, and finally generated without cracks or wrinkles. The properties of the films were highly dependent on the polarity of coagulants. Methanol film exhibited the most homogeneous structure due to the gentle diffusion of methanol during coagulation, the good miscibility of carbohydrates and lignin, and the unparalleled orientation of cellulose II planes to the surface of methanol film. Methanol film also had higher temperature for the maximum decomposition peak (354 °C) than DMAc/ water or water film (338 °C), mainly resulting from its high-molecular-weight lignin. In addition, the tensile stress of the films was between 37-70 MPa. Methanol film had the highest tensile strength which indicates that lignin has two-side effect on the film properties. Lignin can increase the cross-links among the biopolymers. However, an excessive amount of lignin can make the films brittle. The high cross-link density and uniform structure may contribute to the higher mechanical properties of the methanol film.

In the third section, by increasing interaction of autohydrolyzed biomass with IL, the biomass had low recalcitrance, and was completely enzymatically fractionated to high

yield and purity carbohydrates and lignin streams. First, a portion of hemicellulose (55%) was extracted from the biomass by autohydrolysis (160 °C for 60 min) with small amount of lignin and cellulose. The extracted biomass was then activated with [C_2mim][OAc] at 60 °C for 3 h followed by an enzymatic hydrolysis to hydrolyze the carbohydrates into monosugars and generate the lignin fraction. The cellulose I of autohydrolyzed biomass was activated by IL and transformed into cellulose II within 3 h. The enzymatic conversion of cellulose in the IL-regenerated autohydrolyzed biomass was almost complete within 6 h. The saccharification kinetics and carbohydrates conversion yields revealed that a combination of both autohydrolysis and IL activation significantly reduced the recalcitrance of the IL-regenerated autohydrolyzed biomass, making it more susceptible to enzymatic hydrolysis than each treatment separately. Through this fractionation process, each biopolymer was isolated with high mass recovery and purity. Approximately, 87% of cellulose, 81% of hemicellulose, and 70% of lignin with a purity of 90.1% were produced. In addition, two-dimensional ^{1}H-^{13}C HSQC NMR spectroscopy indicated that the main linkages of lignin in hybrid poplar were preserved during the fractionation process. The isolated lignin may have a structure more similar to native lignin due to the low severity of each step in the fractionation process. The isolated lignin also had much higher glass transition temperature (181 °C) than organosolv lignin (135 °C). The unique characteristics of the isolated lignin may suggest its potential to produce lignin-based materials with superior physical and mechanical properties.

5.2 Recommendations for future works

Future work based on the contribution of this dissertation includes:

(1) Investigating higher loadings of autohydrolyzed biomass in IL since higher loadings

would be an attractive route to decrease pretreatment cost, increase the efficiency, and improve the profitability of biorefineries.

(2) In chapter 3, methanol film showed better mechanical properties than DMAc/water or water film. The high cross-link density between carbohydrates and lignin could result in its good mechanical property. Nuclear Overhauser effect spectroscopy (NOESY) could be a useful tool to quantify the distance between the biopolymers of the films, and further investigate the impact of coagulating solvents on biomass films.

(3) The optimum carbohydrates to lignin ratio can be investigated to produce films with the higher mechanical properties.

(4) The biopolymers films can be generated by the biopolymer blend (cellulose, hemicellulose and lignin)/IL solution. The comparison of the physicochemical properties of biopolymers films and lignocellulosic films could reveal the impact of biopolymers interactions on the quality of films.

(5) Biomass fibers can be produced by wet-spinning from the autohydrolyzed biomass/IL systems. The optimum conditions for wet-spinning can be investigated by measuring the viscosity of the biomass/IL solution and the cross-over point of storage modulus and loss modulus.

(6) The in-situ enzymatic saccharification of activated biomass can be investigated to combine the IL activation and enzymatic saccharification as one step in order to improve the efficiency and reduce the cost of the fractionation process.

(7) This research shows that hemicellulose is the major factor for inhibiting the diffusion of IL to biomass. A novel ionic liquid, which can efficiently hydrolyze hemicellulose, and lower cellulose crystallinity and convert it into cellulose II while not impacting lignin could

achieve the same performance as the combined autohydrolysis-IL treatment.

(8) Regarding the high glass transition temperature and good thermal stability of the isolated lignin from the fractionation process, there will be possibilities to generate high value-added products, e.g. lignin carbon fiber and lignin-based films with good physical and mechanical properties.

VITA

Jing Wang attended the Northeast Forestry University, Harbin, China and received her bachelor degree of chemical processing engineering of forest products and Master degree. After graduation, she continued her graduate study in the Department of Biosystems Engineering and Soil Science, University of Tennessee, Knoxville (UTK) to pursue graduate education in 2012. Jing joined Dr. Labbe's research group in spring of 2013.